Spring 2017

Radiographic assessment of lung anatomy, physiology, and disease in a porcine model of cystic fibrosis and people with cystic fibrosis

Ryan J. Adam
University of Iowa

RADIOGRAPHIC ASSESSMENT OF LUNG ANATOMY, PHYSIOLOGY, AND DISEASE IN A PORCINE MODEL OF CYSTIC FIBROSIS AND PEOPLE WITH CYSTIC FIBROSIS

by

Ryan J. Adam

A thesis submitted in partial fulfillment
of the requirements for the Doctor of
Philosophy degree in Biomedical Engineering
in the Graduate College of
The University of Iowa

May 2017

Thesis supervisor: Professor David A. Stoltz

Graduate College
The University of Iowa
Iowa City, Iowa

CERTIFICATE OF APPROVAL

_____

PH.D. THESIS

_____

This is to certify that the Ph.D. thesis of

Ryan J. Adam

has been approved by the Examining Committee for the thesis requirement for the Doctor of Philosophy degree in Biomedical Engineering at the May 2017 graduation.

Thesis committee: _____
David A. Stoltz, Thesis Supervisor

_____
Mahmoud Abou-Alaiwa

_____
Eric A. Hoffman

_____
Lynda S. Ostedgaard

_____
Joseph M. Reinhardt

_____
Jessica C. Sieren

“Progress in pediatrics: cystic fibrosis of the pancreas and its relation to celiac disease”

Dorothy Andersen
American Journal of Diseases of Children, 1938

To people, past and present, adversely affected by cystic fibrosis

ACKNOWLEDGEMENTS

This work would not have been possible without the contributions of many. I would like to thank members of my graduate thesis committee: David A. Stoltz, Mahmoud Abou-Alaiwa, Eric A. Hoffman, Lynda S. Ostedgaard, Joseph M. Reinhardt, and Jessica C. Sieren. I thank the Department of Biomedical Engineering. I would like to extend a special thank you to Joe Zabner and Mike Welsh. I would like to extend a special thank you to our research study participants. I would like to thank members of the CF research group: Sarah Horgen, Mahmoud Abou-Alaiwa, Lynda Ostedgaard, Tony Fischer, Ian Thornell, Nemo, Xiao Xiao Tang, Mark Hoegger, Viral Shah, James McMenimen, Conner Parker, Phil Karp, Sarah Ernst, Tom Moninger, Jan Launspach, Brie Hilkin, Eugene Chang, Patrick Allen, Cullen Shanrock, Alejandro Comellas, Paul McCray, Xiaopeng Li, Luis Vargas-Buonfiglio, Nick Gansemer, Oriana Vargas-Buonfiglio, Emma Hornick, Jade Rivera, David Dickey, Tom Gross, Doug Hornick, David Meyerholz, Joe Reinhardt, Sandeep Bodduluri, Ben Steines, Kortney Webber, Lee Beaumont III, Jenna Sapasap, Carley Stewart, Zach Noonan, Sandeep Bodduluri, Meghan Hartry, Alejandro Pezzulo, Brad Hamilton, Leah Reznikov, Sarah Horgen, and Theresa Mayhew.

I would like to extend a very special thank you to Geoffrey and Chris McLennan. I got my start as an undergraduate assistant in your laboratory. Thank you.

I would like to extend a very special thank you to David Stoltz. I would also like to extend a special thank you to Stoltz Laboratory members: Andy Michalski, Amit Diwakar, Dan Cook, Keyan Zarei, Linda Powers, Lee Beaumont III, Peter Taft, Maged Awadalla, Drake Bouzek, Michael Rector, and Mal Stroik.

I would like to extend a special thank you to my family, John Adam, Penny Adam, and Katie Bangs. I would like to extend a special thank you to Marissa Decker.

ABSTRACT

Mutations in the gene encoding the cystic fibrosis transmembrane conductance regulator (CFTR) cause cystic fibrosis (CF). Despite affecting many organ systems, the leading cause of death in the CF population is lung disease characterized by accumulation of mucus in the airways, chronic infection, and chronic inflammation. For the current studies we investigated elements of CF lung disease in a porcine model of CF and in people with CF. Our primary analysis tool was chest computed tomography (CT).

Evidence suggests that CF lung disease begins very early in life, likely within weeks of birth. Despite this, early CF lung disease is relatively poorly understood. Because studies in neonates with CF are extremely limited, we investigated early-life CF lung disease in pigs with CF. From prior studies we knew that newborn CF pig lungs lack mucus accumulation, infection, and inflammation at birth, but have a number of congenital airway abnormalities including airway size reduction, irregularly shaped airways, and a massive, irregular tracheal smooth muscle bundle. For the current study we tested two hypotheses: first, that airway growth is abnormal in CF, and second, that lung disease would initiate spontaneously and be apparent on CT within weeks of birth. We tested our hypothesis by comparing three week old non-CF and CF pigs.

We found three week old CF pigs to have proximal airway size reduction, airways of reduced circularity on cross-section, and a large tracheal smooth muscle bundle that is visible on CT. Three week old CF pig airways were less distensible but had a greater coefficient of variation in distensibility. From these data we concluded that airway development is dependent upon CFTR in pigs, and may contribute to lung disease pathogenesis.

On CT, three week old CF pig lung parenchyma was more heterogenous in density than three week old non-CF pigs, especially in the right cephalad lung. The degree of lung tissue heterogeneity in CF pigs correlated with the degree of lung infection, as quantified by the number of bacterial colony forming units. Three week old CF pigs also had significantly more air trapping upon exhalation than non-CF pigs, and the degree of air trapping correlated with the degree of mucus accumulation in the

airways as seen on histology. These data suggest that CF pigs spontaneously develop hallmark features of CF lung disease within weeks of birth, apparent on CT. This study helped set the foundation for future comparative studies involving CF therapeutics, for example, antibiotics and mucolytics.

In adults with CF we performed a before drug, after drug study. The drug was ivacaftor, and it largely restores CFTR function in people with *G551D-CFTR*. We hypothesized that abnormal airway smooth muscle behavior in people with CF, "CF asthma," is, in part, a primary consequence of CFTR disruption. We tested our hypothesis by assaying smooth muscle tone before and after administration of ivacaftor. We limited the time duration to two days. We reasoned two days was long enough for ivacaftor to become effective, but not long enough to reverse long standing lung infection and inflammation, which potentially could independently alter smooth muscle function. The implication being, that observed changes would be primary to CFTR restoration. We observed an increase in airway distensibility as measured from chest CT scans, and a reduction in vascular smooth muscle tone, as measured by pulse wave analysis. Furthermore, the change in airway distensibility correlated with the change in vascular smooth muscle tone. These data suggest that smooth muscle tone is, in part, regulated by CFTR, and that irregular smooth muscle behavior may represent one pathogenic mechanism of CF lung disease.

Many of the people in our two day ivacaftor study returned for follow up after one year of ivacaftor therapy. We hypothesized that radiographic features of lung disease, including bronchiectasis, airway wall thickening, and air trapping, would improve following one year of ivacaftor therapy. We observed no change in total lung capacity, but a reduction in residual volume following one year of ivacaftor therapy. Interestingly, approximately half of this reduction occurred within two days of ivacaftor therapy. These data imply ivacaftor to relieve air trapping, and that a major component of ivacaftor's mechanism to be fast acting. Our airway measurements were confounded by an error in scan reconstruction. Several published findings report airway wall thinning following long term ivacaftor administration (quantified with CT scan scoring systems), while published findings on the long term effects of ivacaftor on bronchiectasis are

mixed. Taken together, these studies of pigs with CF and people with CF, help us understand this disease.

PUBLIC ABSTRACT

Despite affecting many organ systems, the leading cause of morbidity and mortality in the cystic fibrosis (CF) population is lung disease. For the current studies we investigated elements of CF lung disease in a porcine model of CF and in people with CF. Our primary analysis tool was chest computed tomography (CT).

To investigate early CF lung disease we examined three week old CF and non-CF pigs. We found three week old CF pigs to have large, irregular tracheal smooth muscle bundles, airways of reduced size, airways of irregular shape, and airways of abnormal distensibility.

Three week old CF pig lung parenchyma was more heterogenous in density than three week non-CF pigs, especially in the right cephalad lung. The degree of lung tissue heterogeneity in CF pigs correlated with the degree of lung infection. Three week old CF pigs also had significantly more air trapping upon exhalation, evidence of airflow obstruction, than non-CF pigs. The degree of air trapping correlated with the degree of mucus accumulation in the airways. These data show that CF pigs spontaneously develop hallmark features of CF lung disease within weeks of birth, and that abnormal airway growth and development in CF may contribute to lung disease. This study helped set the foundation for future comparative studies involving CF therapeutics, for example, antibiotics and mucolytics.

In adults with CF we performed a before drug, after drug study. The drug was ivacaftor, and it restores the basic underlying defect in a subset of people with CF: impaired function of a particular anion channel. We hypothesized that abnormal airway smooth muscle behavior in people with CF, known as “CF asthma,” is, in part, a primary pathogenic mechanism of CF lung disease. We tested our hypothesis by assaying smooth muscle tone before and after administration of ivacaftor. We limited the time duration to two days. We reasoned two days was long enough for ivacaftor to become effective, but not long enough to reverse long standing lung infection and inflammation which could affect smooth muscle function independently. The implication being, that observed changes would be directly due to restoration of the CF defect. We found evidence

suggesting relaxation of airway and vascular smooth muscle tone. And, the change in airway smooth muscle tone correlated with the change in vascular smooth muscle tone. These data suggest that impaired smooth muscle function is a primary element of CF lung disease.

Many of the people in our two day ivacaftor study returned for follow up after one year of ivacaftor therapy. We hypothesized that radiographic features of lung disease would improve following one year of ivacaftor therapy. We observed no change in lung volume upon inspiration, but a reduction in expiratory lung volume, approximately half of which occurred within two days. Our airway measurements were confounded by errors in scan reconstruction, however, other published studies report airway wall thinning over long term ivacaftor administration. Taken together, these studies of pigs with CF and people with CF, help us understand this disease.

TABLE OF CONTENTS

LIST OF FIGURES

CHAPTER 1: INTRODUCTION AND AIMS

Mutations in the gene encoding the cystic fibrosis transmembrane conductance regulator (CFTR), an anion channel, cause cystic fibrosis (CF). Although CF adversely affects a number of organ systems, the leading cause of morbidity and mortality in the CF population is lung disease. CF lung disease is characterized by chronic infection, chronic inflammation, and mucus accumulation. The life expectancy for a person born today with CF in the U.S. is about 40 years [1].

The manner by which loss of CFTR impairs lung function can be divided into two categories: those primary to loss of CFTR, and those secondary to loss of CFTR. Disease manifestations primary to loss of CFTR are caused directly by loss of CFTR's anion channel function. These represent "root problems" of CF lung disease. An example of a likely primary defect we discovered in the newborn CF pig pertains to bacterial killing [2-3]. Loss of CFTR results in a reduction of bicarbonate secretion resulting in abnormally acidic airway surface liquid. This acidic pH, in turn, impairs the airway's ability to kill bacteria. Abnormally acidic pH illustrates one primary consequence of CFTR disruption, because it was caused directly by loss of CFTR, in this case, loss of bicarbonate secretion.

Primary effects of CFTR disruption lead to secondary consequences. Secondary consequences are not caused *directly* by loss of CFTR. For example, loss of bacterial killing may lead to chronic infection. Chronic infection is not caused directly by loss of CFTR. Thus, infection is a secondary consequence of CFTR disruption. Infection may lead to inflammation and accumulation of airway mucus. In CF, the triumvirate of infection, inflammation, and mucus accumulation form a vicious, self-perpetuating, progressive cycle of lung injury, remodeling, and functional decline.

Identification of primary defects is of great importance, because it may lead to therapeutics that target "root" problems rather secondary manifestations. To date, CF therapeutics have been mostly restricted to treatment of secondary consequences (e.g. antibiotics for infection). This is largely because identification of primary defects is confounded by the presence of secondary defects. The timing of disease onset also poses

a challenge. CF lung disease begins very early in life, likely within weeks or months of birth [4-5]. Thus, the window to identify primary defects prior to the onset of secondary manifestations is extremely small. In short, we poorly understand the origins and events that are important in the pathogenesis of CF lung disease. In the current studies we worked toward illuminating these unknowns.

We had a two pronged approach to studying initiation of CF lung disease: one in pigs with CF, and one in people with CF. For our pig studies, we used a porcine model of CF; pigs that lack CFTR. We then investigated the initiation of CF lung disease mainly through CF to non-CF pig comparisons. In humans, we implemented the converse: *restoration of non-functional* CFTR. In this study we investigated CF lung disease by comparing adults with CF before and after CFTR restoration. We used a recently developed drug, ivacaftor, to restore CFTR function. Ivacaftor is effective, but only for people with the *G551D* mutation of *CFTR* (and some related mutations), about 5% of the CF population.

A major goal of our CF pig project was to characterize early CF lung disease. What do we already know of the CF pig lung phenotype? We know the newborn CF pig lung lacks overt, CF characteristic lung disease. That is, it lacks evidence of mucus accumulation, infection, and inflammation [6-7]. It does, however, have a number of airway congenital abnormalities including airways of irregular size and shape [7-9]. We also know that over months to years the CF pig develops hallmarks of CF lung disease including mucus accumulation, infection, and inflammation [6].

Thus, for the CF pig, we know the beginning, and we know the end. We do not know the "in-between." Understanding this "in-between" period is critical to understanding the transition from relative health at birth, to advanced CF lung disease later in life. Hence, we investigated the CF pig lung phenotype at three weeks of age, an "in-between" time point. Our central analysis tool was the chest CT scan, with augmentation by bacterial analysis, and histology.

In people we performed a before drug, after drug study using ivacaftor in adults with CF with at least one *G551D-CFTR* allele. Based upon airway smooth muscle

abnormalities in people with CF [10-17], and in newborn CF pigs [8, 18], we hypothesized that abnormal airway smooth muscle is a primary consequence of CFTR disruption, and hence, represents one pathogenic mechanism of CF lung disease. We therefore tested smooth muscle tone before and after administration of ivacaftor. Importantly, we limited our study duration to two days. We reasoned that longstanding lung infection and inflammation would minimally change over two days, but CFTR function would. Thus, observed physiological changes would be primary, but unlikely secondary, to CFTR restoration. We assessed smooth muscle tone with chest CT, spirometry, and pulse wave analysis.

When these people began taking ivacaftor, they were in fact beginning ivacaftor for life. Many of the people in the two day ivacaftor study, returned after one year of ivacaftor therapy for chest CT scans and spirometry. From these we sought to characterize the long-term effect of ivacaftor on lung structure and function. Would ivacaftor halt progression of CF lung disease? Would it reverse CF lung disease? Would it have no impact? Observed changes over a one year period would likely represent the summation of changes in primary and secondary consequences of CFTR restoration.

Our central analysis tool for the human and pig studies was the chest CT scan. We used chest CT because it is a common clinical tool, is relatively non-invasive (radiation), and permits quantification of various disease measures in a standardized manner. Collectively, our goal for these studies was to identify radiographic features/correlates of CF lung disease and CFTR-dependent anatomy/physiology in CF pigs and people with CF. Specific aims are detailed below and the experimental design summarized by Figure 1.

Specific Aim 1: Investigate CFTR-dependent lung/airway development and disease in newborn and three week old pigs with CT based tools.

Specific Aim 1a: Does loss of CFTR affect airway growth in CF pigs?

Congenital airway abnormalities may represent an underappreciated aspect of early CF lung disease. Identification and characterization of these congenital abnormalities will elucidate their potential contribution to lung disease. In addition, a number of developing therapeutics, similar to ivacaftor, are designed to target CFTR directly [19-21]. Even if these approaches are successful in restoring CFTR function, because they would be administered postnatally, their effect on congenital airway defects is unclear and probably limited. Thus, developmental airway defects may represent a long term disease manifestation, even after CFTR restoration. For the current study, we hypothesized airway growth in pigs to be CFTR-dependent, and thus, without functional CFTR, CF pigs will have abnormal airway growth. We present the results of this study in Chapter 3.

Specific Aim 1b: What are the early radiographic features of CF lung disease? Do radiographic features of CF lung disease in pigs correlate with infection, inflammation, and histological findings?

There is increasing evidence that CF lung disease begins very early in life [4-7, 22-23]. Despite this, relatively little is known of early CF lung disease. This, in large part, is because studies are extremely difficult to conduct in the neonatal period. A main goal of the "three week old CF pig project" was to characterize early CF lung disease. We hypothesized there to be lung infection, inflammation, and mucus accumulation in three week old CF pigs. We hypothesized three week old CF pigs to have radiological evidence of disease including air trapping, and parenchymal density abnormalities. We hypothesized these radiological abnormalities to correlate with measures of infection, inflammation, and mucus accumulation. This study helped establish the "normal progression" of early CF lung disease. We present the results of this study in Chapter 4.

Specific Aim 2: Investigate the effects of acute CFTR restoration on human CF airway disease.

Specific Aim 2a: Does two days of ivacaftor treatment improve pulmonary function?

Ivacaftor is a bioavailable, small molecule that induces a conformational change in G551D-CFTR (a specific mutation of CFTR). This conformational change, in effect, greatly increases CFTR function [24-25]. Early trials of ivacaftor in people with *G551D-CFTR* indicate a rapid and sustained improvement in pulmonary function [26-31]. Ivacaftor is the first therapeutic that targets the underlying CFTR defect, rather than treat symptoms of its disruption.

We performed a before ivacaftor-after ivacaftor study over a two day time interval. This abbreviated time window was designed to minimize changes in airway mucus accumulation, lung infection, and lung inflammation. Ivacaftor is estimated to reach blood serum steady state levels in three to five days [32], and there was no published data over a two day time interval. Hence, we did not know if ivacaftor would be efficacious over only two days. We hypothesized that it would. We tested this hypothesis by obtaining spirometry and measuring sweat chloride concentration (a biomarker of CFTR function) before and after ivacaftor. We present the results of this study in Chapter 5.

Specific Aim 2b: Does CFTR potentiation affect smooth muscle function?

Given airway smooth muscle abnormalities in people with CF, and the newborn CF pig, we hypothesized that abnormal airway smooth muscle function in people with CF, including evidence of increased tone, was caused, at least in part, directly from CFTR impairment. Based upon this, we hypothesized ivacaftor to have a smooth muscle relaxing effect. We tested for smooth muscle tone with spirometry before and after bronchodilator, with airway measurements obtained from chest CT scans, and from pulse wave analysis, a method used to assay vascular smooth muscle tone. Importantly, we reasoned that alterations in longstanding infection and inflammation would be minimal over only two days, thus observed changes would likely reflect augmentation of CFTR function. If loss of CFTR function directly impacts smooth muscle behavior, it follows that abnormal smooth muscle behavior is a primary pathogenic mechanism of CF lung disease. Twelve people were in this study. We present the results in Chapter 5.

Specific Aim 3: Investigate the effects of long term (~one year) CFTR restoration on human CF airway disease.

Seven of the twelve people who participated in the two day study returned for chest CT scans after one year of ivacaftor therapy. The effect of ivacaftor on lung structure and function over a one year interval is not well described. We hypothesized that long term administration of ivacaftor would limit progression, if not reverse, aspects of CF lung disease. This study will enable us to compare lung structure and function from three time points: baseline, after two days of ivacaftor therapy, and after one year of ivacaftor therapy. We present the results of this study in Chapter 6.

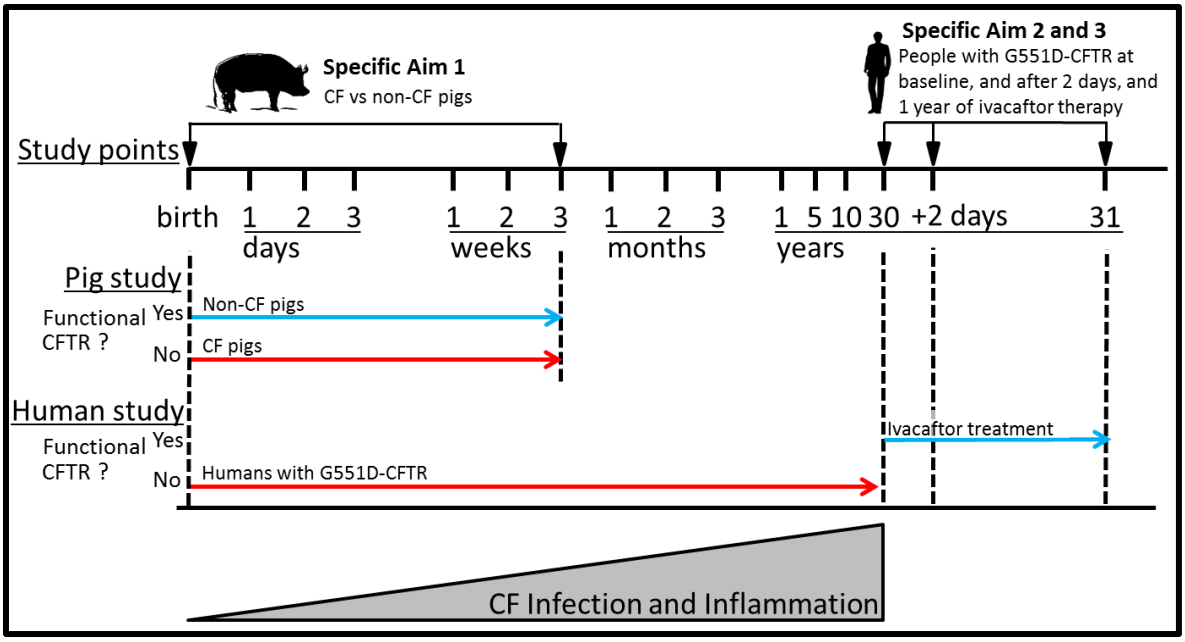

Figure 1. Study designs. We examined non-CF and CF pigs at birth, prior to the onset of airway mucus accumulation, infection, and inflammation, and at the three week time point, when airway mucus accumulation, infection, and inflammation are likely present. In adults with CF, we performed a before ivacaftor, after ivacaftor study over a two day time interval. The abbreviated time interval was designed to limit changes in airway mucus accumulation, infection, and inflammation. With these "secondary" manifestations held constant, we could infer that observed changes were likely caused directly by CFTR restoration. In addition, we examined these adults one year after initiation of ivacaftor therapy. Changes at this time point could reflect changes both primary and secondary to CFTR restoration.

CHAPTER 2: BACKGROUND INFORMATION

A brief background section was included to provide information of topics relevant to the presented work. This includes general background about CF and the CF pig. This chapter also includes description of several experimental techniques used to complete these studies such as sweat chloride concentration, chest CT, spirometry, and pulse wave analysis. Additional background is provided on an as-needed basis in other chapters.

2.1. CYSTIC FIBROSIS

CF is caused by mutations in the gene encoding CFTR, a protein that channels anions including chloride and bicarbonate. Lack of CFTR function results in ion and water imbalances at the cellular level. These imbalances, in turn, adversely affect a number of organ systems (Figure 2).

At the gastrointestinal level, approximately 10% of newborns with CF have meconium ileus, a life-threatening condition in which newborns fail to pass their first stool [33-36]. In the pancreas, duct obstruction impairs secretion of digestive enzymes, often leading to pancreatitis, and contributing to malnutrition [37]. Nutrition is further impaired in people with CF due to abnormally acidic intestinal pH [30]. CF affects the reproductive tract of women and men with CF. Reduced fertility occurs in women with CF, in part, because of abnormal cervical mucus, and over 90% of men with CF are sterile due to congenital bilateral absence of the vas deferens [38-40]. In addition, sweat concentration of sodium and chloride is elevated. The "salty sweat" phenotype is relatively benign, but is used extensively diagnostically [41].

Although affecting many organ systems, the leading cause of morbidity and mortality in the CF population is progressive lung disease, often most pronounced in the upper lobes [42-43]. One hallmark of CF lung disease is abnormal airway mucus. In a healthy lung, the airways are lined with mucus. This mucus provides a protective layer to the epithelial surface and entraps inhaled particulate and bacteria. In health, the airway

mucus is continually cleared from the airways through the action of mucociliary clearance. In CF, airway mucus is abnormal. CF airway mucus is commonly excessive in volume, tenacious, and mucopurulent [38]. This abnormal mucus impairs mucociliary clearance and accumulates in airways often resulting in partial or complete obstruction (Figure 3). A study by Rowe *et al.* illustrates abnormal mucus behavior in CF. They found CFTR potentiation (augmentation of CFTR function) to improve mucociliary clearance and lung function in adults with CF [30]. These results suggest that 1) CFTR maintains airway mucus homeostasis, and 2) that abnormal mucus in CF impairs lung function [30].

Static and abnormal airway mucus predisposes individuals with CF to bacterial infection, another hallmark of CF lung disease. Lung infection begins early in life for people with CF and is often chronic in nature. For example, Kerem *et al.* reports 10% of people with CF to have chronic lung infection by *Pseudomonas aeruginosa* at age 6 and approximately 55% by age 25 [44]. Although people with CF may be infected with an array of bacteria, *P. aeruginosa* is among the most prevalent, and for a number of reasons, among the most damaging. First, *P. aeruginosa* itself elicits an injurious inflammatory response. Second, *P. aeruginosa* through the release of toxins, may damage the host independent of inflammation. Third, *P. aeruginosa* spontaneously forms biofilms. These biofilms shelter the bacteria from antibiotics and innate defense [45-46]. Chronic lung infection, by *P. aeruginosa* and by other bacteria, is a major component of CF lung disease.

Chronic lung infection contributes to chronic lung inflammation in people with CF. CF lung inflammation also commonly begins early in life. For example, in 1997 Armstrong *et al.* discovered elevated inflammatory markers on bronchoalveolar lavage in infants (~ 3 months old) with CF including elevated neutrophil counts, IL-8, and neutrophil elastase [23]. While inflammation is an important component of the immune system, imbalanced or protracted lung inflammation may result in irreversible tissue damage. For example, neutrophil elastase is associated with bronchiectasis and airway dilatation in people with CF [4]. Airway remodeling in response to inflammation impairs lung function, is often irreversible, and may include wall thickening, dilatation, cyst

formation, and more [38, 47]. Inflammatory tissue damage often results in reduced lung function in people with CF.

Abnormal airway smooth muscle behavior is also a common feature of CF lung disease and is referred to as "CF asthma [13]." Airway hyper-responsiveness, the excessive narrowing of airways in response to a stimuli [48], is present in an estimated 40-60% of adults with CF [49-50]. Moreover, the presence of bronchodilator reversible airway obstruction in people with CF suggests increased basal airway smooth muscle tone [51]. Narrowed airways increase the work of breathing by increasing resistance to airflow.

In summary, although CF adversely affects many organ systems, the leading cause of morbidity and mortality in the CF population is lung disease. CF lung disease begins early in life and is characterized by a vicious cycle of infection, inflammation, airway hyper-reactivity, remodeling, and mucus buildup. Collectively, these result in functional decline. The life expectancy of someone born today with CF in the U.S. is about 40 years [1].

2.2 THE CYSTIC FIBROSIS PIG

Our lab generated a porcine model of CF [52-53]. CF pig gastrointestinal pathology resembles that of humans with CF [54]. *CFTR-/-* pigs experience meconium ileus, pancreatic duct obstruction, micro-gallbladder, and congenital absence of the vas deferens in males [54]. We are unable to compare *CFTR-/-* pig sweat chloride to humans with CF because pigs lack sweat glands anatomically [53].

What is the CF pig's lung phenotype? At birth, the CF pig lacks lung infection, inflammation, and airway mucus accumulation [6]. However, despite this, the newborn CF pig lung is not normal. On the anatomical level, it has a trachea of reduced caliber and irregular shape [8]. The tracheal size reduction extends into the proximal, but not distal airways [7]. The newborn CF pig also exhibits a number of functional deficits. First, newborn CF pig tracheal airway smooth muscle exhibits irregular contractile behavior, including evidence of increased basal tone [18]. Second, the newborn CF pig lacks

bacterial infection, but does exhibit an impaired ability to kill bacteria [2-3, 6]. This impairment has been tied to abnormally acidic airway surface liquid pH [2-3]. Third, the newborn pig lacks accumulation of mucus in the airway, but does exhibit abnormal mucus behavior. Submucosal glands secret mucus onto the airway surface. Once there, the mucus helps to entrap particulate before ultimately being expelled by the action of mucociliary clearance. CF animal submucosal glands secret mucus as non-CF animals do, but once secreted, the CF mucus strands fail to efficiently detach from the gland, resulting in impaired mucociliary clearance [55-56]. Fourth, acidic pH increases the viscosity of airway surface liquid in newborn CF pigs [57].

Although the newborn CF pig lacks overt signs of lung disease, it has several functional deficits that, in effect, set it up to develop lung disease over time. Evidence of disease in months old CF pigs include classic signs of human CF lung disease [6, 58]. These include accumulation of airway mucus, that at times, results in complete airway obstruction (Figure 4). Evidence of lung disease on chest CT includes airway wall thickening and parenchymal consolidation with the right upper lung zone often showing the most involvement (Figure 5) [6]. Infection occurs with an array of bacteria, suggesting a host vulnerability to a wide assortment of bacteria. The CF pig recapitulates many aspects of human CF lung disease.

2.3 SPIROMETRY

Perhaps the most commonly used method of assessing lung function in people is spirometry. To obtain spirometry, one must perform breathing maneuvers through a specialized mouthpiece known as a spirometer. The spirometer converts the subject's breathing maneuvers into volume-time curves, or flow-volume loops, referred to as spirograms (Figure 5). Spirograms provide various measures of lung volume and function. We acquired spirometry from the people who participated in our ivacaftor project. (We did not perform spirometry on our pigs.)

Spirometers can obtain a number of lung volume measurements (Figure 5). Tidal volume (TV) is the volume of gas that is inhaled or exhaled during normal, quiet breathing at rest. Lung volume at the end of tidal exhalation is functional residual capacity (FRC). Total lung capacity (TLC) is the lung volume after a maximal inspiration. Inspiratory reserve volume (IRV) is the difference between TLC and the peak of tidal volume. The lung volume after a maximal expiration is known as the residual volume (RV), and the difference between TLC and RV is vital capacity (VC). The difference between FRC and RV is the expiratory reserve volume (ERV). It should be noted that spirometry can measure changes in volumes but not absolute lung volumes. Consequently, neither TLC, FRC, or RV can be measured using spirometry. RV can be measured by volume analysis of CT scans, body plethysmography, and other methods, and once known, can be used to calculate FRC and TLC using other spirometric measures (e.g. RV + VC = TLC) [59].

Changes in specific lung volumes are associated with specific pulmonary functional deficits. For example, air trapping is the excessive retention of air upon exhalation, and as such, results in an elevated RV, elevated FRC, but not necessarily an elevated TLC. Consequently, VC is reduced. In contrast, hyperinflation is associated with elevated TLC, and an elevated RV, while VC is relatively unaffected [48].

A dynamic spirometric measure relevant to this work is forced expiratory volume in 1 second (FEV_1). FEV_1 is the volume of air (liters) that can be forcibly exhaled from TLC in 1 second (Figure 5). FEV_1 is measured in liters, but is commonly converted from liters to "% of predicted" after normalization by height, age, race, and gender. FEV_1% predicted is often regarded as a "whole lung average" assessment of lung function. An FEV_1 of 80% predicted or greater is considered relatively normal, while an FEV_1 below 80% of predicted may indicate lung disease. To illustrate, the FEV_1% of predicted at baseline (before ivacaftor treatment) for the adults with CF in our ivacaftor study ranged from the 34% (severe disease) to 101% (relatively healthy) [60].

Another dynamic spirometric measure relevant to this work is FEF_{25-75}. FEF_{25-75} is the average flow rate (L/s) between the 25th and 75th percentile of a forced expiratory maneuver from TLC (Figure 5). FEF_{25-75} is regarded as a measure of small and medium

airway obstruction [48], and like FEV_1, is often expressed as % of predicted. To illustrate, the FEF_{25-75} % of predicted at baseline for the adults with CF in our ivacaftor study ranged from 9% (severely impaired function) to 69% (comparatively better function) [60].

2.4 CHEST CT SCANS AND MEASUREMENT

CT scanners obtain X-ray radiographs from a number of different angles, and then use computer algorithms to reconstruct the information from the X-rays into a stack of cross-sectional images. In contrast to conventional X-ray radiographs where the three-dimensional anatomy is projected onto a two-dimensional image resulting in superimposition of anatomy, CT scans produce a volumetric image where each "slice" within the scan is a two-dimensional image that represents a two-dimensional cross-section of anatomy with no superimposition [61].

CT images are grayscale, where the voxel intensity is typically in Hounsfield Units (HU). HU is a measure of radiodensity, or the ability of a material to absorb X-ray photons. The HU scale is standardized such that the same material should have the same HU (or close to it) across scanners and between scanning centers. Lower HU values appear relatively dark on CT and correspond to materials with little ability to absorb X-ray photons (radiolucent). High HU values, appear relatively bright on CT, and correspond to materials that efficiently absorb X-ray photons (radiodense).

Generally, there is correspondence between radio and physical density (mass/volume), such that materials of high physical density also have high radiodensity, and vice-versa [62-64]. For example, air, of relatively little radio and physical density, has an HU of -1000. In contrast, water, of greater radio and physical density, has an HU of 0. Blood has an HU of approximately 30, bone may range from 500 to 3000 HU. The lung, largely composed of air and blood, generally ranges in HU from -1000 to 30. Figure 6 illustrates various HU values in a pig chest CT scan slice.

CT scans are a common means by which to assess lung structure and function. In the current studies we assessed lung density profiles through HU histogram analysis. A

lung HU histogram, as the name suggests, is simply a histogram of the lung HU values from CT. HU is a measure of radiodensity, but because of the correspondence between radio and physical density, HU histograms may be used to assess lung density profiles. For example, the lung density profile naturally changes through the course of breathing. The lung is generally less dense upon inspiration than upon expiration, largely on account of changes in lung gas volume. Differences between inspiratory and expiratory lung HU histograms reflect respective differences in lung density (Figure 7).

Disease may alter the lung density profile. For example, emphysematous parenchymal destruction reduces lung density, and consequently would likely result in a leftward shift in the lung HU histogram [65-66]. In contrast, fluid accumulation in ARDS, would make the lung relatively more dense, causing a rightward shift of the HU curve [67-68]. In addition, general lung infection and infiltration may lead to neutrophilic infiltration, consolidation, and alveolar flooding, all of which could increase lung density. Histogram statistics (e.g. mean HU, mode HU, etc.) may be used to compare two histograms (e.g. non-CF vs. CF) against each other statistically.

Airway measurements can also be obtained from lung CT scans. We collected airway measurements for the current studies primarily using VIDA Diagnostic's Apollo Software. It produces a wide array of airway measurements. The ones we report in the current studies include airway lumen cross-sectional area, airway diameter, airway wall thickness, and airway circularity. Airway circularity is a unitless 2D shape descriptor that ranges in value from 0 (not at all circular) to 1 (a perfect circle). We are interested in it because newborn CF pigs have reduced airway circularity compared to non-CF controls [8]. Mathematically, circularity = $4\pi A/P^2$, where A = lumen area, and P = lumen perimeter. Apollo does not directly produce a measure of airway circularity, but it does produce measures of lumen perimeter and lumen cross-sectional area, which can be used to calculate lumen circularity. The Apollo measurements we used were obtained perpendicular to the airway lumen tree centerline. These measurements represented the average of a number of measurement samples over the airway segment's middle third.

2.5 SWEAT CHLORIDE CONCENTRATION

People with CF have elevated sweat sodium and chloride concentration. The mechanism behind increased sweat salt concentration in CF is well understood. The sweat duct interstitium naturally reabsorbs both sodium and chloride from the sweat gland duct. Without functional CFTR, reabsorption of chloride is impaired, and as a consequence, sodium is also poorly reabsorbed (Figure 8) [38]. In contrast to other ducts in people with CF, sweat gland ducts do not become obstructed, inflamed, or pathological aside from elevated sodium and chloride concentration. However, people with CF are more vulnerable to salt depletion, particularly during strenuous exercise or in hot weather.

For decades, the "sweat test" has been a gold standard, diagnostic test for CF. The diagnostic threshold of sweat chloride concentration for CF is 60 mmol/L. Sweat chloride concentration in people without CF is generally between 10 and 30 mmol/L [69]. The average baseline sweat chloride concentration of the adults with CF in our ivacaftor study was 94 mmol/L [60]. As previously mentioned, pigs lack sweat glands anatomically.

2.6 PULSE WAVE ANALYSIS

Pulse wave analysis, also known as applanation tonometry, is the assessment of arterial blood pressure waveforms, a relatively non-invasive means to measure many aspects of cardiovascular health (Figure 9) [70-71]. We used it to assess arterial stiffness in adults with CF before and after ivacaftor therapy. One modulator of vascular stiffness is smooth muscle tone [72]. We hypothesized ivacaftor to relax smooth muscle tone, and thus we expected a reduction in arterial stiffness.

We obtained two measurements. The first was pulse wave velocity. This is simply the propagation velocity (m/s) of the blood pressure pulse through the vasculature. The second was augmentation index (AIx). The blood pressure pulse emanates from the heart and is directed toward the distal arteries. Part of the blood pressure pulse is

reflected in a retrograde fashion through the vasculature. This reflected pressure augments systolic blood pressure. AIx measures the magnitude of this reflection. Vascular stiffening leads to increased pulse wave velocity and increased AIx. We have not adapted pulse wave analysis for use on pigs.

An experiment by Wilkinson *et al.* provided proof of concept for the pulse wave analysis portion of our ivacaftor project [72]. Nitric oxide (NO) is naturally produced by vascular endothelium and results in vascular smooth muscle relaxation. Wilkinson *et al.* showed that pharmacologic inhibition of NO synthase results in a dose dependent increase in vascular stiffness, as measured by AIx (pulse wave velocity not reported) [72]. In short, they pharmacologically increased smooth muscle tone and observed an increase in AIx. In our ivacaftor study we hypothesized the converse, that a reduction in vascular tone, through administration of ivacaftor, would decrease pulse wave velocity and AIx.

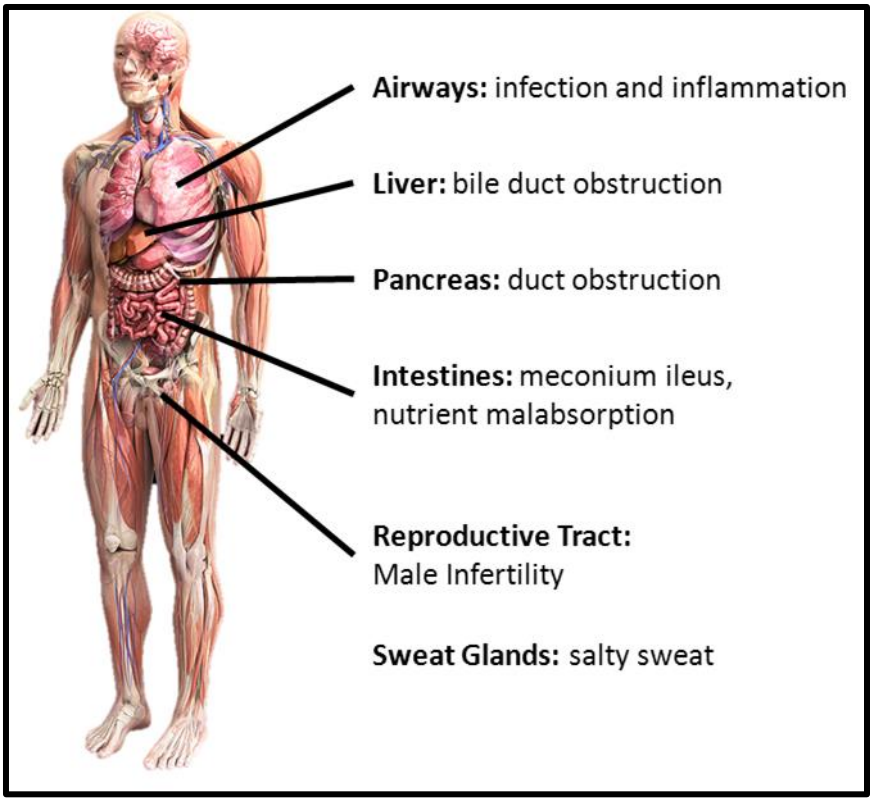

Figure 2. Cystic fibrosis affects many organ systems. Adapted from [41].

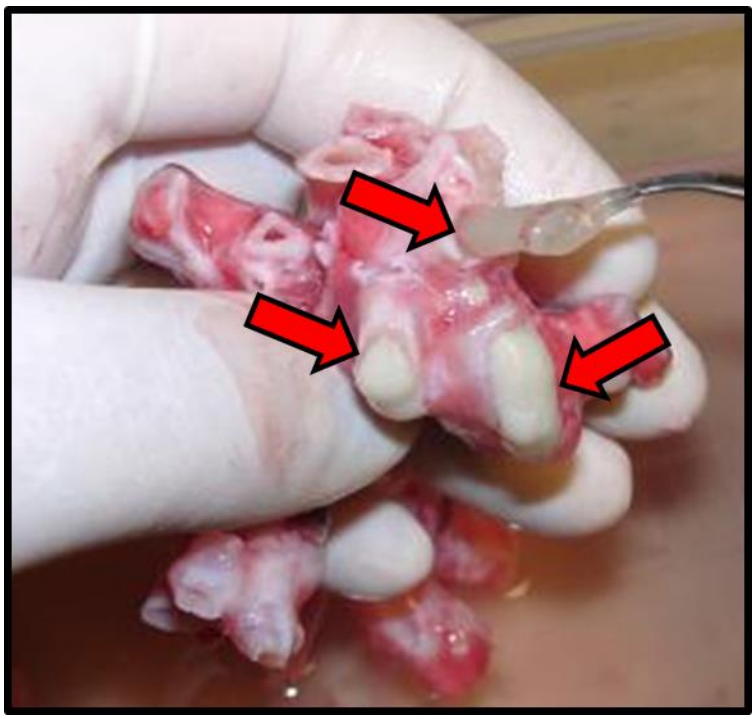

Figure 3. A freshly excised sample from a human CF lung explant. Accumulation of mucus may result in complete obstruction, even in relatively large airways (arrows). Photo obtained by the Laboratory of Jeffrey Wine.

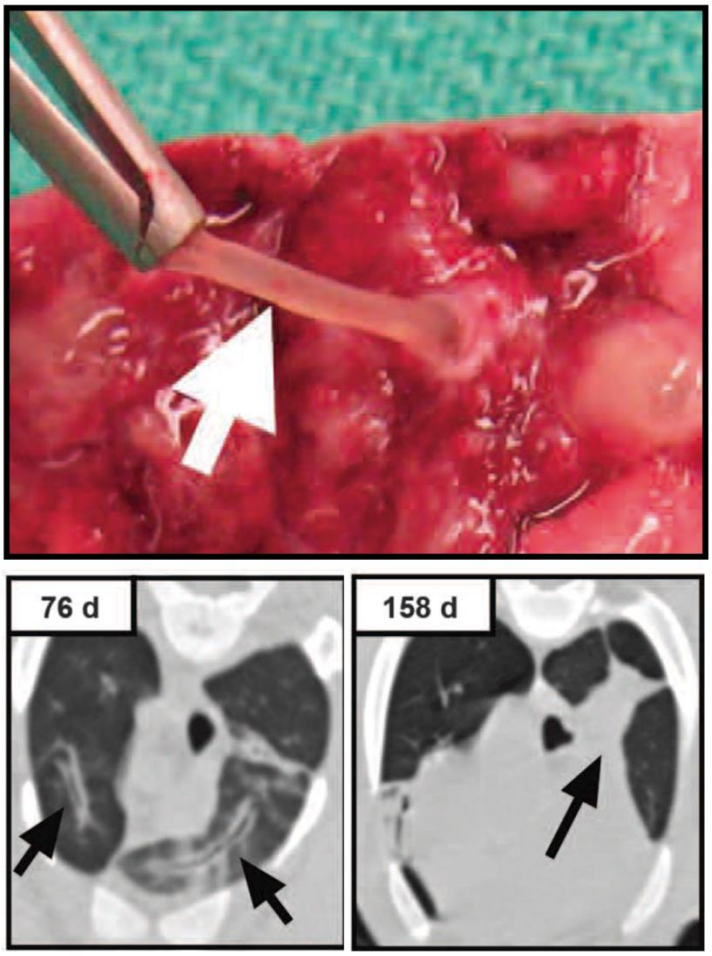

Figure 4. Lung disease in CF pigs that are months old. (Top) Tenacious mucus that completely obstructs an airway and maintains its shape when pulled with forceps. (Lower Left) Transverse CT scan slice. Arrows highlight airway wall thickening. (Bottom right) Transverse plane chest CT slice. Arrow highlights consolidation. Images adapted from [6].

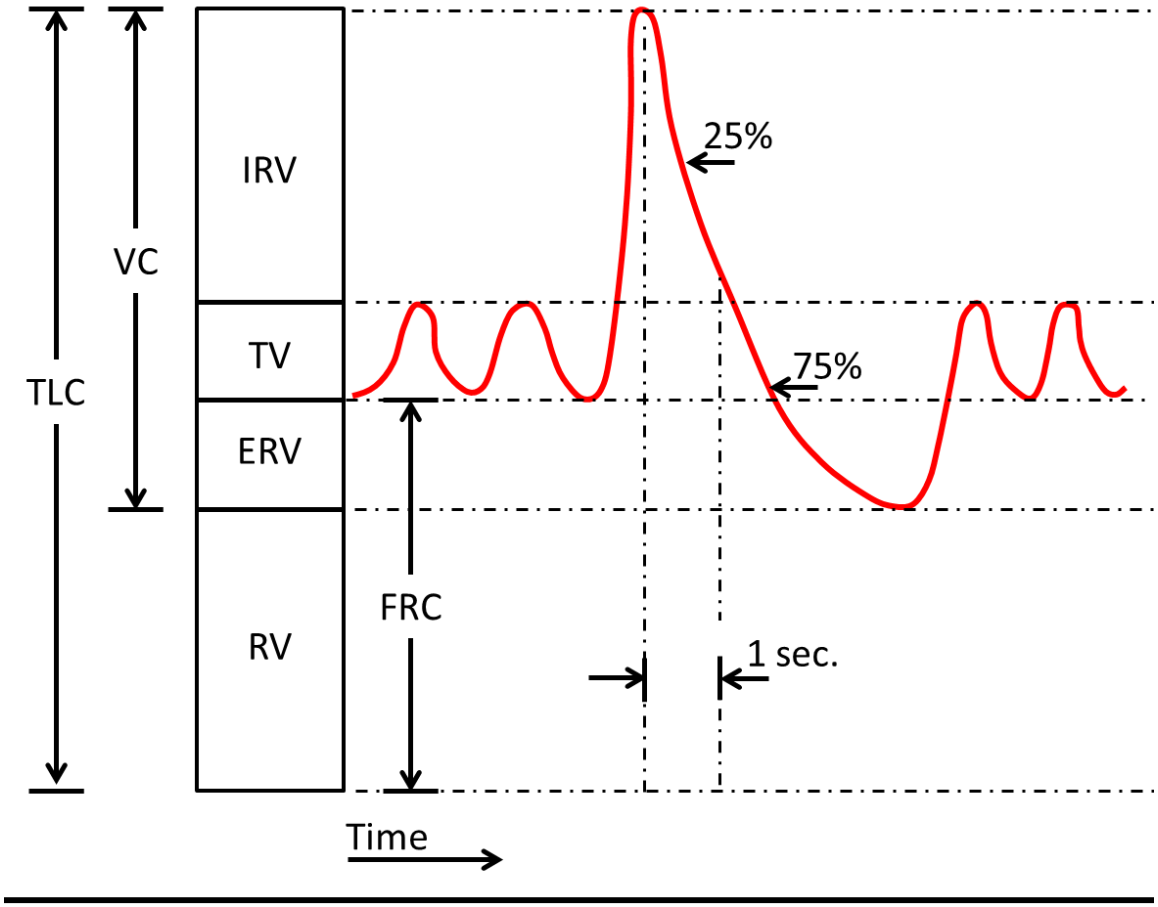

Figure 5. Spirogram tracing. Y-axis is volume. X-axis is time. FEV_1 is the volume that can be forcibly exhaled from a maximal deep inspiration. FEF_{25-75} is the flow rate (L/s) between 25% and 75% of vital capacity (VC) during this forcible exhalation. TLC = total lung capacity. IRV = inspiratory reserve volume. TV = tidal volume. ERV = expiratory reserve volume. RV = residual volume. FRC = functional residual capacity.

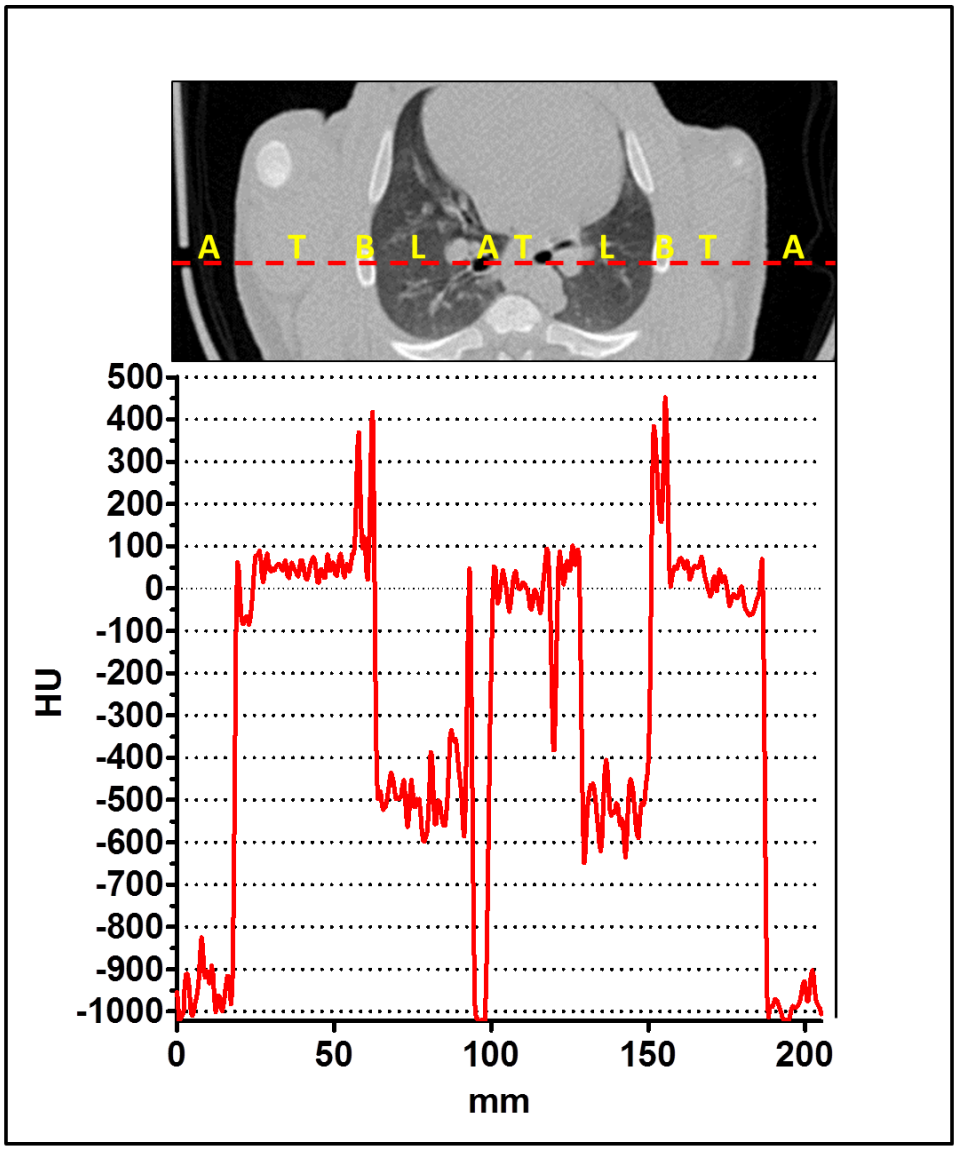

Figure 6. HU profile. A slice from a pig chest CT scan. The HU values along the dashed line are shown in the below graph. The CT slice and graph spatially correspond. Consequently, the HU for a specific point in the CT slice is located directly below it in the graph. The letters denote various tissues or air. T = general body tissue, B = bone, and L = lung, A = air.

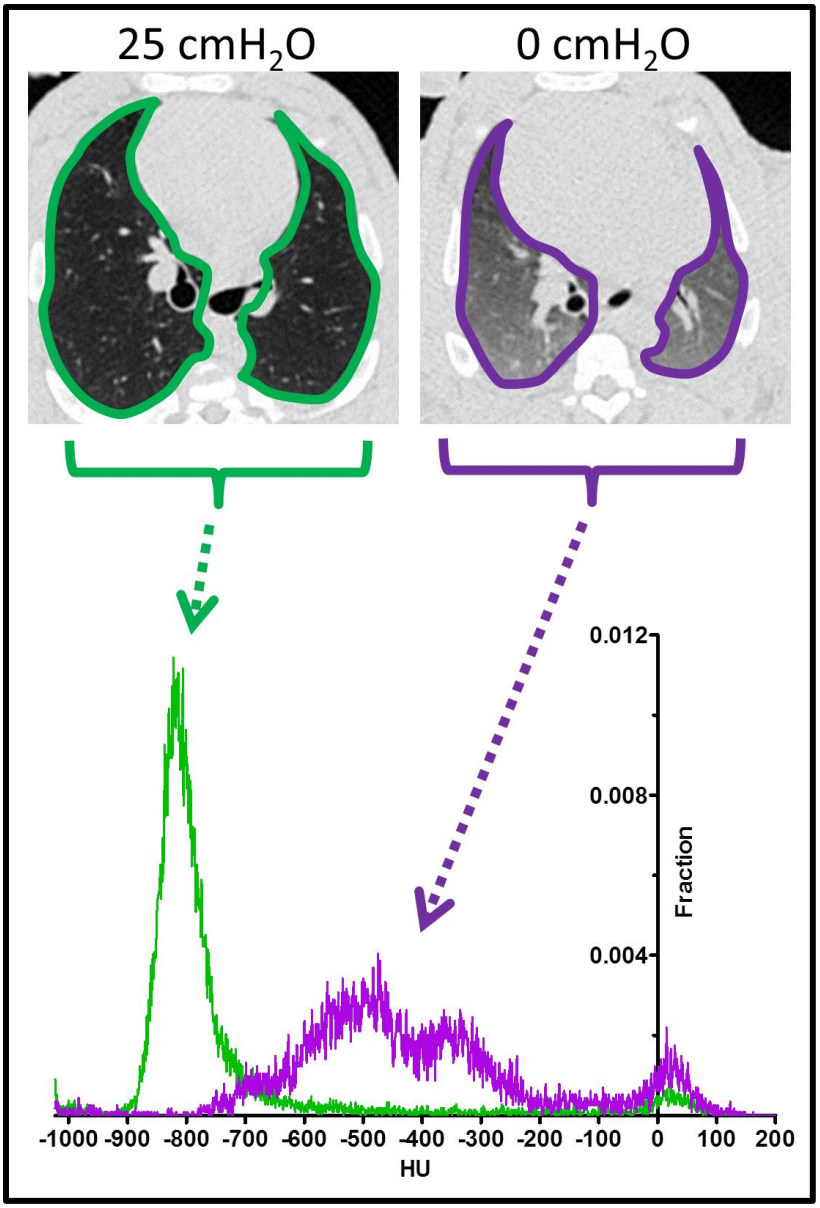

Figure 7. Lung HU histograms. Slices from a pig chest CT scan obtained at a pressure of 25 cmH_2O (top left) and 0 cmH_2O (top right). The lungs have been outlined from each scan slice, and their respective HU histograms are shown below. The lung at 25 cmH_2O is filled with air, appears relatively dark visually, and is largely made up of low valued HUs. In contrast, the 0 cmH_2O has less air, appears brighter visually, and its curve is rightward shifted relative to the 25 cmH_2O curve.

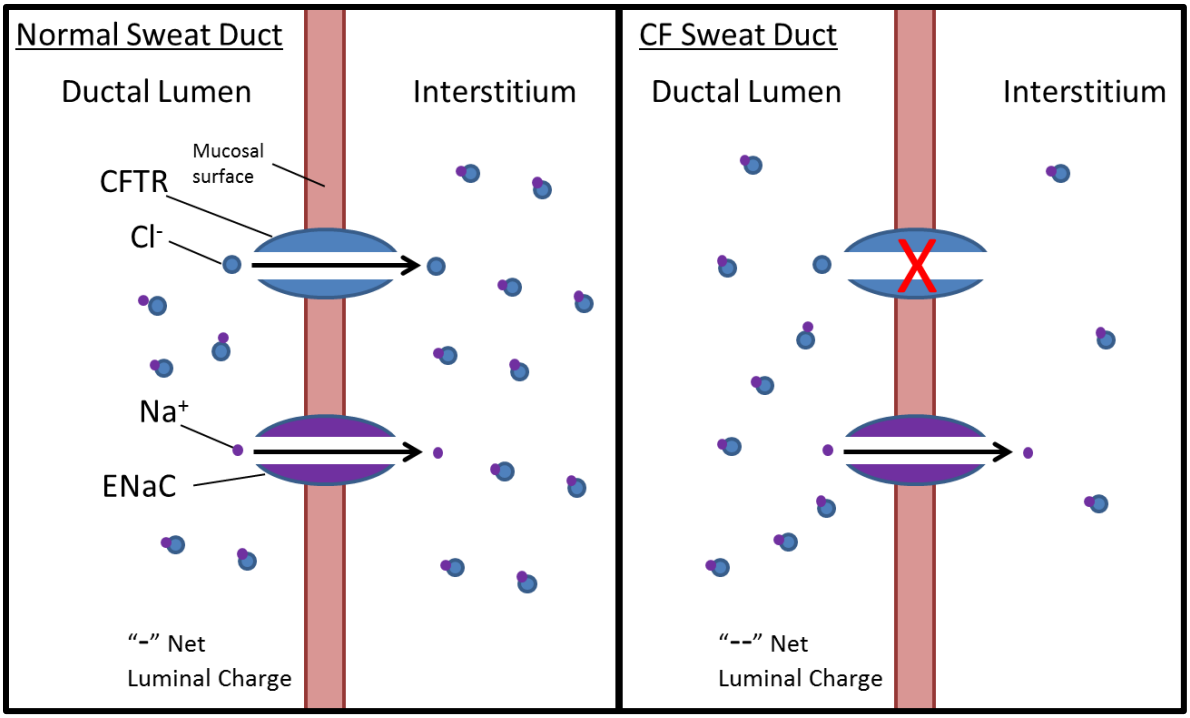

Figure 8. People with CF have salty sweat. In the normal sweat duct (left), functional CFTR and epithelial sodium channel (ENaC) permit reabsorption of chloride and sodium from the sweat ductal lumen into the interstitium. Without CFTR (right), reabsorption of chloride is largely inhibited. This alters the electrochemical gradient across the mucosal surface, impairing sodium reabsorption, resulting in salty sweat. Figure based upon one from Rowe *et al.* [38].

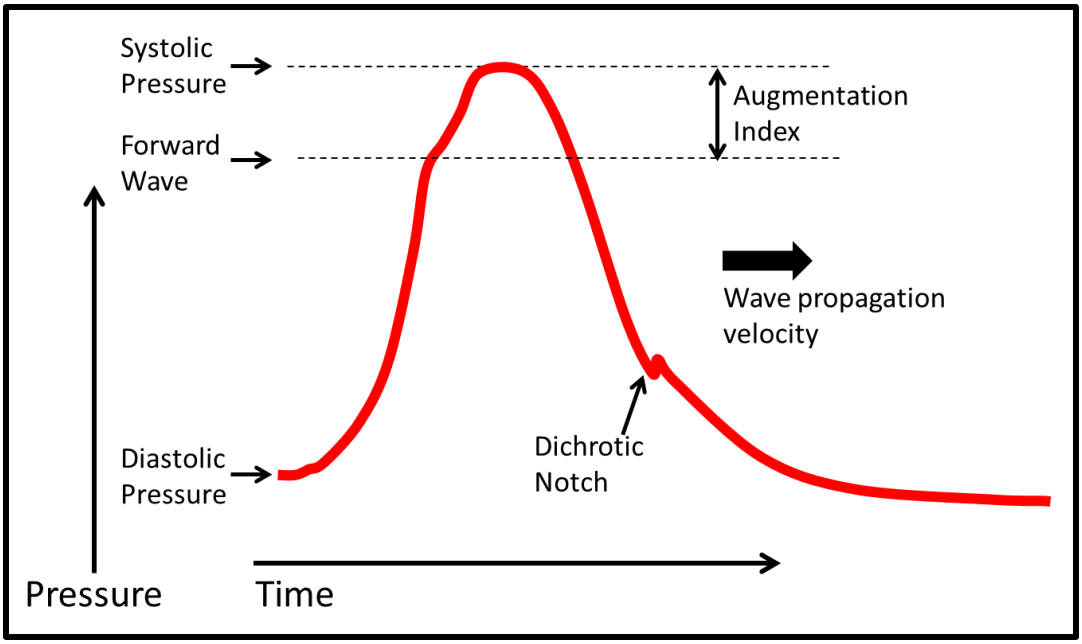

Figure 9. Pulse wave analysis. Pulse wave analysis is the assessment of arterial blood pressure pulses. We focused on two measurements. The first was pulse wave velocity. This is the propagation speed of the blood pressure pulse, measured in m/s. The second was augmentation index (AIx). The pressure pulse propagates from the heart through the arteries. Part of this wave is reflected back from the vasculature, and augments systolic pressure. The AIx measures the magnitude of this reflection. Pulse wave velocity and AIx are each a measure of vascular stiffness, where increased stiffness results in greater pulse wave velocity and a greater AIx.

CHAPTER 3: ABNORMAL AIRWAY GROWTH IN CF PIGS

3.1 INTRODUCTION

There is increasing evidence of abnormal lung structure and function in infants and children with CF. For example, anatomically, a retrospective analysis revealed infants with CF to have tracheas of reduced caliber [8]. In addition, children with CF are shown to have tracheas of reduced circularity on cross-sectional imaging [8], increased airway smooth muscle mass on biopsy [11], and to collapse (tracheomalacia) at over ten times the rate of the general population [73-74]. Functionally, as many as two of three infants with CF have air trapping on CT, a sign of obstruction to airflow [5].

The newborn CF pig lung phenotype has much in common with the early-life phenotype of people with CF. Anatomically, newborn CF pigs have tracheas of reduced size and circularity [8], and evidence of increased smooth muscle mass in the form of large, longitudinally oriented tracheal smooth muscle bundles [8]. Functionally, newborn CF pigs have increased resistance to airflow, and air trapping upon exhalation [7].

Based upon these observations, we hypothesized airway and lung growth to be abnormal in CF pigs. We tested our hypothesis by examining the airways and lungs in three week old non-CF and CF pigs, primarily using CT imaging. We chose chest CT as our primary analysis tool, because it is relatively non-invasive (radiation), permits quantitative morphological assessment, and is a common clinical tool.

This study will be informative in a number of ways. First, establishing and identifying abnormal airway structure is a prerequisite for determining the potential contribution of abnormal growth and development to functional deficits. Second, this study will help establish a basis of comparison for future CF pig studies involving therapeutics, challenges, and manipulations (e.g. CFTR modulators), many of which would be impossible to perform on people with CF. Lastly, this study will inform upon the early-life phenotype of people with CF. Significantly, this period is very difficult to study in people, yet likely represents the age at which CF lung disease begins.

3.2 METHODS

CT Scan Acquisition and Analysis

The CT scans of the newborn CF and non-CF pigs used in the current study were retrospectively analyzed from a prior study [7]. The three week old non-CF and CF animals studied for the current study were prospectively imaged with the same CT scanning protocol as the newborn CF and non-CF pigs [7]. In brief, animals were anesthetized, paralyzed, and underwent a tracheostomy. A lung recruitment maneuver was performed prior to scanning. Two scans were acquired per animal. The first was at an airway pressure of 25 cmH_2O (inspiratory). This scan was followed by a scan acquired at an airway pressure of 0 cmH_2O (expiratory). Scan specs were as follows: 190 mA, 120 KeV, 0.28 s of exposure time, slice thickness of 0.6 mm, slice spacing of 0.3 mm, and a pitch of one [7].

The chest CT scan of the 347 day old CF pig followed a different protocol. This animal was anesthetized and then scanned while spontaneously breathing. This animal was not paralyzed and did not undergo a tracheostomy.

Airway and lung measurements were obtained using VIDA Diagnostic's Apollo Software. Measurements obtained from Apollo for the current study included lung volume, airway wall thickness, airway lumen area, inner airway circularity (circularity of inner airway wall), outer airway circularity (circularity of outer airway wall), and airway distensibility. We calculated airway distensibility based upon matched airway measurements of inspiratory and expiratory chest CT scans. We defined distensibility as follows: 100*[(insp. airway lumen area – exp. airway lumen area)/exp. airway lumen area)]. Airway distensibility coefficient of variation was calculated for each airway segment of the left and right main bronchus that was visible on both the inspiratory and expiratory chest CT scans. Airway distensibility was calculated on a per animal average basis as follows: STDEV(X)/AVG(X), where X equals all of measured bronchial airway segment's distensibility within an animal.

Tracheal Smooth Muscle Bundle Scoring

Three genotype blinded reviewers scored inspiratory pig CT scans for the presence of tracheal smooth muscle bundles. Scans of newborn non-CF and CF as well as scans of three week old non-CF and CF animals were scored. For scoring purposes, a bundle was defined as a protuberance into the airway lumen space. The presence of a bundle was indicated by a positive score from at least two of the three reviewers. If a bundle was observed, the bundle width was measured in ImageJ with the tape-measure tool, and the circumferential location within the trachea was recorded, where the anterior aspect of the trachea was 0^0, the right 90^0, the posterior 180^0, and the left 270^0. When "Average Bundle Angle" is reported, this represents the average bundle angle across all four scored locations, across all scorers. "Average Bundle Width" was similarly calculated.

Histopathology

One newborn non-CF and CF trachea were fixed in 10% neutral buffered formalin. Ten histological sections were prepared from each trachea. Staining was with hematoxylin and eosin. The histology was prepared by the laboratory of Dr. David Meyerholz.

3.3 RESULTS

Trachea Size and Shape

The newborn CF pig has a trachea of reduced caliber and circularity, despite having normal lung volume [7-8]. We asked if this phenotype persisted through three weeks of age. Three week old CF pigs weighed less than three week old non-CF pigs.

Consequently, we report our findings after body mass normalization. All airway and lung measurements were performed at an airway pressure of 25 cmH_2O unless otherwise noted. Despite no difference in lung volume, three week old CF pigs had tracheas of reduced cross-sectional area, (Figure 10A-E). There was no significant difference between genotypes in average tracheal wall thickness (Figure 10F), but CF pigs did have reduced inner circularity (Figure 10G).

Tracheal Smooth Muscle Bundles on CT

Our research group previously discovered the presence of a large, longitudinally oriented, tracheal airway smooth muscle bundle in newborn CF pigs that at times protrudes into the luminal airspace [8]. There is no evidence of these bundles in newborn non-CF pigs [8]. Based upon these observations we formed two hypotheses. First, that three week old CF pigs would also have these bundles. Second, that the bundles would be visible on CT in both newborn and three week old CF pigs.

To test these hypotheses we had genotype blinded reviewers score CT scans for the presence of bundles. Chest CT scans from newborn non-CF, newborn CF, three week old non-CF, and three week old CF pigs were scored. If observed, bundle width and circumferential angle of location within the trachea were measured. We assessed CT scans for the presence of bundles at four tracheal locations based upon anatomical landmarks. These four locations included: just above the tracheal bronchus, just below the tracheal bronchus, halfway between the tracheal bronchus and the carina, and just above the carina. The tracheal bronchus is an airway pigs have but humans do not. It branches directly off of the trachea proximal to the carina and is the central airway of the pig's tracheal lobe (porcine equivalent of the right upper lobe) [75]. Placement of the endotracheal tube prohibited assessment more proximally.

Only 1 of 8 newborn non-CF and 1 of 11 three week old non-CF pigs were positively scored for a bundle at any of the four tracheal locations. In contrast, 8 of 8 newborn CF pigs and 15 of 17 three week old CF pigs were scored to have a bundle

present at any of the four measured locations (Figure 11A). In general, these data agreed with our previously published observation that CF pigs have tracheal bundles and non-CF pigs do not [8].

We realized that tracheal airway smooth muscle bundles could reduce tracheal lumen circularity independent of an intrinsic airway shape defect. Hence, we also measured tracheal outer wall circularity, which we reasoned would be minimally affected by the bundle's presence. Outer wall circularity was significantly reduced in three week old CF pigs.

We next determined the location of bundles within CF pig tracheas. For both newborn and three week old CF pigs, the longitudinal tracheal location most often found to have a bundle was just below the trachea bronchus (Figure 11B). Circumferentially, the bundles were always located on the posterior, right side (Figure 11C, 11D).

Tracheal bundle width was greater for three week old CF pigs than for newborn CF pigs (Figure 11E). In addition, we observed a statistically significant, linear correlation between bundle width and animal body mass (Figure 11F). Based upon this finding we hypothesized the bundle to represent a long term phenotype. To test this hypothesis we retrospectively assessed a chest CT scan from a 347 day old CF pig. We found this CF pig to have a bundle present on CT. Similar to newborn and three week old CF pigs, it was located on the posterior, right side of the trachea between the tracheal bronchus and the carina (Figure 11G).

To verify our CT scan findings we performed a histological assessment from one newborn non-CF and CF pig (Figure 12). For this, we took histological samples from precise locations up and down the trachea including the four specific locations at which CT scans were scored. Our findings from histology corroborated our findings from CT. First, that CF pigs have airway smooth muscle bundles while non-CF pigs do not. Second, in CF pigs, bundles are located circumferentially within the trachea on the posterior, right side. Third, bundles are on the order of 1 mm in width. Last, longitudinally, bundles are most prominent between the carina and the tracheal bronchus.

Bronchial Size, Shape, and Distensibility

We found tracheas of reduced size and circularity in three week old CF pigs. Does this phenotype extend into the bronchi? To answer this question, we collected airway measurements from every airway segment of the right and left main bronchus visible on CT (Figure 13A). We defined an airway segment as the portion of airway from one airway bifurcation to the next, and measurements were made with VIDA Diagnostic's Apollo Software. We first measured bronchial airway wall thickness. We found that, on average (average of all measured segments of the right and left main bronchus combined), there was no statistically significant difference between genotypes (Figure 13B). However, we did observe a reduction in average bronchial inner circularity (Figure 13C).

We observed airway size reduction in the proximal but not distal measured airways (Figure 13D). More specifically, we observed the proximal most measured bronchial airway segments to be reduced in size for CF animals. This size reduction lessened with distal airway tree progression, such that, there was virtual size equivalence between genotypes in the distal-most measured airways. This pattern of proximal airway size reduction is reminiscent to that previously found in a micro-CT study of the newborn CF pig tracheal lobe (porcine equivalent of the right upper lobe) [7].

Airway smooth muscle tone is one factor that can influence airway distensibility, the ability of an airway to change in size in response to a change in pressure. Increases in smooth muscle tone can lead to a decrease in airway distensibility [60, 76]. We know from prior work that newborn CF pigs have increased airway smooth muscle tone at baseline [18]. Based upon this observation we hypothesized airway distensibility to be decreased in three week old CF pigs.

To measure bronchial distensibility we collected CT scans at both 25 cmH_2O (inspiratory) and 0 cmH_2O (expiratory). We measured airway distensibility in the trachea and in each airway segment of the right and left main bronchus that were visible on both the expiratory and inspiratory scan. We defined distensibility as follows: 100*[(insp. airway lumen area – exp. airway lumen area)/exp. airway lumen area)], similar to

previously published studies [60, 76]. We found no difference in tracheal distensibility (Figure 14A), but that airway bronchial distensibility was reduced in three week old CF pigs (Figure 14B). We also observed the average airway distensibility coefficient of variation to be increased in CF animals (Figure 14C). That is, the within animal variation in distensibility between bronchial airway segments was greater for CF than non-CF pigs.

3.4 DISCUSSION

Tracheal Smooth Muscle Bundles

What can we infer about CF pig tracheal smooth muscle bundles based upon our observations? We know bundles are unlikely formed in response to infection and inflammation as newborn CF pigs have a tracheal smooth muscle bundles but not airway infection and inflammation. We know the size and location of the bundles within the trachea to be consistent between CF animals. This does not suggest a stochastic developmental mechanism, but instead, a developmental mechanism that is distinct and repeatable. What might this mechanism be? Perhaps the *TMEM16A* mouse offers a clue. Interestingly, the *TMEM16A-/-* mouse (a chloride channel knockout) has tracheal airway smooth muscle bundles reminiscent of the CF pig (CFTR channels chloride). These observations may suggest chloride secretion to be important in the normal growth and development of airway smooth muscle.

The presence of tracheal airway smooth muscle bundles may have a number of functional implications. First, because they protrude into the lumen airspace, they could be obstructive to tracheal airflow. Even modest reduction in effective airway radius, which the bundle could cause, can appreciably increase resistance to airflow [59]. Moreover, bundle protrusion may alter tracheal airflow profiles and particle deposition patterns. Second, because the bundle is composed of airway smooth muscle, it could contribute to airway hyper-reactivity, which people with CF commonly exhibit [51]. Last, children with CF have increased airway smooth muscle mass on biopsy [11]. Evidence of increased airway smooth muscle mass in newborn and three week old CF pigs may

suggest that increased airway smooth muscle mass in children with CF may, in part, be a direct consequence of CFTR disruption.

Airway Size, Shape, and Distensibility

Three week old CF pigs have size reduction of proximal but not distal airways. This unique pattern of size reduction is highly similar to that observed in newborn CF pigs. In newborn CF pigs, we initially attempted to identify the pattern of airway size reduction with conventional CT imaging. However, with this imaging modality we lacked sufficient spatial resolution to visualize any but the proximal most airways of newborn pigs. Instead, we used micro-CT, which has greater image resolution than conventional CT, to image pig's right upper lobe. In this lobe, we found proximal but not distal airway size reduction [7].

Proximal airway size reduction in three week old CF pigs and newborn CF pigs is likely to have the same causal mechanism. We previously speculated this pattern of size reduction to be related to the temporal order of *CFTR* expression *in-utero*. There is evidence that *CFTR* is more highly expressed in early gestation than later gestation [77-79]. Therefore, it could be that CFTR is more important to airway development in early gestation than in later gestation. The temporal order of *CFTR* expression may overlap with the temporal order of airway formation *in-utero*, where large airways form prior to distal airways.

On the functional level airway size reduction would likely increase airway resistance. We did not measure airway resistance for the current study, but newborn CF pigs have airway size reduction and increased airway resistance [7]. In addition, airways of reduced size may be more susceptible to obstruction by mucus.

In 1974, Malcolm Green *et al.* coined the term "dysanapsis" (Greek: *dys*, "unequal;" *anaptixy*, "growth") to describe disproportionate growth between the lungs and airways[80]. CF pigs have dysanaptic growth because their proximal airways are small compared to their lung volume. At the functional level, decreased airway size would

reduce anatomic deadspace, and thus increase the percentage of inhaled air participating in gas exchange, while at the same time increasing airway resistance to airflow [81]. Green *et al.* observed that people with disproportionately large airways had greater maximal expiratory flow rates [80].

The CF pig may inform upon the limits of lung and airway dysanapsis. Three week old non-CF pig trachea cross-sectional area normalized by lung volume ranges from 0.08 to 0.18 mm^2/cm^3 at 25 cm H_2O. This wide range implies that under normal conditions (non-pathological), there is a large amount of plasticity between airway and lung growth: nature permits variation in size between the two. However, there must exist an upper and lower limit. The CF pigs in this study range from 0.04 to 0.10 mm^2/cm^3, and thus between both genotypes the range is 0.04 to 0.18 mm^2/cm^3. We therefore know, this range to be compatible with life in three week old pigs, with the CF pigs possibly approaching the lower limit.

Airway distensibility was reduced in the right and left main bronchus of three week old CF pigs. There are at least two likely contributors to this. First, reduced distensibility may stem from abnormal CF airway allometry. If bronchial wall thickness is no different between genotypes, yet the CF airways are reduced in lumen size, then the ratio between wall thickness and airway lumen size would be elevated in CF pigs. This may function like structural reinforcement, and consequently, the airways resist change in size and are less distensible.

Second, abnormal airway smooth muscle may contribute. We know from prior studies that newborn CF pigs have increased basal airway smooth muscle tone [18]. We also know that acute augmentation of CFTR using ivacaftor in adults with *G551D-CFTR* results in increased airway distensibility, most likely caused, in part, by a relaxation of airway smooth muscle (Chapter 5) [60]. We have not directly assessed smooth muscle tone in three week old CF pigs, but studies of newborn CF pigs, and adults with *G551D-CFTR* raise the possibility of increased tone, which could, in turn, contribute to decreased CF pig airway distensibility.

The airway distensibility coefficient of variation was greater for CF than non-CF animals. What might cause increased CF heterogeneity? Abnormal airway structure may contribute. Evidence of structural defects in newborn CF pigs includes abnormal tracheal cartilage rings, and decreased airway circularity. We did not assess cartilage structure in the current study, but we did find three week old CF pigs to have reduced tracheal and bronchial circularity. These could be evidence of underlying structural irregularities. Irregular airway structure could biomechanically destabilize airways, perhaps predisposing them to collapse, even independent of an increased wall thickness to lumen size ratio. In support, the *TMEM16A-/-* mouse has irregular tracheal cartilage and tracheomalacia [82].

Abnormal airway smooth muscle behavior could contribute to this heterogeneity. Perhaps, there is more variation in airway smooth muscle tone between bronchial segments of CF airways than non-CF airways, and the differences in distensibility heterogeneity reflect this. In support, asthmatics exhibit more variable airway size reduction in response to methacholine than do non-asthmatic controls [83-84]. Granted, the mechanisms of airway size change between the asthmatics study and our study in pigs was different (methacholine vs. airway pressure), but the results are analogous, and both consistent with heterogenous smooth muscle behavior.

Heterogenous CF airway distensibility could have a number of functional implications regarding obstruction, particularly if our findings in the right and left main bronchus are representative of the airway tree as a whole. Increased heterogeneity suggests variability in the way airways change in size in response to pressure changes. It suggests that some airways have limited size change in response to pressure changes, while others change greatly. The ones that change greatly may be predisposed to collapse, potentially causing obstruction of all downstream airways. Air trapping is a consequence of obstruction and is present in newborn CF pigs [7], and as many as 2 of 3 infants with CF [5]. Perhaps heterogenous airway distensibility contributes to this phenotype.

Congenital Defects and CFTR Restoration

Over 5% of people with CF are taking the CFTR potentiator, ivacaftor. Additional drugs targeting other *CFTR* mutations are currently being tested and developed. Recent advances in gene therapy have shown evidence of *CFTR* restoration in animal models [19-20, 85], raising the possibility of *CFTR* gene therapy for people with CF. Clinicians and researchers envision a future in which CFTR can be rescued by a drug, or replaced by a virus, theoretically providing cure-like treatment for people with CF.

What effect would such therapies, presumably applied postnatally, have on congenital airway abnormalities? Congenital defects, similar to those found in the pig, may spontaneously correct themselves in the face of CFTR restoration. Such a result would have several implications. It would suggest that chronic loss of CFTR is required to "maintain" defects throughout airway growth and development. It would also emphasize the importance of newborn screening for CF. Presumably, CFTR restoration would be more effective at rescuing airway growth and development defects if applied earlier in life than later.

In contrast, it is possible that post-natal CFTR restoration would not rescue congenital airway defects. In this scenario, with CFTR restored, and presumably minimized lung disease and general morbidity (e.g. pancreatitis, sinusitis, etc.), abnormal airway growth and development may represent the most salient manifestation of *in-utero* CFTR disruption. What impact might congenital defects have? Newborn pigs with CF have reduced airway size [7-8]. This abnormality likely contributes to their increased resistance to airflow [7]. Infants with CF may share this phenotype [8]. In addition, infants and children with CF have increased rates of tracheomalacia, potentially life-threatening episodes of tracheal collapse [73]. In this scenario, prevention of congenital defects would require restoration of CFTR *in-utero*.

3.5 CONCLUSION

Study strengths. First, our study benefited from high-quality, standardized chest CT scans acquired at 0 cmH_2O and 25 cmH_2O. Second, studies of infants with CF are hampered by a lack of non-CF controls. Here, we assessed CFTR-dependent airway development through non-CF to CF comparisons. Third, we were able to gain additional insight by comparing the respective phenotypes of newborn and three week old CF pigs.

Study limitations. First, analogous studies in infants and children with CF would be greatly informative. However, such studies are limited by technical and ethical challenges. Hence, we examined three week old CF and non-CF pigs. Second, we were unable to assess airway cartilage in the current study. However, given tracheal cartilage abnormalities in newborn CF pigs (imaged with optical coherence tomography) [8], CF mice [86], CF rats [87], and adults with CF [88], we believe it likely that three week old CF pigs have airway cartilage abnormalities. Third, we focused our airway assessment on the right and left mainstem bronchi. Additional studies are required to determine if the phenotype of the left and right main bronchi extend to other airways. Last, we were unable to rule out infection and inflammation as causal factors in the CF pig airway phenotype described here. However, the airway phenotype in three week old CF pigs is highly similar to that of newborn CF pigs, which lack evidence of lung infection and inflammation, suggesting a predominantly CFTR-dependent mechanism.

In three week old CF pigs we observed proximal airway size reduction, reduced circularity in the trachea, reduced bronchial circularity, no difference in airway wall thickness, and reduced, but relatively more variable bronchial distensibility. These findings reinforce the possibility that CFTR plays a role in airway growth and development, and that when CFTR is disrupted, abnormal airway development ensues.

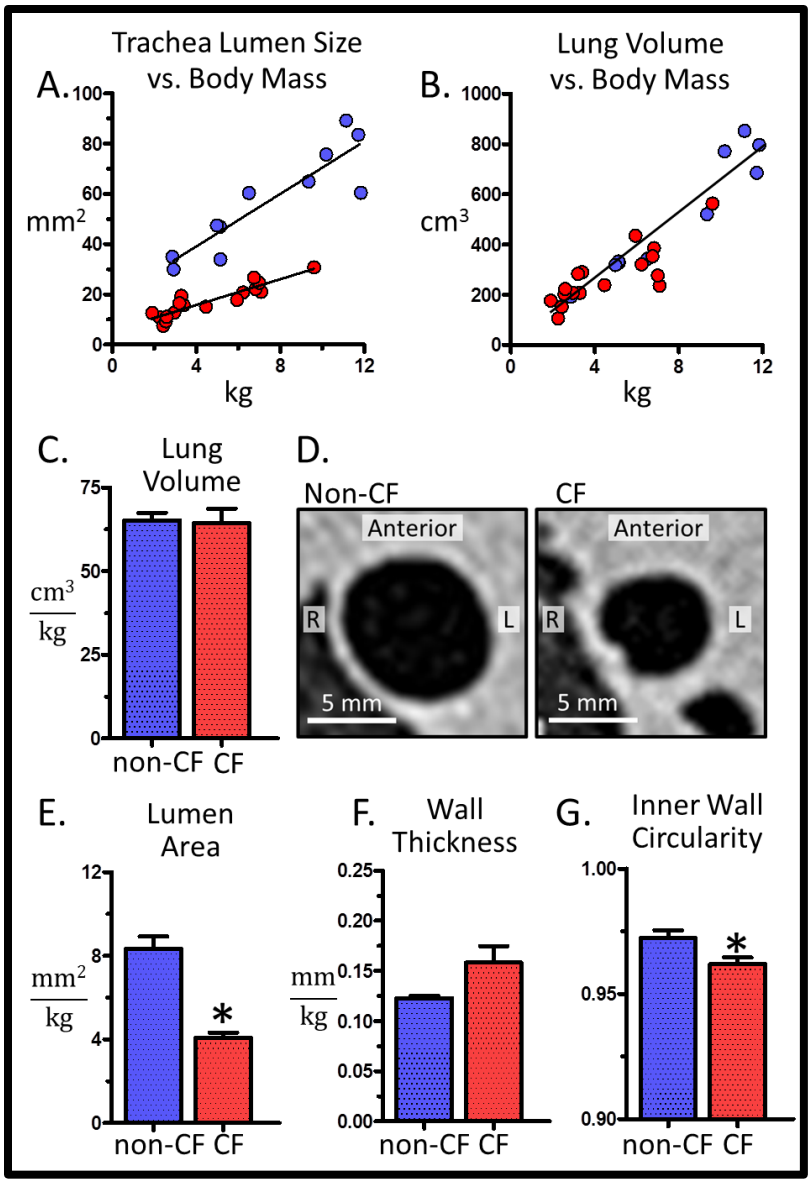

Figure 10. Lung volume and tracheal measurements in three week old CF pigs. All measurements and images obtained from CT scans acquired at an airway pressure of 25 cmH_2O. (A) Tracheal lumen cross-sectional area vs. animal body mass. $P<0.05$ for non-zero slope, for both genotypes, respectively. (B) Lung volume vs. animal body mass. $P<0.05$ for non-zero slope. (C) Lung volume normalized by body mass. (D) CT scan images of a three week old non-CF and CF pig trachea. (E) Tracheal lumen cross-sectional area normalized by body mass. (F) Average tracheal wall thickness normalized by body mass. (G) Tracheal inner wall circularity. Data are mean and SEM. *$P<0.05$

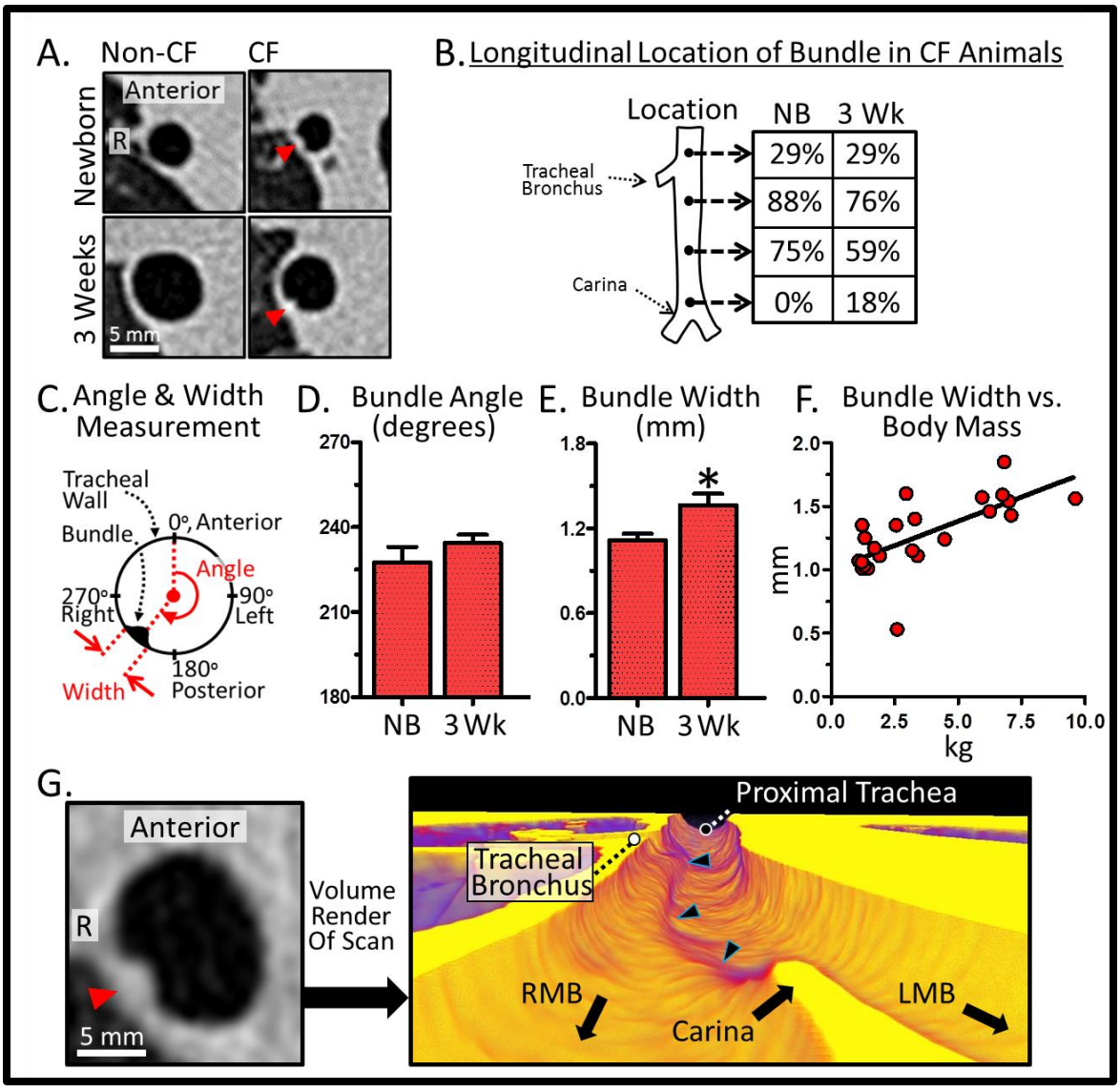

Figure 11. A CT-based description of tracheal airway smooth muscle bundles in CF pigs. (A) Newborn and three week old CF animals have tracheal airway smooth muscle bundles (arrows) on CT while non-CF pigs lack them. (B) Longitudinal location of bundles in newborn (NB) and three week (3 Wk) old CF pigs. Data presented as percentage of CF animals scanned. (C) Diagram illustrating bundle angle and width measures. (D) Bundle angle in newborn and three week old CF pigs. (E) Bundle width in newborn and three week old CF pigs. (F) There was a statistically significant, linear correlation between bundle width and pig body mass. (G) A bundle on CT (arrow) of a 347 day old CF pig (left), and corresponding CT scan volume render (right). In the volume render the anterior half of the scan has been cut away to more easily visualize the bundle (arrows), pseudo-colored. Data are mean and SEM. *P<0.05

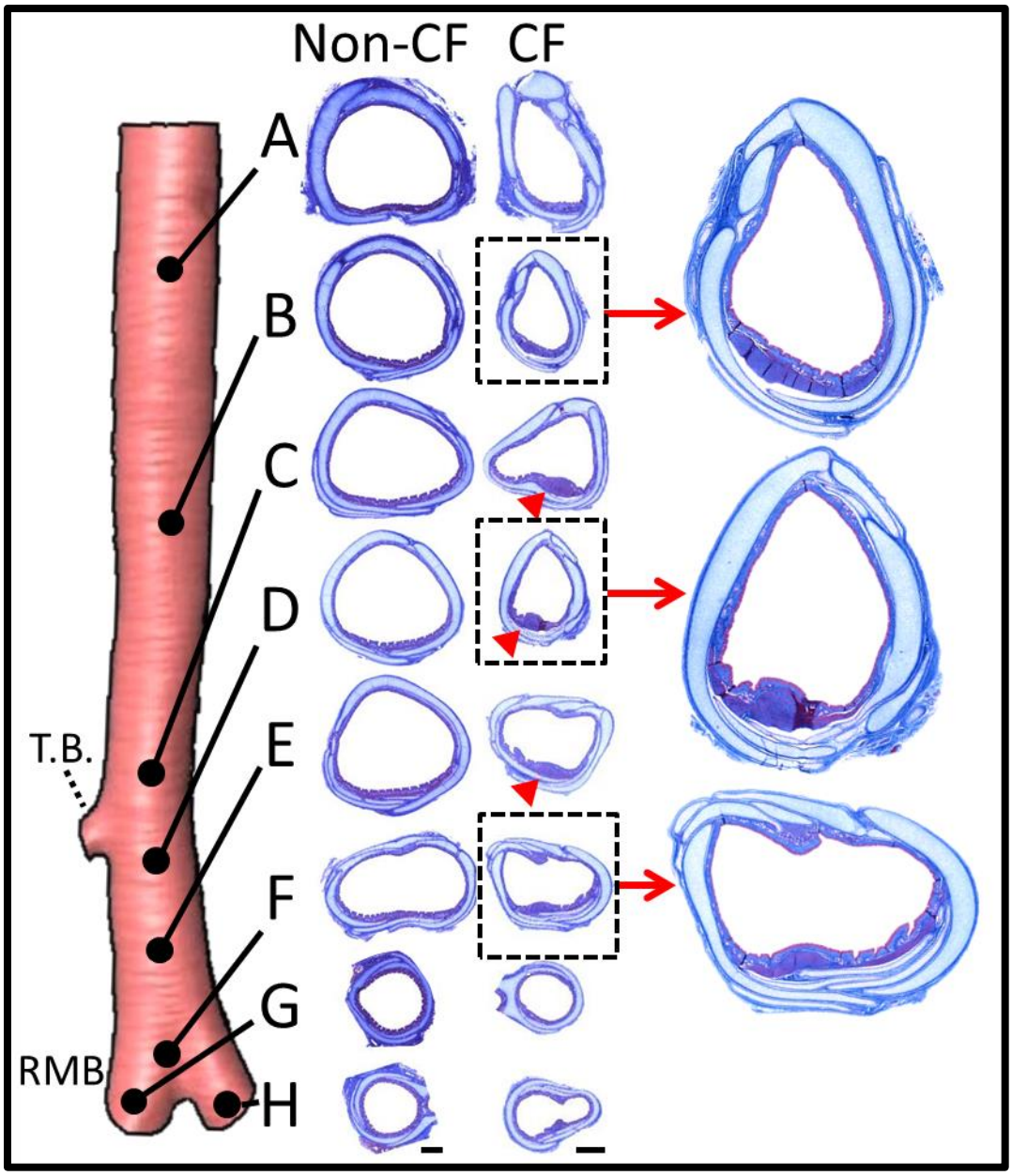

Figure 12. Tracheal histology from one newborn non-CF and CF pig. The non-CF trachea lacks evidence of tracheal airway smooth muscle bundles. The CF trachea does have a smooth muscle bundle, most prominent at location C, D, and E (arrows). Three CF pig sections are enlarged. Scale bar is 1 mm for both non-CF and CF, respectively. Staining with Masson's trichrome.

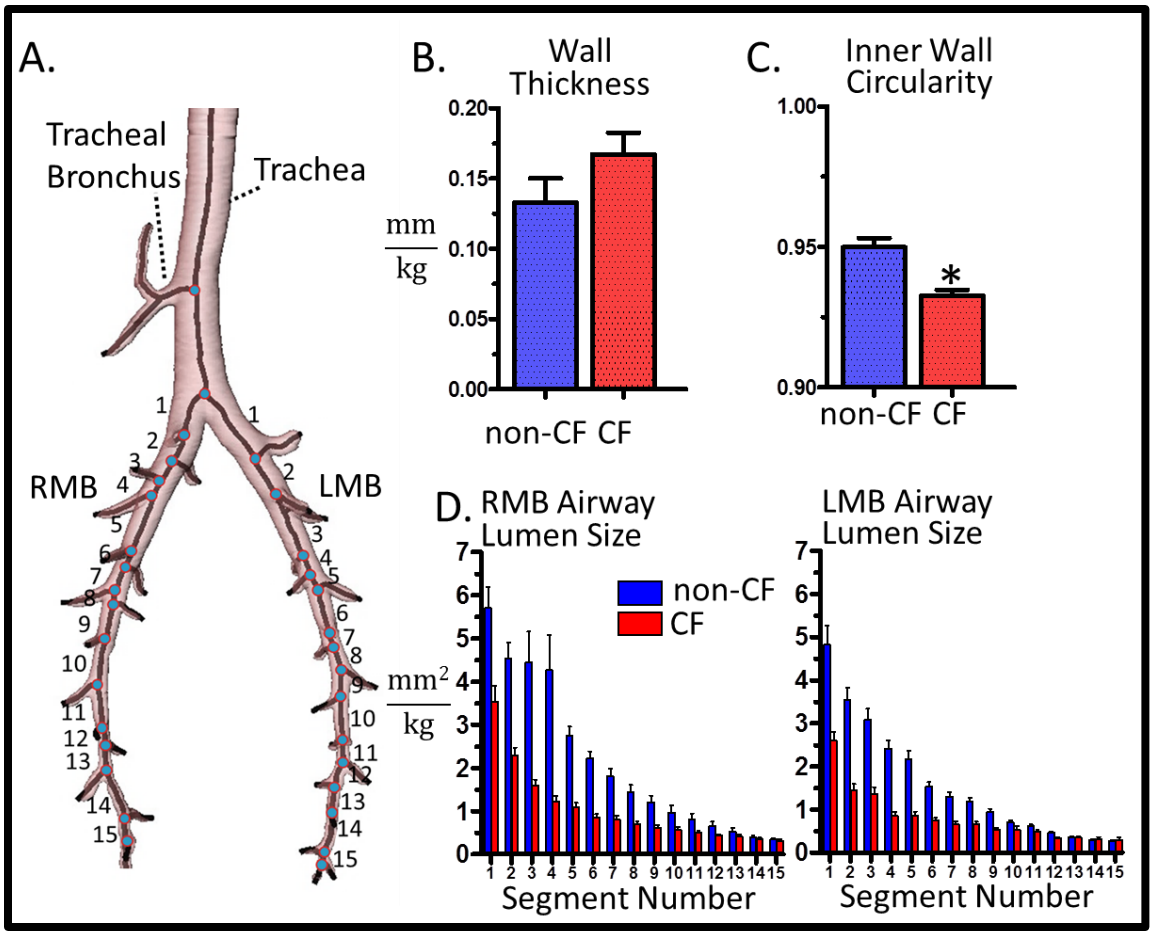

Figure 13. Bronchial airway measurements. (A) A three week old non-CF porcine airway lumen tree. Many airways have been digitally pared to focus on the trachea and airway segments (numbered) of the right and left main bronchus. (B) Average bronchial wall thickness. (C) Average inner circularity. (D) Bronchial airway lumen size ordered by bronchial segment numbers that correspond to the airway lumen diagram in Part A. Data are mean and SEM. *P<0.05

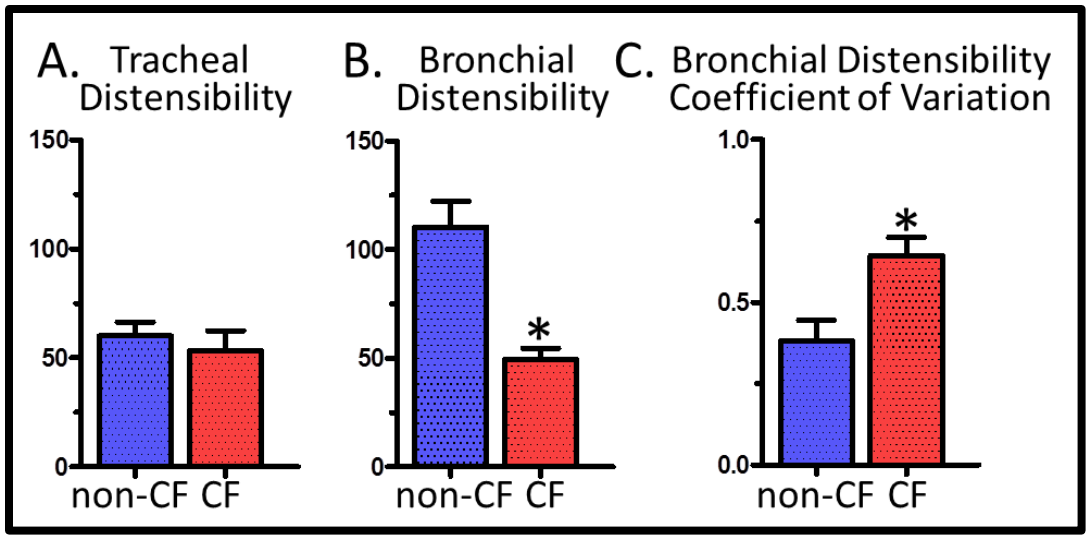

Figure 14. Airway distensibility. (A) Tracheal distensibility. (B) Bronchial distensibility is reduced in three week old CF pigs. (C) Three week old CF pigs have increased distensibility coefficient of variation. Data are mean and SEM. *P<0.05

CHAPTER 4: CF PIG LUNG DISEASE ON CT IMAGING AT THREE WEEKS OF AGE AND CORRELATIONS WITH HISTOLOGY AND BACTERIA

4.1 INTRODUCTION

People with CF are thought (with limited evidence) to have relatively normal and healthy lungs at birth. Over years and decades their lungs transition from health to advanced disease. While advanced CF lung disease is well characterized, the transition from health to disease is not. Understanding the mechanisms behind this transition is required to prevent CF lung disease pathogenesis.

Characterizing this transition would be very difficult in children and neonates with CF, the time at which CF lung disease likely begins. Reasons like this are why we created a porcine model of CF. We know that at the newborn time point, CF pigs lack lung infection and inflammation. We also know that over months to a year they develop advanced lung disease [6]. Similar to people with CF, we do not how the CF pig lung transitions from relative health at birth to advanced disease later on.

To better understand this transition process we studied non-CF and CF pigs at the three week age point. Primarily using chest CT, we sought to answer a number of questions. Do three week old CF pigs show signs of disease on CT? If so, can we quantify it? Do CT findings correlate with measures of infection and inflammation? Answering these questions will help us better understand early aspects of CF lung disease. This study will help establish the "normal progression" of CF pig lung disease through three weeks of age, setting the table for invaluable future comparative studies involving various therapeutics.

4.2 METHODS

This is intended to be a brief methodological description. Additional methodology is presented on an as needed basis throughout the Results and Discussion sections.

CT Scan Acquisition and Analysis

We previously described the CT scan acquisition methodology in Chapter 3. It is also as described in a previously published manuscript from our group [7]. We generated left and right lung masks with Apollo. Apollo generated an initial lung mask, and then these masks were edited manually as needed. We then used the lung masks and scans to generate HU histograms in Matlab.

We generated a number of HU histograms for each lung CT scan. These included whole lung histograms, histograms on a lung thirds basis (both cephalad, middle, and caudal, as well as anterior, middle, posterior), and histograms on a lung sixths basis – along the same axis as the lung thirds. Our Matlab code generated 18 descriptive statistics for each histogram. These included the following: % of voxels between -1024 and -950 HU, % between -950 and -850HU, % between -850 and -500HU, % greater than -500HU, maximum HU, minimum HU, histogram skewness, histogram kurtosis, mean HU, standard deviation of HU, HU coefficient of variation, lung volume, % of voxels less than -856 HU, mode HU, HU quartile 1, HU quartile 2 (median), HU quartile 3, and HU IQR. Although we generated many histogram statistics, we report only upon mode HU, mean HU, and HU IQR. We generated histograms at 25 cmH_2O and 0 cmH_2O for 8 newborn non-CF pigs, 8 newborn CF pigs, 17 three week old non-CF pigs, and 11 three week old CF pigs, a total of 110 scans. Sandeep Bodduluri of the Reinhardt Laboratory helped with histogram data generation.

Bacterial Analysis

Small tissue samples were obtained from six lung zones at necropsy. These zones included: the right and left cephalad (toward the head), the right and left middle, and the right and left caudal (toward the tail). Lung homogenate samples were serially diluted and plated onto agar. Standard microbiological procedures were used to identify and quantify bacteria, including the number of colony forming units (CFU). Bacterial analysis was similar to that described in Stoltz *et al.* [6]. Drake Bouzek of the Stoltz Laboratory led this portion of the project.

Histological Scoring

Lung tissue samples were collected at necropsy and prepared for histology. Histology was scored for the presence and degree of mucus accumulation in the airways. Mucus scores ranged from 0 to 3 where 0 indicated normal mucus, 1 indicated a mild rim along the wall or mucus string into the lumen, 2 indicated partial, but less than 50%, lumen obstruction, and a score of 3 indicated greater than 50% obstruction of the airway lumen by mucus. Histology was also scored for the presence and degree of inflammation. A score of 0 was considered normal. A score of 1 indicated rare exocytosis of polymorphonuclear cells (PMNs) into the airways. A score of 2 indicated multifocal PMN aggregates in the airways. A score of 3 indicated locally extensive regions of PMN infiltration into airways. Histological scoring was completed by the laboratory of Dr. David Meyerholz.

4.3 RESULTS

Air Trapping and Airway Mucus in Three Week Old CF Pigs

Air trapping is the excessive retention of air upon exhalation, and is caused by obstruction to airflow. In people with CF air trapping is among the earliest signs of disease on CT [5, 89], is predictive of future pulmonary exacerbations [90], and is a risk factor for bronchiectasis [4]. Air trapping may also contribute to abnormal airway smooth muscle behavior. By reducing vital capacity, air trapping impairs the ability of a deep inspiration to relax airway smooth muscle [91].

We previously reported that newborn CF pigs have more lung zones (left, right, upper, middle, lower) with air trapping than newborn non-CF pigs [7]. We hypothesized this phenotype to persist through three weeks of age. Similar to studies of infants with CF [5], and consistent with prior published work from our lab [7], we implemented a scoring system to quantify air trapping in non-CF and CF pigs. We had genotype blinded pulmonologists independently score for the presence of air trapping within each lung zone on expiratory (0 cmH_2O) scans (Figure 15A, 15B). Air trapping was considered present if at least two of the three scorers indicated air trapping. We found that, on average, three week old CF pigs had more lung zones with air trapping present than three week old non-CF pigs.

Air trapping is often caused by airway obstruction. One chief cause of airway obstruction in CF is accumulation of mucus in the airways. Based upon this, we hypothesized that the degree of airway mucus accumulation would correlate with the degree of air trapping. We quantified the degree of airway mucus accumulation with a histological based scoring system. The scores ranged from 0 to 3 where 0 indicates no mucus abnormality, and a score of 3 indicates that over 50% of the airway lumen was obstructed by mucus. Histological scoring was completed by the laboratory of Dr. David K. Meyerholz. We found three week old CF pigs to have significantly more mucus in their airways than three week old non-CF pigs (Figure 16A). In addition, we found a statistically significant, positive, linear correlation between the degree of mucus

accumulation in the airways on histology, and the degree of air trapping as scored from chest CT scans (Figure 16B).

Lung Hounsfield Unit Analysis – 0 cmH_2O

We performed lung HU analysis of chest CT scans taken of three week old non-CF and CF pigs at an airway pressure of 0 cmH_2O (Figure 17). We assessed HU histograms on both a whole lung and regional lung basis. Perhaps HU analysis will reveal disease-caused alterations in CF pig lung density.

We first asked if there were genotype differences in whole lung HU histograms (Figure 18). Upon visual inspection, the HU histograms do not clearly differ from each other. Although we collected many HU histogram shape descriptors (listed in methods), here we focused on average HU, mode HU, and HU IQR. Whole lung average HU, mode HU, and HU IQR did not significantly differ between genotypes at 0 cmH_2O.

We know that CF lung disease can affect some regions of the lung more than others. Given this, we next repeated HU histogram analysis but on a regional basis. Toward this, we digitally divided the lung into thirds on CT. The thirds consisted of the upper (toward the head), middle, and lower (toward the tail) (Figure 19). There were no statistically significant differences between genotypes in average HU, mode HU, or IQR HU for any lung third (Figure 20).

There were statistically significant regional differences within non-CF and CF pigs, respectively. In non-CF and CF pigs, average HU and mode HU were greatest in the lower lung, intermediate in the middle lung, and the least in the upper lung. HU IQR significantly differed between lung thirds in non-CF pigs, with the middle third having the greatest IQR. However, there was no statistically significant difference in HU IQR between lung thirds in CF pigs (Figure 20).

We next repeated our histogram analysis but for the lung zones (left, right, upper, middle, lower). We found no differences between genotypes in average HU and mode

HU for any of the six lung zones (Figure 21, 22). HU IQR was significantly greater in CF pigs than non-CF pigs in the right upper zone, but none of the other five zones. We plotted average HU, mode HU, and HU IQR as paired data points (Figure 23), and found no statistically significant differences between genotypes. We did not find significant correlations between HU histogram statistics and the air trapping scores.

Lung Hounsfield Unit Analysis – 25 cmH_2O

We performed HU histogram analysis at an airway pressure of 25 cmH_2O (Figure 24). Upon visual inspection, the whole lung histograms for non-CF and CF pigs appeared similar to each other. Whole lung average HU, mode HU, and HU IQR were not statistically different between genotypes (Figure 25). Lung third HU histograms were not clearly different between genotypes upon visual inspection (Figure 26). Moreover, there were no statistically significant differences between genotypes in average HU, mode HU, and HU IQR for any lung third (Figure 27). There were statistically significant differences in average HU, mode HU, and HU IQR between lung regions within non-CF but not CF pigs (Figure 27).

Histogram analysis by the six lung zones (Figure 28) revealed no statistically significant differences in average HU, or mode HU between non-CF and CF pigs for any of the six lung zones. HU IQR was significantly greater in the CF pig right upper zone compared to non-CF, but was not significantly different between genotypes for the other five lung zones (Figure 29).

Closer examination of the histogram shape descriptors suggested additional genotype differences. The IQR, though only statistically different between non-CF and CF pigs in the right upper zone, was elevated, on average, for all six lung zones. If CF pigs were no different than non-CF pigs, we might expect the IQR HU for CF pigs to be greater than the non-CF IQR HU in half of the zones, and less than the average non-CF IQR HU in the other half. An elevation in all six zones was statistically significant with a Chi-square test ($P<0.05$). Average HU was increased for CF in five of six zones

(P>0.05). Average HU and HU IQR, but not mode HU, were significantly different between genotypes if plotted as paired per animal averages (Figure 30). These data suggest there are differences in the lung density profile between three week old non-CF and CF pigs at 25 cmH_2O.

Lung Hounsfield Unit Histogram Analysis – Variability Score and Lung Infection

HU histogram analysis suggests that three week old CF pig lungs may be more variable in tissue density than non-CF animals. What might cause such variability? One possibility is infection. Infection may result in radiographic opacities in the lung, which in turn, may cause more variability in HUs (Figure 31). We therefore hypothesized tissue variability on CT to correlate with bacterial infection in CF pigs. We measured bacteria by enumerating the number of bacterial colony forming units (CFU) from lung samples acquired from respective lung zones, where a higher CFU corresponds to more bacteria (more severe infection). We found CF pigs to have a trend for elevated levels of bacteria (P=0.06).

We first asked if whole lung HU IQR correlates with a whole lung average of CFU. We found that the linear correlation between these two variables did not reach statistical significance. Knowing that manifestations of CF lung disease often exhibit regional dependency, we next assessed correlations between CFU and HU IQR on a regional basis. Figure 32 illustrates the IQR within each of the six lung zones for each three week old non-CF and CF pig included in the study.

How should we correlate HU IQR with CFU? Should we correlate per animal average of IQR across the six lung zones with CFU? We should not, because to correlate that with whole lung CFU would require a weighted average where each zone is weighted by its respective fraction of total lung volume. If we did that, then it would become a whole lung average. We already investigated that and did not find a correlation.

Should we correlate the "Animal Max" (from Figure 32) with lung CFU? The problem with this approach is that density variation within the lung is regional dependent.

Would an "Animal Max" from Figure 32 represent variation due to infection, or natural variation between lung regions? For example, recall from Figure 27, that the lower lung is naturally more variable than the middle and upper lung.

To solve this problem we created a *Difference Matrix* (Figure 33C). To generate the Difference Matrix we subtracted respective CF animal regional IQRs from the across animal *average* non-CF IQR of the corresponding region. The Difference Matrix measures the *relative* difference between CF and non-CF variability within specific regions. See Figure 33 caption for additional explanation and an example.

Given the natural differences between respective lung regions, we then normalized the Difference Matrix by the non-CF standard deviation on a regional basis, Figure 33D. The rationale for normalization of the Difference Matrix by standard deviation is to place all of the difference measures on the same scale. This way, we can fairly compare across regions within the lung. The concept is similar to a Z-score in statistics. For example, is the value of "12" in the Difference Matrix a large or small difference? Answer: it depends upon the underlying distribution. If the standard deviation of the underlying distribution is, for example, "500," then we can infer a difference of 12 to be relatively small, only 12/500 of one standard deviation. In contrast, if the standard deviation of the underlying distribution is 3, then we know that a difference of 12 is 4 standard deviations above the mean, a large difference. Figure 34 further illustrates the rationale behind standard deviation normalization.

Normalization using standard deviation is meaningful if the underlying distributions are normally distributed. To test this we formed QQ-plots of non-CF IQR on a regional basis, (Figure 35). A straight QQ plot line indicates a normal distribution. Our QQ plots resemble straight lines, suggesting they do not greatly differ from a normal distribution. This implies there is utility in normalization of the Difference Matrix by non-CF standard deviation.

Figure 36 summarizes the process by which we converted regional IQR measures into the standard-deviation-normalized Difference Matrix, henceforth referred to as the "Variability Score." Figure 36A shows the equation used to calculate the Variability

Score. It is very similar to a Z-score in statistics. This score indicates the variability of lung tissue HUs within specific lung regions of CF animals, relative to the average tissue variation across non-CF animals within the same region. By mathematical definition, a CF animal with a Variability Score of 0 would have the same tissue variability as the non-CF average. A Variability Score below zero indicates less tissue variability than the average non-CF animal, and a Variability Score above zero indicates more tissue variability than the non-CF animal average (Figure 36B). Figure 36C shows the Variability Scores for each lung zone within each CF animal. Importantly, the Variability Score controls for natural variations between different regions within the lung, and consequently we are able to fairly compare across different lung zones.

Does the Variability Score pass the "eye test?" Does the gross appearance of the scans visually match the Variability Score? Figure 37 shows an example. In this figure we juxtaposed CT scan images with their respective Variability Scores. Upon visual inspection, the regions with low Variability Scores appear to have little parenchymal variation, and the regions with high Variability Scores have more parenchymal variation. In Figure 38, we extended this juxtaposition to the entire data set. Again, upon visual inspection the Variability Score appears to match the appearance of HU variation.

Does the Variability Score correlate with infection? We performed a regional bacterial analysis from the same six regions of the lung that we used for CT scan analysis (six lung zones). We quantified bacteria by enumerating the number of bacterial colony forming units (CFU) that the lung samples produced. There was a statistically significant, positive, linear correlation between Variability Score and CFU when we included every lung zone from every animal (Figure 39C). In addition, there was a statistically significant, positive, linear correlation between the region of maximum Variability Score within an animal with the region of maximum CFU within an animal (Figure 39D).

Which region of the lung was the most variable? To answer this question we identified the region within each CF animal with the highest Variability Score (Figure 40A). The right upper zone was the most variable in 5 of 9 animals, the right lower in 2 of 9 animals, the left middle and left lower in 1 of 9 animals, and the left upper and right

middle in 0 of 9 animals. This distribution significantly differed from that of a random distribution (Chi-square test, $P<0.05$, Figure 40B).

We next computed the Variability Score for newborn CF pigs, using newborn non-CF animals as the reference (analogous to using three week old non-CF pigs as the reference for three week old CF pigs). We then compared the newborn CF pig Variability Score to the three week old CF pig Variability Score (Figure 41A, 41B). We know from previous publications that newborn CF pigs lack infection and inflammation at birth. Given this, we hypothesized Variability Scores in three week old CF pigs to exceed those of newborn CF pigs. On average, Variability Scores in three week old CF pigs were elevated compared to newborn CF pigs in all six lung zones ($P<0.05$, Chi-square Test, Figure 41C). After regionally pairing, Variability Scores were significantly greater in three week old CF pigs than newborn CF pigs, especially in the right upper zone, Figure 41D. Right upper zone Variability Scores had a linear, statistically significant relationship with bacterial CFU in three week old CF pigs (Figure 41E).

4.4 DISCUSSION

Mucus and Air Trapping

At birth, CF pigs have more air trapping than non-CF pigs. This phenotype persists through three weeks of age. What might cause air trapping in CF pigs? We know that air trapping in newborn CF pigs is not due to accumulation of mucus, infection, or inflammation, because newborn CF pigs lack evidence of these in the lungs [7]. However, it is possible that congenital airway abnormalities including reduced airway size and circularity contribute to air trapping in newborn CF pigs [7].

One likely contributor to the air trapping phenotype in three week old CF pigs is accumulation of mucus in the airways. CF animals had more accumulation of airway mucus than non-CF animals, and the degree of airway mucus accumulation in CF animals

correlated with the degree of air trapping. Accumulation of mucus in the airway can cause air trapping by preventing airflow downstream to the site of mucus obstruction.

Previously published papers illustrated a mucus defects in the newborn CF pig. First, in submucosal glands in the airways of newborn CF pigs secrete mucus, however, after secreted, the mucus strands often fail to detach from the submucosal gland resulting in a stagnant strand of airway mucus [55]. Second, newborn CF pigs have increased airway surface liquid viscosity [57]. These phenotypes, which are present at birth in the CF pig, may have contributed to the increased accumulation of airway mucus in three week old CF pigs, and to their air trapping phenotype. This is further supported by the observation that three week old CF pigs had significantly more air trapping than newborn CF pigs, which lack evidence of mucus accumulation [8].

Air trapping caused by mucus obstruction in CF pigs parallels findings in human CF studies. Robinson *et al*. published a study examining the relationship between airway mucus and air trapping in children with CF [92]. They performed a double-blind, placebo controlled, before drug-after drug study using Dornase alfa, an aerosolized DNase. Dornase alfa reduces airway mucus viscosity by selectively cleaving DNA suspended in mucus. This DNA is largely from dead neutrophils and bacteria. In the Dornase alfa group they observed an increase in FEV_1 and a reduction in air trapping. These results suggest that abnormal mucus can cause airflow obstruction and result in air trapping.

Regional variation in HU within non-CF and CF animals

The upper lungs were less dense on CT at both 0 cm H_2O and 25 cmH_2O in non-CF animals. This likely reflects natural density gradients between the dependent and nondependent regions of the lung. The nondependent lung is less dense because 1) due to gravity more blood is drawn to the dependent lung than the nondependent lung, and 2) the intrapleural pressure is greater in the nondependent lung which helps pull open the alveoli, lowering the density [70, 93].

For a pig scanned supine, the dependent zone would be the posterior aspect, and the nondependent zone the anterior aspect. We performed our histogram analysis on an upper (cephalad), middle, lower (caudal) basis. This begs the question, why do our histograms follow the pattern of dependent and nondependent lungs? The likely answer is that the lower lung (caudal), by natural porcine anatomy, is half or more made up of posterior (dependent) lung of a supine scanned pig (Figure 42) while the upper third has the greatest percentage of nondependent lung, and the density pattern we observed in the histograms is a reflection of this.

The natural density gradient between dependent and nondependent regions can be altered by various lung pathologies, for example, emphysema and ARDS [94-96]. Given this, it is interesting to note that in non-CF pigs, at 25 cmH_2O, there were statistically significant differences between the upper (cephalad), middle, and lower (caudal) lung in average HU, mode HU, and HU IQR, but not in CF pigs. Might this be an early sign of CF lung disease?

Lung Hounsfield Units: Genotype Differences

Three week old CF pig lungs had greater variability in parenchymal density profiles at 25 cmH_2O. Increased heterogeneity was likely caused mostly by an increased number of focal opacities. These focal opacities increased the average HU but had little effect upon mode HU which is relatively outlier robust. Genotype differences were less pronounced on 0 cmH_2O scans. Why might this be? Likely, regional opacities in CF animals were "camouflaged" at 0 cmH_2O, a pressure at which lung volume is naturally reduced and lung density naturally increased.

How do these data compare with the literature? To our knowledge, there are no studies featuring HU analysis in people with CF. In fact, there are few quantitative CT scan studies in the CF literature, and even fewer that include non-CF controls. However, our finding of increased HU heterogeneity in CF pigs agreed with a *qualitative* assessment made by Lynch *et al.* in a CT scan study of 12 infants with CF (median age 8

months): "The most common abnormal finding [in CF] was a poorly defined heterogeneity of lung density [97]."

Our findings seem to be consistent with a number of studies that invoked scoring systems for quantification of CT findings. For example, Davis *et al.* used the Brody Score to quantify lung disease in children under 4 years old with CF [98]. These children with CF were CT scanned following a pulmonary exacerbation (visit 1), and then CT scanned again after intravenous antibiotics and airway clearance therapy (visit 2). On visit 1 they found airway wall thickening, focal opacities, airway dilatation, and hyperinflation. Note that all of these could contribute to HU heterogeneity. After antibiotics and airway clearance therapy, Brody Scores decreased, reflecting improvement. They did not perform HU histogram analysis. However, the Brody Score assesses CT manifestations tied to HU heterogeneity (e.g. focal opacities). Therefore, a reduction in Brody Score may be consistent with a reduction in HU heterogeneity. Because this was a before antibiotics, after antibiotics study, it then follows that a possible reduction in parenchymal heterogeneity was associated with a reduction in bacterial infection, although additional studies would be required for verification.

Lung Infection and Tissue Variability on CT

From prior studies we know CF pigs lack lung infection at birth, but do have an impaired ability to kill bacteria, and over time (months) develop lung infection with an array of bacteria [3, 6]. Given this, it was not surprising that three week old CF pigs had evidence of bacterial infection. Early life lung infection in the CF pig is consistent with a number of studies that report lung infection in neonates with CF. First, Sly *et al.* reports 21% of infants with CF (median age 3.6 months) to be classified as infected, including with *Staphylococcus aureus*, and *Pseudomonas aeruginosa* [5]. Second, using broncho-alveolar lavage, Dakin *et al.* found lower respiratory bacteria in 14 of 22 infants with CF, mean age 23 months [99]. Third, Hilliard *et al.* classified 12 of 25 infants with CF in their study as infected [100].

We found the degree of infection in three week old CF pigs to correlate with the degree of lung parenchymal heterogeneity, as measured by HU IQR. These observations have a number of implications. First, correlation between infection and lung tissue variability may suggest that the status of one can be inferred, to a degree, by measuring the other. Second, HU heterogeneity on CT may have been caused, in part, by bacterial infection. Third, the structural lung disease commonly observed in adults with CF, may initiate very early in life, and this initiation likely involves bacterial infection. This initial infection may contribute to inflammation, tissue remodeling, and functional deficits. Fourth, one three week old CF pig had no detectable lung infection and had very little HU heterogeneity on CT. Interestingly, in the aforementioned studies by Sly, Dakin, and Hilliard, not all neonates were classified as infected. Are some with CF spared early infection, and if so, why? Answering these questions, while beyond the scope of the current study, could inform upon CF lung disease pathogenesis. Fifth, this study raises a number of questions regarding early life treatment of people with CF. At what age is it appropriate to begin antibiotics? Should we begin antibiotics prior to evidence of infection? What are the effects of chronic antibiotics on growth and development in infants and children? These, and similar questions, have been raised before [5-6, 101], and additional studies are required to answer them.

Right Upper Lung Zone Disease

The lung zone with the most variable tissue in three week old CF pigs was the right upper. This finding was consistent with prior CF pig and human CF studies [6, 42-43]. More specifically, a prior study of older CF pigs (months to a year old) qualitatively found the upper right zone to often have the most disease involvement on CT [6]. In a human CT scan study, Maffessanti *et al.* reported the right upper zone to have the most disease in children (avg. 13 y.o.) with CF [43].

What does the current study teach us about CF right upper lung disease? The CF pig has a host of congenital airway abnormalities, might upper right lung disease be in part congenital? This is unlikely, as Variability Scores of newborn CF pigs show the

right upper zone to be, on average, the least variable zone. In three week old CF pigs, the right upper zone was found to have the highest Variability Score in 5 of 9 pigs. The right upper zone was most variable in only 1 of 8 newborn CF pigs. From this observation we may infer the right upper tissue variability found in three week old CF pigs to develop postnatally.

People stand upright, while pigs stand on four legs, yet people with CF and CF pigs both get upper (toward the head) right lung disease. How should we interpret this? Does this suggest a gravity nondependent mechanism? How might gravity affect disease progression in the lung?

One illustration of gravity dependent pathology is infection by *Mycobacterium tuberculosis*. This regional preference is associated with the ventilation to perfusion ratio (V/Q). In lung physiology, V/Q is greatest in the nondependent lung (apex of the human upright lung), and least in the dependent lung (bottom of the human upright lung, [59]). This, in large part, is due to increased perfusion in the dependent lung, simply because gravity pulls more blood to that region. An increase in V/Q in the upper lung means there is a relative paucity of deoxygenated capillary blood exchanging its CO_2 with the oxygenated air. As a consequence, PO_2 is greater in the nondependent lung than the dependent, and PCO_2 is greater in the dependent lung than the nondependent. *Mycobacterium tuberculosis* naturally prefers higher oxygenation, and thus preferentially infects the nondependent lung (upper) in humans [59].

If a similar process occurred in pigs, not necessarily with *M. tuberculosis*, but with any O_2 loving bacteria, we would expect the pigs to get posterior disease (nondependent lung), rather than right cephalad disease. To test this we calculated Variability Scores as we did before, but instead of dividing the lung into six lung zones, we divided the lung into the following sixths: left, right, anterior, middle, posterior. We found the posterior lung third to have a below average Variability Score (Figure 43).

Regional differences in V/Q could potentially affect bacterial infection by another mechanism. The PCO_2 gradient in the lung (caused by natural regional variation in V/Q) causes the dependent lung to be more acidic than the nondependent lung. We know from

prior studies that acid-base balance plays a key role in airway defense. Newborn CF pigs, which have decreased HCO_3- secretion due to lack of CFTR function, naturally have acidic airways, and an impaired ability to kill bacteria. When their ASL pH is raised pharmacologically, their ability to kill bacteria is rescued [3]. In addition, abnormally acidic pH impairs the effectiveness of antimicrobials β-defensin-3 and LL-37 [102]. Hence, a gravity dependent pH gradient in the lung could possibly lead to regional dependent susceptibilities to infection. If this occurred in pigs, we would expect lung disease to occur anteriorly (dependent lung). We found Variability Scores in the anterior lung of three week old CF pigs to be below the overall Variability Score average. In fact, under this regional stratification, the lung zone with the greatest degree of variability was in the right, middle (along the anterior-posterior axis) zone.

If infection in the CF pig occurred in a gravity dependent manner, we may expect the most disease either in the posterior, or anterior side. This is not what we observed. We observed the most disease, as measured by the Variability Score, in the right upper (cephalad) zone. Moreover, if the mechanism were related to gravity should it affect both the left and right lung equally, rather than one side preferentially?

If right upper lung disease in CF is not congenital and not due to the effects of gravity, then what could cause it? One potential explanation is abnormal particle deposition patterns in CF. In a computational fluid dynamics (CFD) study, Awadalla *et al.* observed that inhaled particles (which could represent dust, bacterial, and miscellaneous particulate) preferentially travel to the right side of the lung. This preference was likely, in part, because the CF pig branching angle at the carina significantly differed from non-CF pigs, and preferentially directed particles to the right side [103]. Although this study observed a preference for *right lung* particle deposition in CF rather than a *right upper lung* preference, it still raises the possibility of abnormal particle deposition as a potential contributor to right upper lung disease in CF. Davis *et al.* cite aspiration of gastroesophageal reflux (GER) as a possible explanation for CF right upper lung disease [98]. Children with CF have increased incidence of GER [104-106], although why GER would preferentially affect the right (as opposed to right and left) is unclear.

This study does not pinpoint a cause for right upper lung disease, but its prevalence in both humans and pigs with CF suggests that it is unlikely caused by a gravity-dependent mechanism. The fact that newborn CF pigs lack evidence of right upper lung disease at birth suggests that it develops postnatally. Infection likely contributes to upper right lung disease because the degree of right lung zone variability on CT correlated with the level of infection on bacterial culture.

Pathogenic Mechanisms of CF Lung Disease

It is extremely difficult to separate primary from secondary defects of CFTR disruption in people with CF. Even infants show signs of lung infection and inflammation. Inability to separate primary from secondary, has limited researcher's ability to identify "the roots" of CF lung disease. Identification of these "roots" is required to treat underlying problems, rather than symptoms of underlying problems. Recognition of this limitation was a key reason why our research group developed the CF pig.

The hallmarks of CF lung disease are relatively well characterized and include accumulation of mucus in the airways, chronic infection, and chronic inflammation. Although the newborn CF pig lacks evidence of these in its lungs, it is primed to develop them. The newborn CF pig has an impaired ability to detach mucus strands from submucosal gland ducts [55], increased airway surface liquid viscosity [57], and has an impaired ability to kill bacteria [3].

Three week old CF pigs have a trend for increased bacterial CFU, and increased accumulation of mucus in the airways, but do not have elevated levels of inflammation. These observations have a number of implications. First, researchers debate whether infection precedes inflammation in CF, or vice-versa [23, 107-110]. The results of this study, and previously published work [6], suggest that infection precedes inflammation in CF pigs. Second, the data in newborn CF pigs and the current study may suggest that an impaired ability to kill bacteria, accumulation of airway mucus, and inflammation are, to

a degree, independent of each other. In support, we were unable to find a correlation between bacterial CFU, airway mucus accumulation, and inflammation in three week old CF pigs. In addition, newborn CF pigs exhibit mucus and bacterial killing abnormalities without infection, inflammation, and mucus accumulation. It then follows, that treatment of a single defect (e.g. antibiotics to help offset impaired bacterial killing) may be insufficient to entirely prevent lung disease. While mucus accumulation, infection, and inflammation likely form a vicious cycle, each may be, to an extent, respectively pathogenic independent of the other two.

This study in three week old CF pigs provides a basis of comparison for future studies involving therapeutics. In such future studies we could systematically target individual, putative, pathogenic mechanisms of CF lung disease. For example, we could test the effect of bacteria on lung disease progression by treating pigs with antibiotics, or raise them in a strictly bacteria free environment. We could test the effects of airway mucus accumulation by treating pigs with mucolytics. We could test the effects of congenital abnormalities by generating *G551D-CFTR* pigs, keeping them off ivacaftor until birth, and then putting them on ivacaftor postnatally, and vice-versa. We could raise CF pigs while on anti-inflammatories to test the effects of inflammation on lung disease. We could assess the effectiveness of CFTR gene therapy approaches. All of these studies would be *extremely difficult* to execute with humans as subjects, would inform upon mechanisms of CF lung disease pathogenesis, and would inform on therapeutic options for people with CF.

4.5 CONCLUSION

This study has a number of strengths and limitations. Strengths include: 1) High quality, pressure controlled chest CT scans enable visualization and quantification of lung characteristics. 2) Many studies of infants with CF are hampered by a lack of non-CF controls. In the present study we drew inferences primarily based upon non-CF to CF comparisons. 3) We were uniquely positioned to match histology to CT and bacterial findings. Such studies are extremely limited in humans. 4) A correlation between air

trapping scoring and histological mucus scoring suggest that each are meaningful and sensitive measures. 5) Similarly, correlations between Variability Score and infection suggest that each are meaningful and sensitive measures. 6) Comparison of the newborn and three week old age points facilitated our analysis of early CF lung disease. Limitations. 1) We used lung tissue heterogeneity as a marker of early CF lung disease in pigs. Future studies are required to determine if this approach is well suited for assessment of advanced CF pig lung disease or human CF lung disease. 2) Our animals were *CFTR*-/-, while many mutations of *CFTR* maintain a degree of residual function (e.g., ΔF508), *CFTR*-/- does not. Although, we previously report that the Δ*F508-CFTR* pig phenotype mimics that of *CFTR*-/- animals [58].

There is a growing appreciation that CF lung disease begins very early in life. We have shown, in prior studies, that newborn CF pigs lack hallmark features of CF lung disease including infection and mucus accumulation. This study shows these to spontaneously develop in CF pigs within weeks of birth, and that several features of CF lung disease are apparent on CT within weeks of birth in CF pigs. This study has helped lay the groundwork for future CF pig studies testing various early-life therapies. Early-life therapeutics may one day be part of normal care for people with CF, especially with broadening implementation of newborn screening for CF. Early medical intervention may alter the course and scope of lung disease in people with CF.

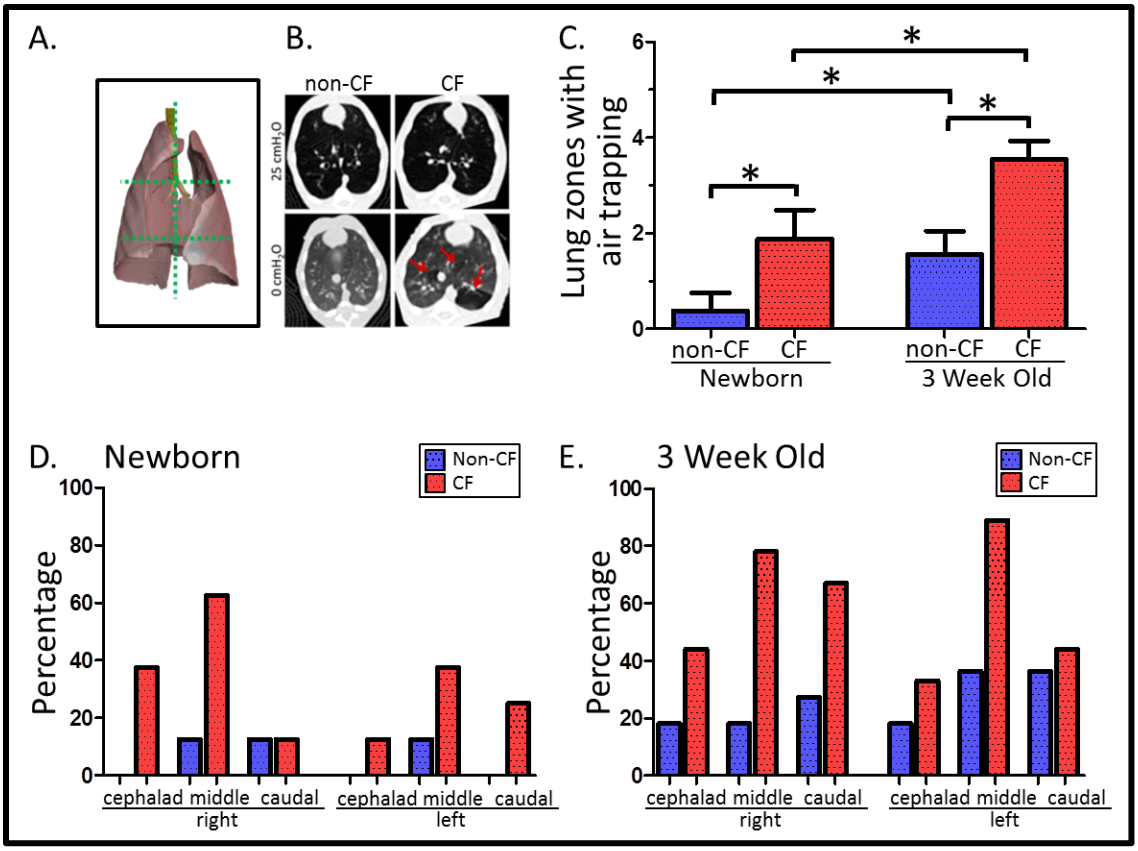

Figure 15. Air trapping scores in newborn and three week old CF pigs. (A) For scoring purposes we divided the lung into six zones. (B) CT scan slices highlighted regions of air trapping (arrows) in a newborn CF pig at 0 cmH_2O. (C) The average number of lung zones scored as positive by genotype blinded pulmonologists. Data are mean and SEM. (D) The percentage of pigs scored positive for air trapping in respective lung zones for newborn and (E) three week old non-CF and CF pigs. Images from A, B, and D were reproduced from [7]. *P<0.05

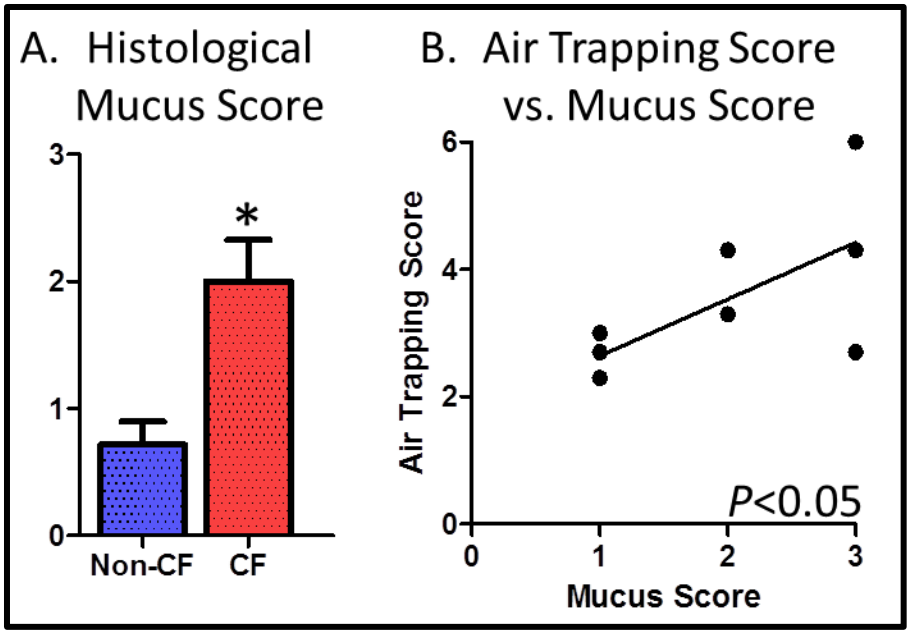

Figure 16. Mucus and air trapping. (A) Genotype blinded histological scoring by a pathologist revealed three week old CF pigs to have more airway mucus than three week non-CF pigs. Data are mean and SEM. (B) There was a statistically significant, positive, linear correlation between the number of lung zones with air trapping present and the histological mucus score. *$P<0.05$

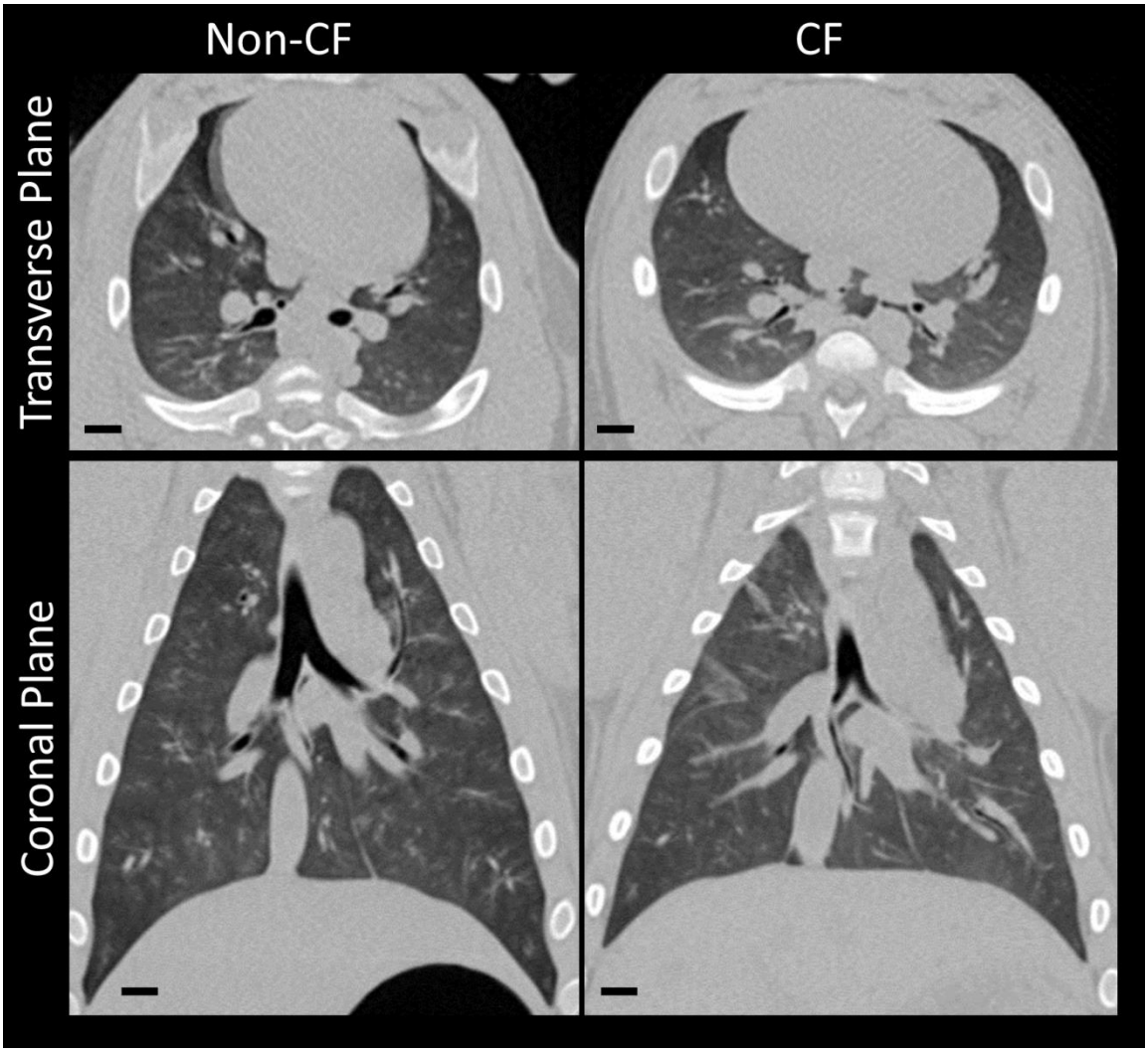

Figure 17. CT images at 0 cmH_2O. Three week old non-CF (Left) and CF pig (right). Scale bar 1 cm.

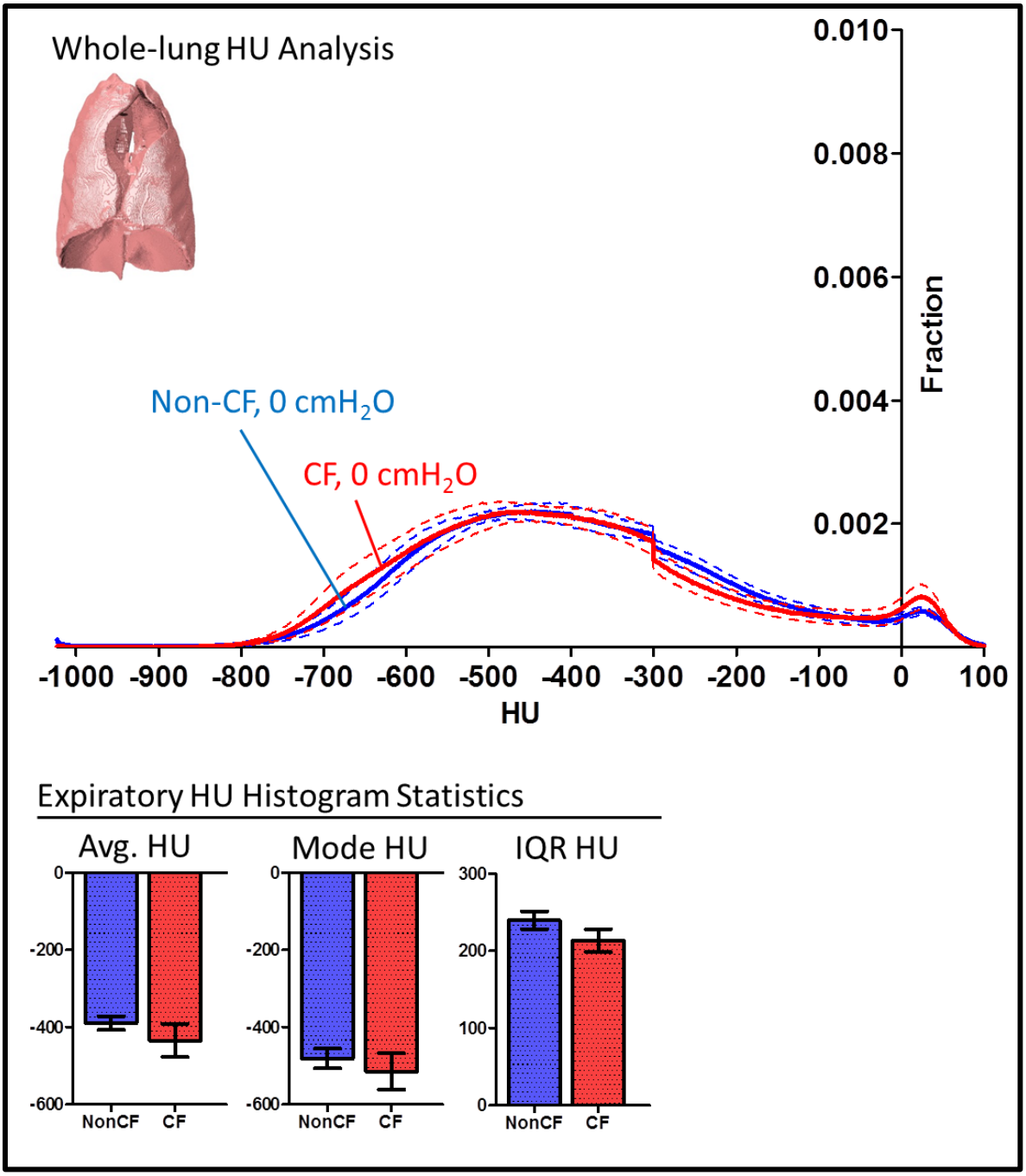

Figure 18. Whole lung HU histograms for three week old non-CF and CF pigs. Average ± SEM of whole lung HU histograms (top) with accompanying histogram statistics (bottom).

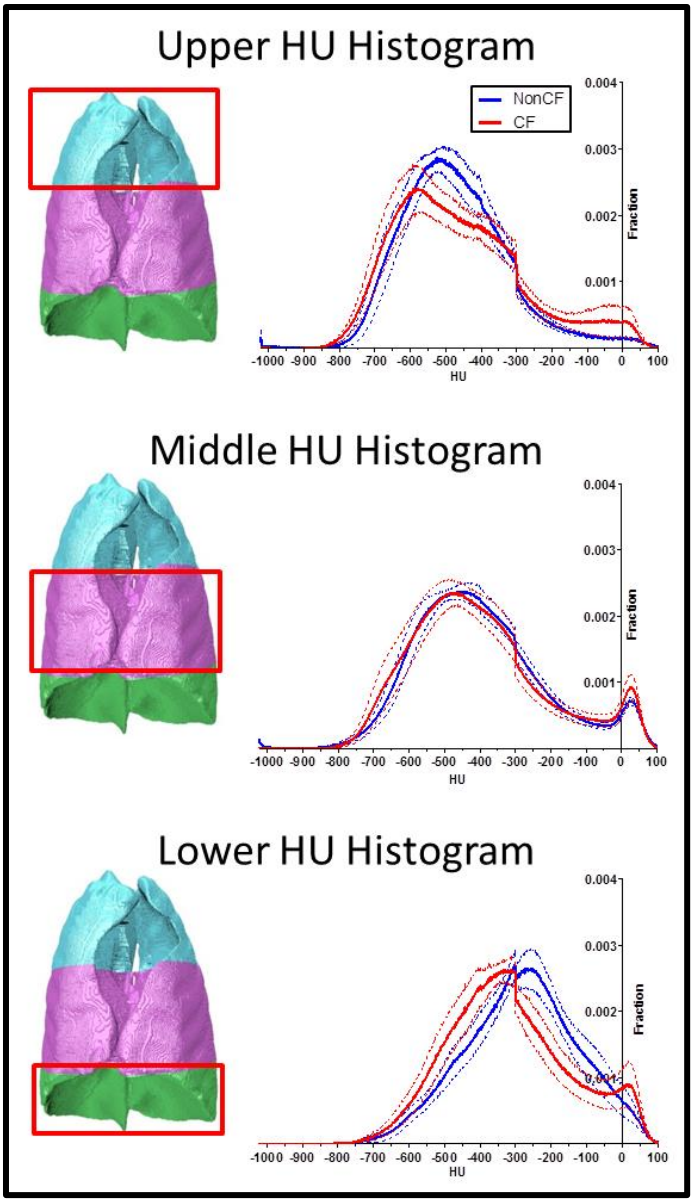

Figure 19. HU histograms by lung thirds at an airway pressure of 0 cmH_2O. Box over lung third at left denotes region of lung HU histogram. Lines are average ± SEM.

Average HU	Non-CF	CF	P-Value
Upper	-473±19	-461±6	NS
Middle	-401±19	-403±31	NS
Lower	-284±23	-317±32	NS
P-Value	S	S	

Mode	Non-CF	CF	P-Value
Upper	-525±30	-534±34	NS
Middle	-489±25	-487±35	NS
Lower	-261±38	-330±50	NS
P-Value	S	S	

IQR	Non-CF	CF	P-Value
Upper	177±9	210±16	NS
Middle	220±9	211±12	NS
Lower	193±10	215±21	NS
P-Value	S	NS	

Figure 20. Histogram statistics for lung thirds at 0 cmH_2O in three week old non-CF and CF pigs. Data are mean ± SEM. P-values in the right column reflect genotype differences within respective regions (Mann-Whitney Test). P-values in the bottom row reflect regional differences within respective genotypes (Friedman Test). $P<0.05$ denoted as "S." $P>0.05$ denoted as "NS."

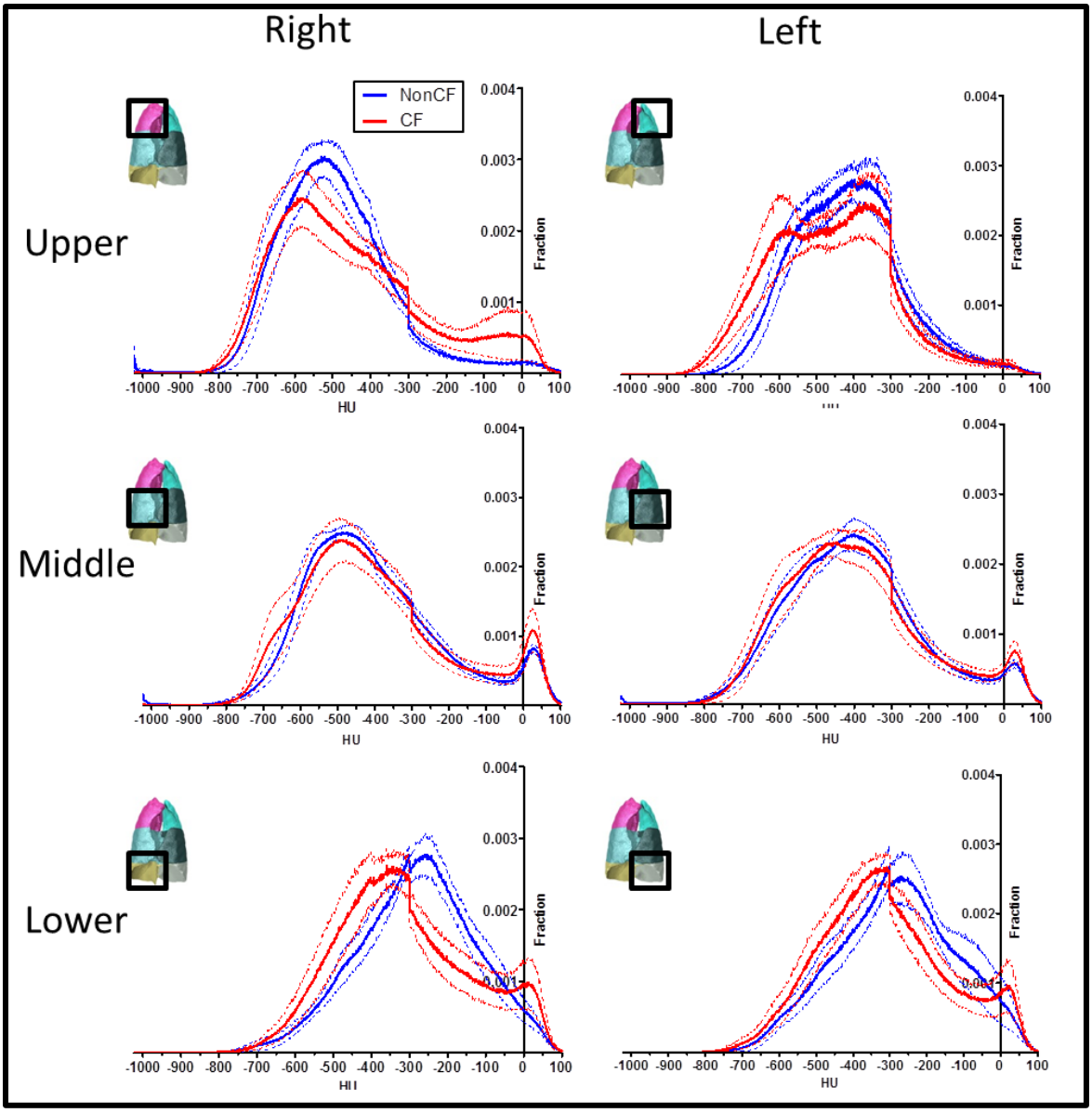

Figure 21. Regional HU histograms for three week old non-CF and CF pigs at an airway pressure of 0 cmH_2O. The solid lines represents an across animal average, and the dotted lines represent SEM. Lung segmentations are on the left side of each histogram and are color coded by lung region. A box encloses the corresponding lung region.

Average HU	Non-CF	CF	P-Value
Right Upper	-492±18	-456±42	NS
Left Upper	-417±21	-459±31	NS
Right Middle	-402±17	-403±33	NS
Left Middle	-397±20	-399±28	NS
Right Lower	-282±19	-321±31	NS
Left Lower	-284±26	-317±31	NS

Mode HU	Non-CF	CF	P-Value
Right Upper	-538±29	-518±67	NS
Left Upper	-420±26	-457±39	NS
Right Middle	-506±20	-458±68	NS
Left Middle	-424±27	-444±33	NS
Right Lower	-273±30	-317±47	NS
Left Lower	-262±42	-316±50	NS

IQR HU	Non-CF	CF	P-Value
Right Upper	160±9	202±16	S
Left Upper	166±9	163±8	NS
Right Middle	220±7	212±12	NS
Left Middle	209±10	202±10	NS
Right Lower	191±9	206±20	NS
Left Lower	189±11	208±24	NS

Figure 22. HU histogram shape descriptors for three week old non-CF and CF pig lungs at 0 cmH_2O. These data correspond to the histograms shown in the previous figure. "NS" denotes $P>0.05$, and "S" denotes $P<0.05$ with Mann-Whitney Test.

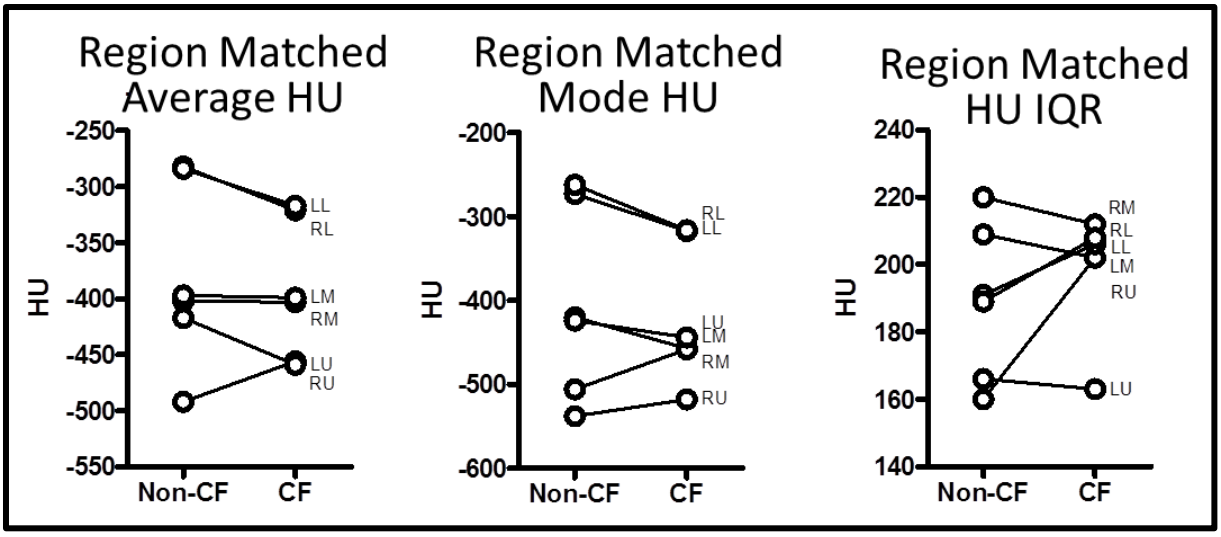

Figure 23. Hounsfield Unit histogram results at 0 cmH_2O for three week old non-CF and CF pigs. These data correspond to the tabular results in the prior figure. Dots represent a per-animal average within respective genotypes, and lines connect respective lung regions between genotypes. Initials mark respective lung regions. *P<0.05

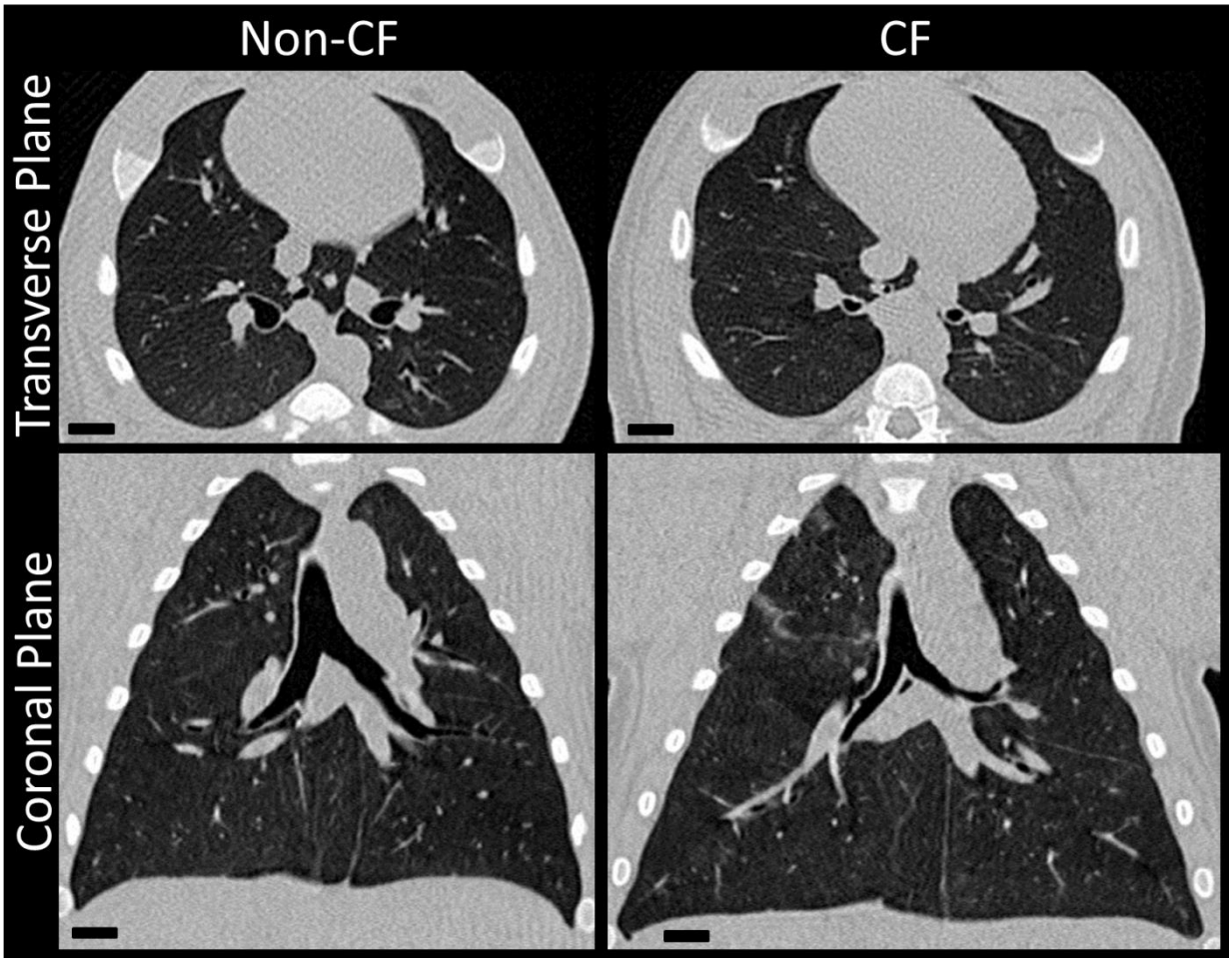

Figure 24. Chest CT scan slices of a three week old non-CF and CF pig in the transverse and coronal plane. Scans acquired at an airway pressure of 25 cmH_2O. Scale bar is 1 cm for all images.

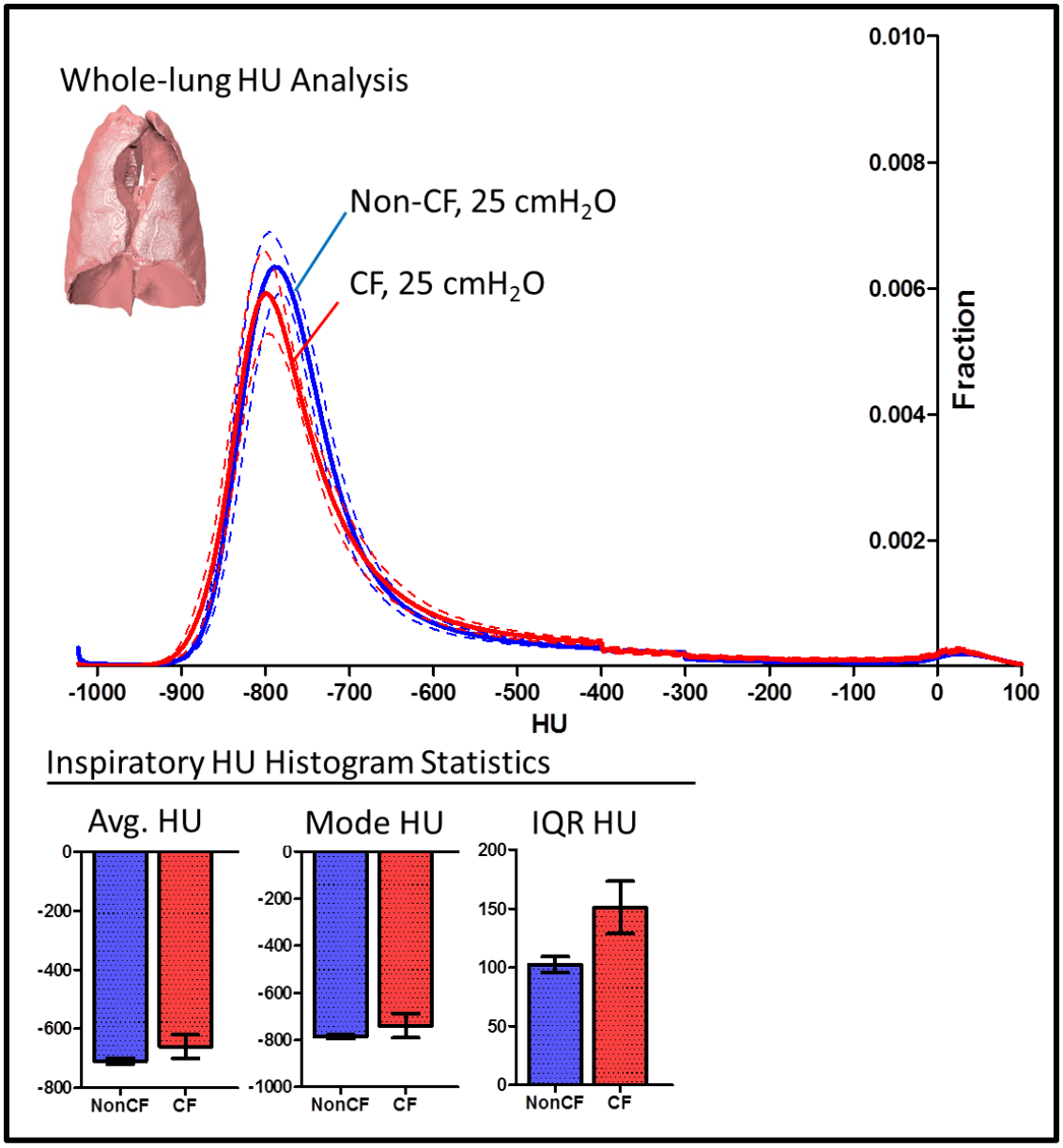

Figure 25. Whole lung histogram analysis at an airway pressure of 25 cmH_2O. (Top) Average (solid line) plus/minus SEM (dotted lines) HU histograms for three week old non-CF and CF pigs. (Bottom) Descriptive statistics of the above HU histograms. There were no statistically significant differences between genotypes in these three descriptive statistics. Bars represent averages ± SEM.

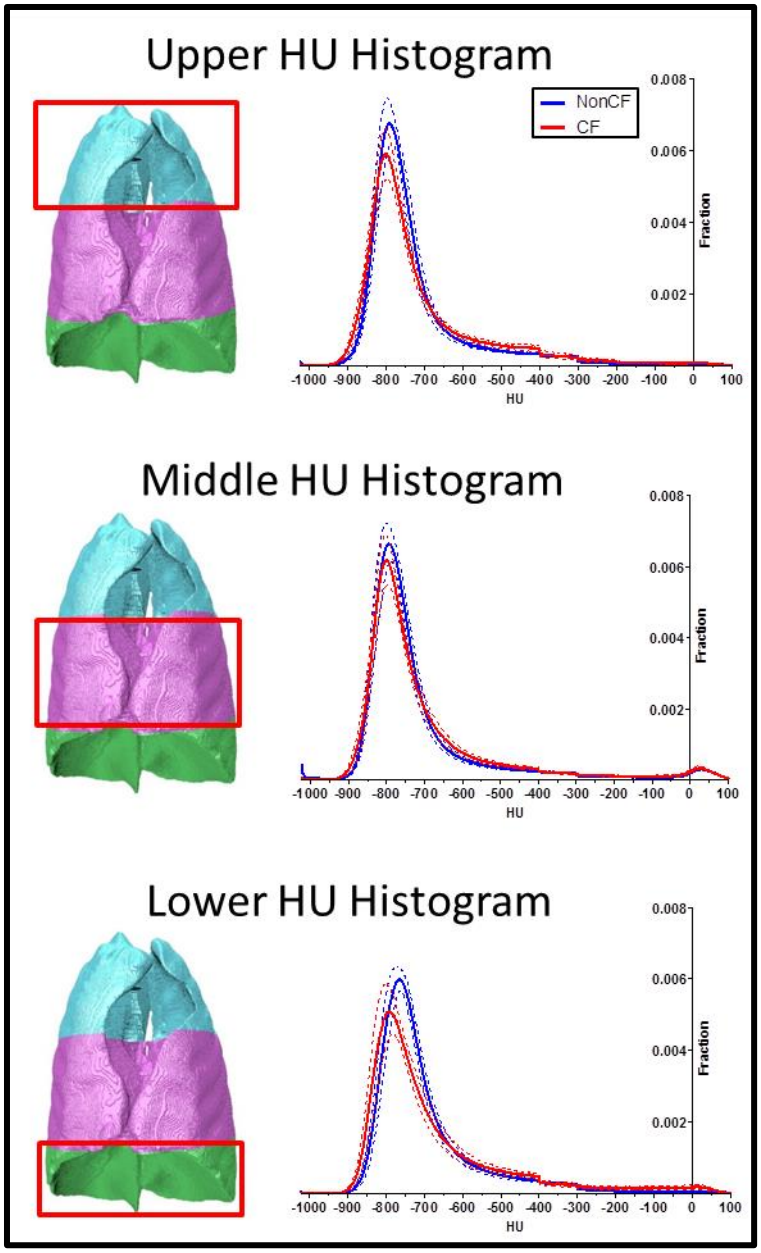

Figure 26. HU histogram at 25 cmH_2O by lung thirds in the three week old non-CF and CF pig. The solid lines represents an across animal average, and the dotted lines represent SEM. Lung segmentations are on the left and color coded by lung third. A box encloses the region of interest.

Average HU	Non-CF	CF	P-Value
Upper	-722±10	-710±19	NS
Middle	-711±11	-698±19	NS
Lower	-696±13	-674±28	NS
P-Value	S	NS	

Mode	Non-CF	CF	P-Value
Upper	-784±9	-794±9	NS
Middle	-789±8	-790±10	NS
Lower	-768±8	-777±11	NS
P-Value	S	NS	

IQR	Non-CF	CF	P-Value
Upper	91±5	142±26	NS
Middle	97±7	129±19	NS
Lower	112±11	161±31	NS
P-Value	S	NS	

Figure 27. HU histogram shape descriptors by lung thirds. Data are mean ± SEM. P-values in the right column reflect genotype differences within respective regions (Mann-Whitney Test). P-values in the bottom row reflect regional differences within respective genotypes (Friedman Test). $P<0.05$ denoted as "S." $P>0.05$ denoted as "NS."

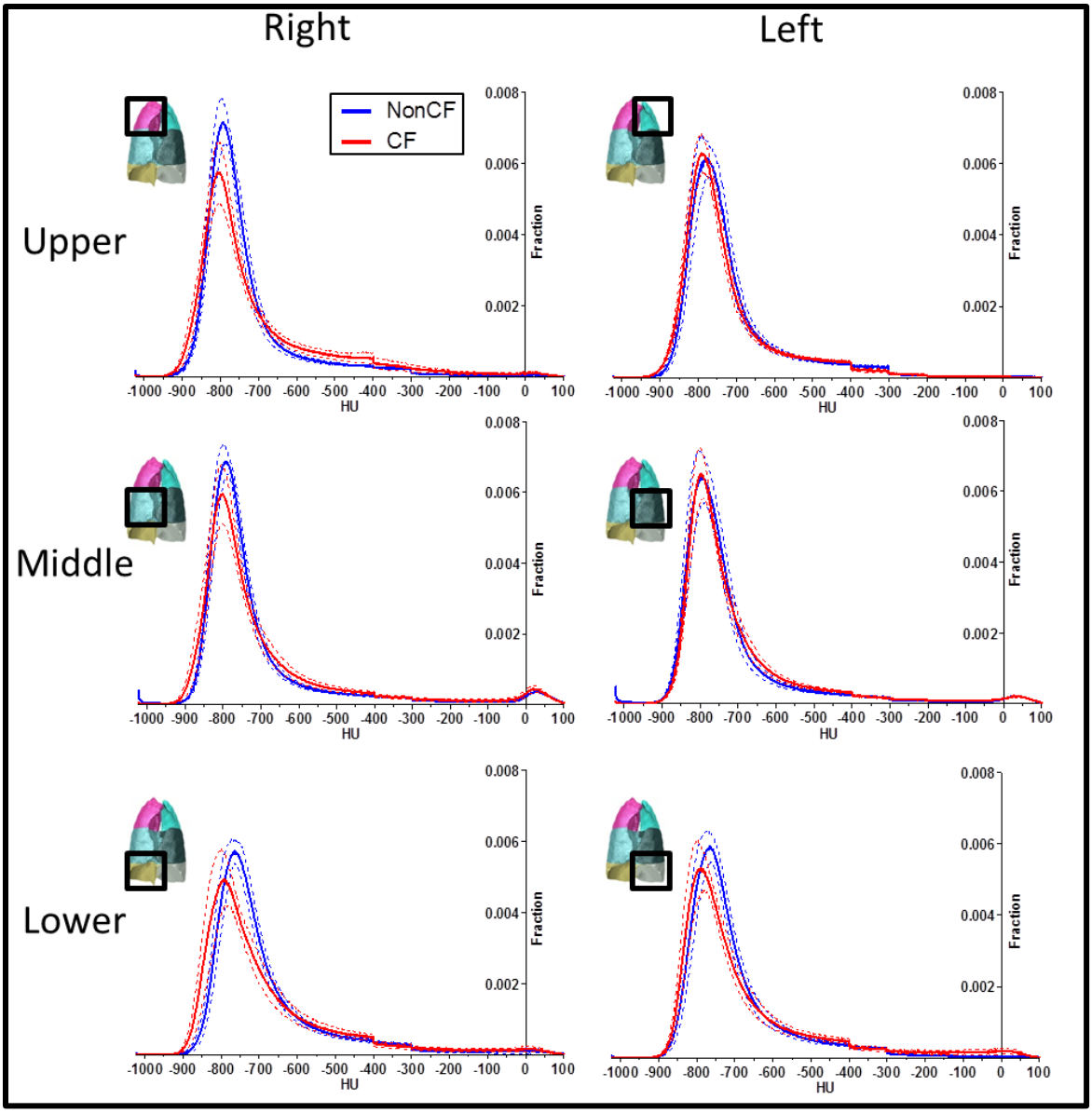

Figure 28. HU histograms of three week old non-CF and CF pigs at 25 cmH_2O for six lung regions. The solid lines represents an across animal average, and the dotted lines represent SEM. Lung segmentations are on the left side of each histogram and are color coded by lung region. A box encloses the corresponding lung region.

Average HU	Non-CF	CF	P-Value
Right Upper	-728±10	-701±28	NS
Left Upper	-710±12	-718±11	NS
Right Middle	-705±10	-692±26	NS
Left Middle	-716±13	-701±14	NS
Right Lower	-695±12	-679±31	NS
Left Lower	-697±14	-674±28	NS

Mode HU	Non-CF	CF	P-Value
Right Upper	-786±8	-794±11	NS
Left Upper	-775±9	-781±8	NS
Right Middle	-792±7	-794±13	NS
Left Middle	-790±10	-787±9	NS
Right Lower	-768±8	-783±13	NS
Left Lower	-770±9	-781±11	NS

IQR HU	Non-CF	CF	P-Value
Right Upper	87±5	152±31	S
Left Upper	100±7	111±11	NS
Right Middle	99±8	137±27	NS
Left Middle	93±7	121±14	NS
Right Lower	111±10	156±31	NS
Left Lower	112±13	164±33	NS

Figure 29. HU histogram shape descriptors for three week old non-CF and CF pig lungs at 25 cmH_2O. These data correspond to the histograms shown in the previous figure. "NS" denotes $P>0.05$, and "S" denotes $P<0.05$ with Mann-Whitney Test.

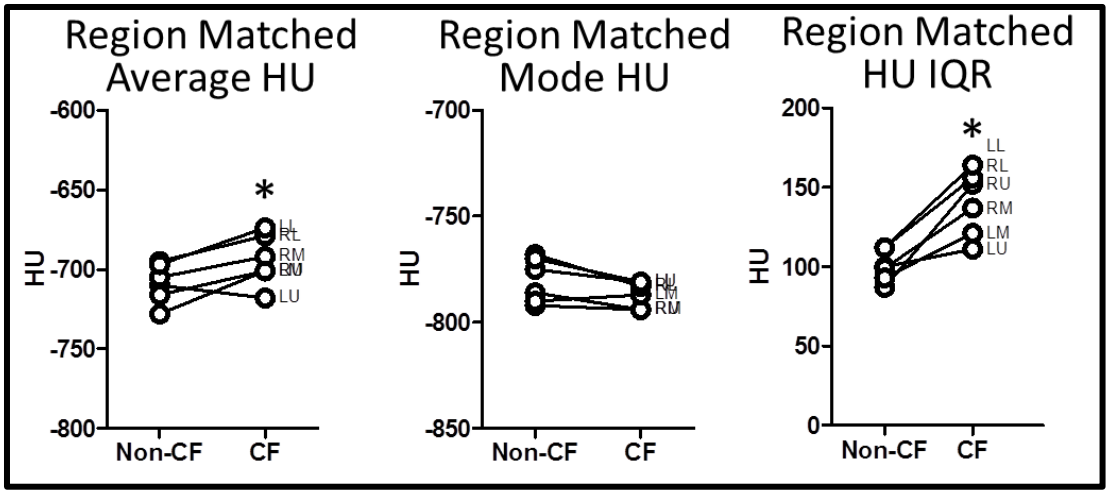

Figure 30. Hounsfield Unit histogram results at 25 cmH_2O for three week old non-CF and CF pigs. These data correspond to the tabular results from the prior figure. Dots represent a per-animal average within respective genotypes, and lines connect respective lung regions between genotypes. Initials label the six lung regions. *P<0.05

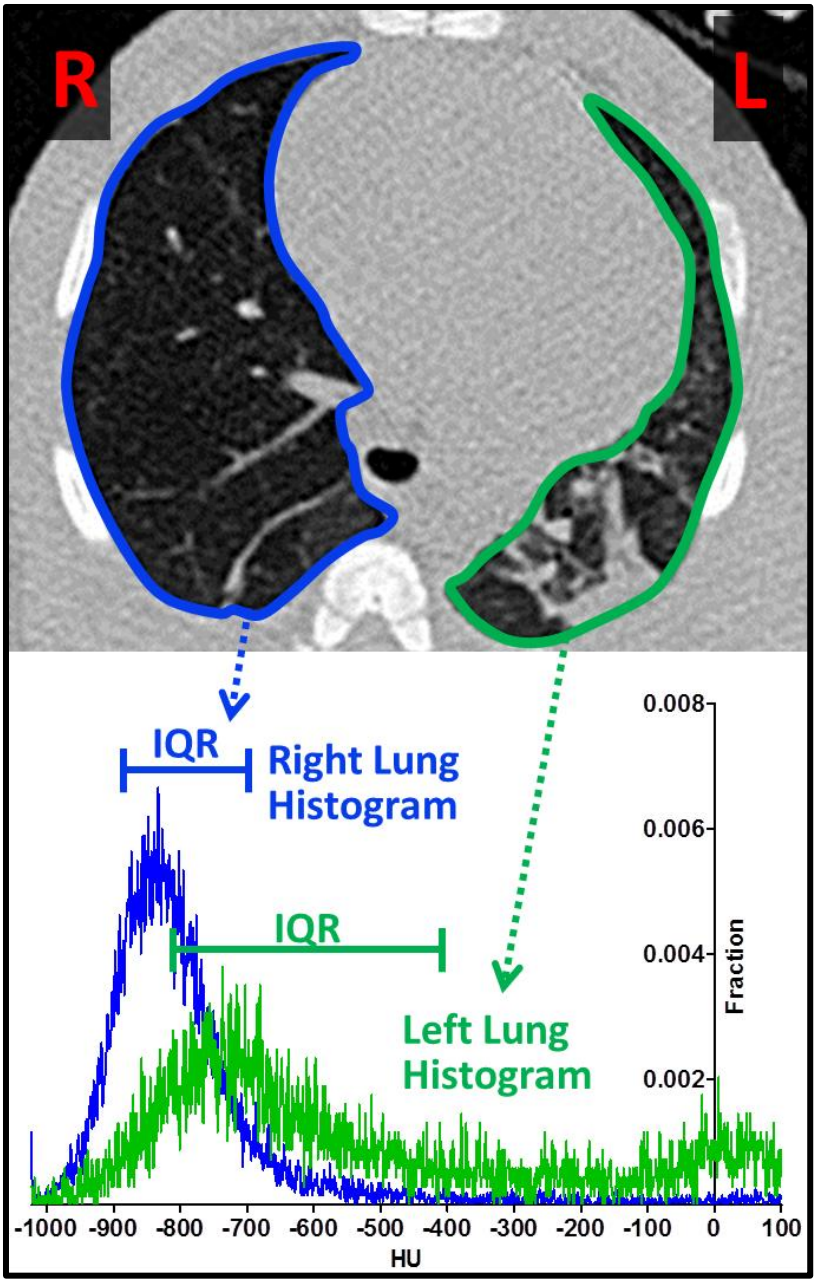

Figure 31. Variability in lung density and variability in lung HU histograms. (Top), one slice from a chest CT scan of a three week old CF pig. The right lung is traced with a blue line and the left lung is traced with a green line. The right lung is relatively homogenous in HU. The left lung is patchy and has radiologic opacities. (Bottom), HU histograms for the right lung (blue line) and left lung (green line). The IQR is overlaid. Compared to the right lung, the left lung HU histogram has more variability, as indicated by its greater IQR.

A. Three Week Old Non-CF Pigs Regional HU IQR

Animal ID	RU	LU	RM	LM	RL	LL	Animal Avg.	Animal Max	Animal STDEV
A	71	79	74	72	72	76	74	79	3
B	72	80	78	70	88	83	79	88	7
C	82	106	92	95	138	177	115	177	36
D	77	83	89	84	94	85	85	94	6
E	94	101	98	88	96	90	95	101	5
F	119	91	103	97	104	100	102	119	9
G	85	105	112	111	142	158	119	158	27
H	85	126	96	84	109	99	100	126	16
I	98	130	151	132	162	137	135	162	22
Reg. Avg.	**87**	**100**	**99**	**93**	**112**	**112**			
Reg. Stdev.	**15**	**19**	**23**	**19**	**29**	**36**			

B. Three Week Old CF Pigs Regional HU IQR

Animal ID	RU	LU	RM	LM	RL	LL	Animal Avg.	Animal Max	Animal STDEV
J	99	92	100	83	71	75	87	100	12
K	177	95	87	79	76	82	99	177	39
L	330	137	323	198	224	300	252	330	78
M	90	92	114	109	257	312	162	312	97
N	94	83	74	75	76	82	81	94	8
O	145	127	162	140	295	228	183	295	65
P	105	98	141	133	183	170	138	183	34
Q	73	100	132	133	143	133	119	143	27
R	251	176	98	138	82	95	140	251	64
Reg. Avg.	**152**	**111**	**137**	**121**	**156**	**164**			
Reg. Stdev.	**87**	**30**	**75**	**39**	**87**	**95**			

Figure 32. Regional HU interquartile range (IQR) in three week old non-CF and CF pigs. (A) IQR for each of the six lung zones denoted as RU, LU, RM, LM, RL, and LL. Animal average, max, and standard deviation (STDEV) as well as regional averages and standard deviation. (B) Shows the same data but for three week old CF pigs.

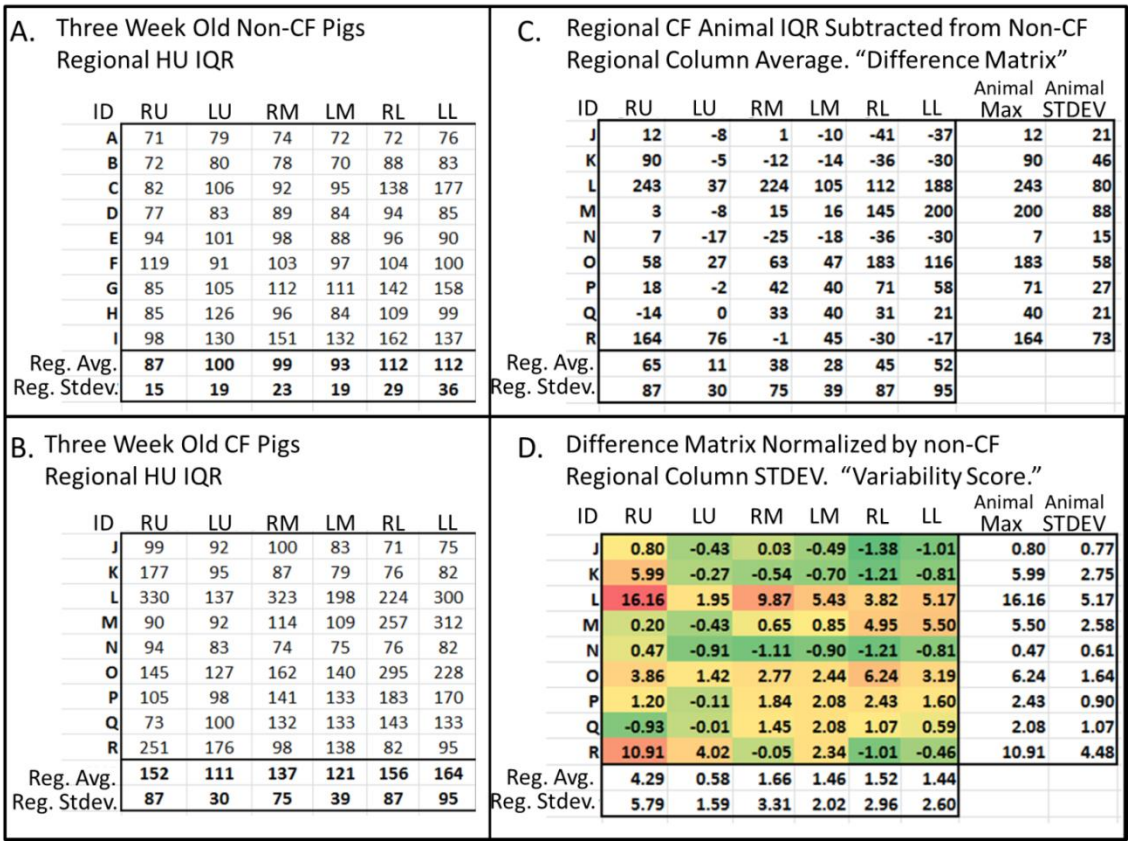

A. Three Week Old Non-CF Pigs
Regional HU IQR

ID	RU	LU	RM	LM	RL	LL
A	71	79	74	72	72	76
B	72	80	78	70	88	83
C	82	106	92	95	138	177
D	77	83	89	84	94	85
E	94	101	98	88	96	90
F	119	91	103	97	104	100
G	85	105	112	111	142	158
H	85	126	96	84	109	99
I	98	130	151	132	162	137
Reg. Avg.	87	100	99	93	112	112
Reg. Stdev.	15	19	23	19	29	36

C. Regional CF Animal IQR Subtracted from Non-CF
Regional Column Average. "Difference Matrix"

ID	RU	LU	RM	LM	RL	LL	Animal Max	Animal STDEV
J	12	-8	1	-10	-41	-37	12	21
K	90	-5	-12	-14	-36	-30	90	46
L	243	37	224	105	112	188	243	80
M	3	-8	15	16	145	200	200	88
N	7	-17	-25	-18	-36	-30	7	15
O	58	27	63	47	183	116	183	58
P	18	-2	42	40	71	58	71	27
Q	-14	0	33	40	31	21	40	21
R	164	76	-1	45	-30	-17	164	73
Reg. Avg.	65	11	38	28	45	52		
Reg. Stdev.	87	30	75	39	87	95		

B. Three Week Old CF Pigs
Regional HU IQR

ID	RU	LU	RM	LM	RL	LL
J	99	92	100	83	71	75
K	177	95	87	79	76	82
L	330	137	323	198	224	300
M	90	92	114	109	257	312
N	94	83	74	75	76	82
O	145	127	162	140	295	228
P	105	98	141	133	183	170
Q	73	100	132	133	143	133
R	251	176	98	138	82	95
Reg. Avg.	152	111	137	121	156	164
Reg. Stdev.	87	30	75	39	87	95

D. Difference Matrix Normalized by non-CF
Regional Column STDEV. "Variability Score."

ID	RU	LU	RM	LM	RL	LL	Animal Max	Animal STDEV
J	0.80	-0.43	0.03	-0.49	-1.38	-1.01	0.80	0.77
K	5.99	-0.27	-0.54	-0.70	-1.21	-0.81	5.99	2.75
L	16.16	1.95	9.87	5.43	3.82	5.17	16.16	5.17
M	0.20	-0.43	0.65	0.85	4.95	5.50	5.50	2.58
N	0.47	-0.91	-1.11	-0.90	-1.21	-0.81	0.47	0.61
O	3.86	1.42	2.77	2.44	6.24	3.19	6.24	1.64
P	1.20	-0.11	1.84	2.08	2.43	1.60	2.43	0.90
Q	-0.93	-0.01	1.45	2.08	1.07	0.59	2.08	1.07
R	10.91	4.02	-0.05	2.34	-1.01	-0.46	10.91	4.48
Reg. Avg.	4.29	0.58	1.66	1.46	1.52	1.44		
Reg. Stdev.	5.79	1.59	3.31	2.02	2.96	2.60		

Figure 33. Interquartile range data, Difference Matrix, and Variability Score. (A) IQR for each lung zone for each three week old non-CF, and (B) CF animal. (C) The IQR Difference Matrix for CF animals. To obtain this matrix we subtracted respective regional IQRs of CF animals from the average regional IQR across non-CF animals. For example, Animal J has a difference of "12" in the right upper zone. To obtain this we subtracted Animal J's right upper zone IQR, which is "99", from the average IQR across all non-CF animals for the right upper zone, this is "87." 99-87 = 12. (D) We next normalized the Difference Matrix by the WT standard deviation (Regional Stdev from Part A). Continuing our example with Animal J…the difference in the right upper zone is "12." We then normalized this by the non-CF standard deviation for the right upper zone; this value is "15." 12/15 = 0.8. We refer to this value as the "Variability Score." This table has been color coded by value, where the greatest value is red, the lowest green, and intermediate values intermediate colors.

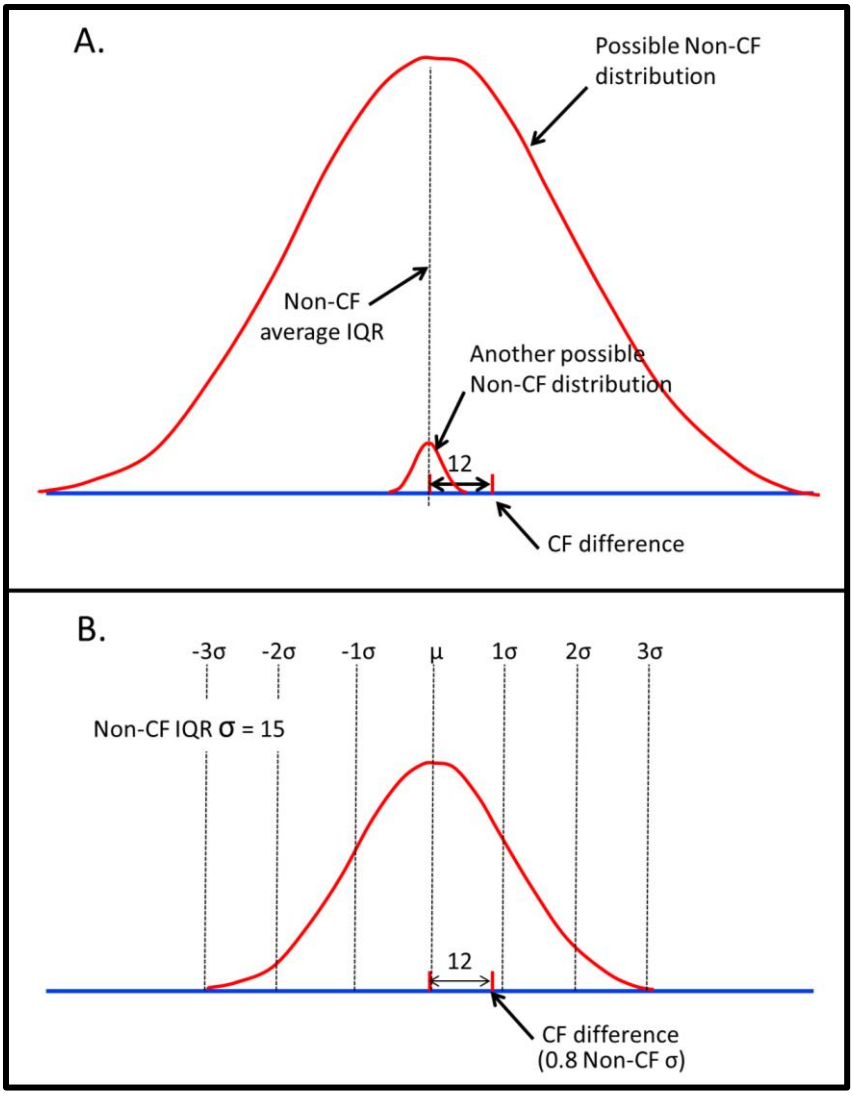

Figure 34. Rationale behind normalization of the Difference Matrix by standard deviation. (A) In this example, the difference is 12. Is that a large difference or a small difference? Anwer: it depends upon the underlying distribution. If non-CF has a wide distribution, then a difference of 12 is not far from the non-CF mean. If non-CF has a narrow distribution, then a difference of 12 is large. (B) In this example, the non-CF IQR standard deviation, denoted as σ, is 15. Continuing this example, 12/15 = 0.8, hence, we know that a difference of 12 is a little less than one standard deviation. Normalization by standard deviation provides scale.

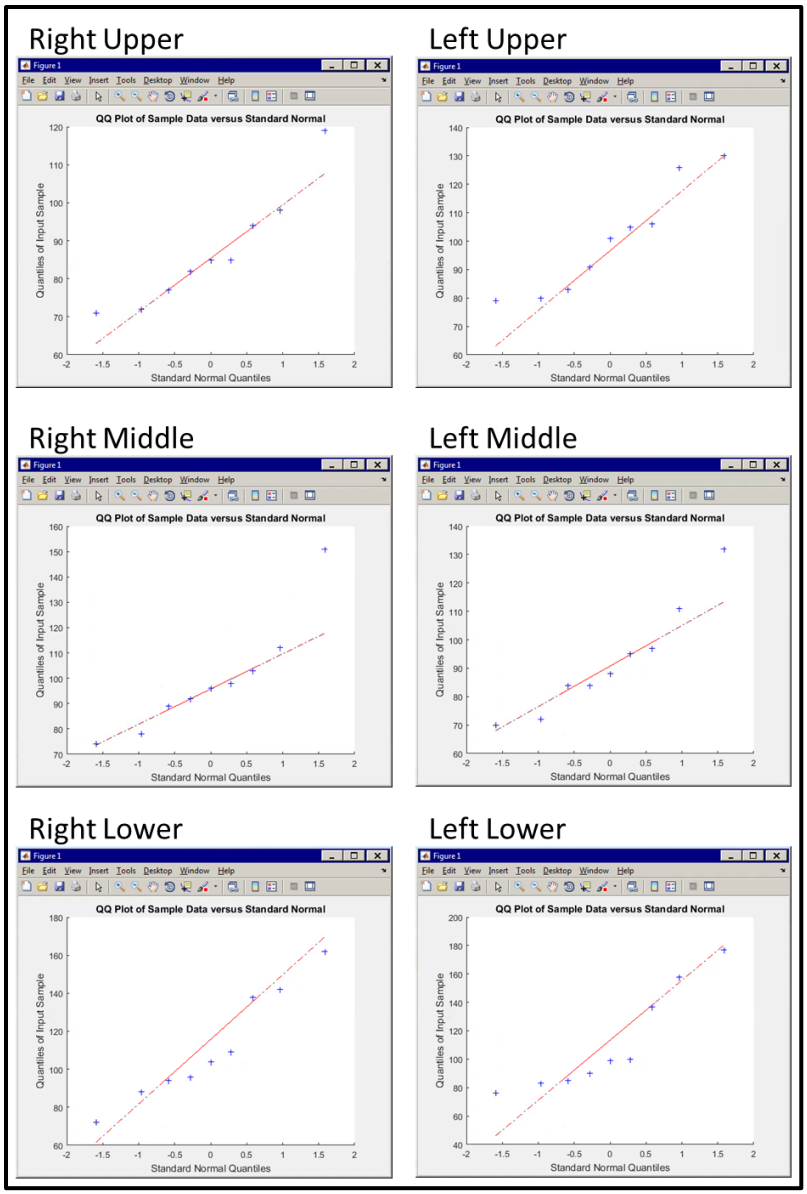

Figure 35. QQ plots of the non-CF HU IQR for each of the six lung regions. QQ plots resemble a straight line suggesting that the non-CF IQR distributions within each zone do not differ greatly from a normal distribution. There are 9 points within each plot, each representing a single non-CF animal.

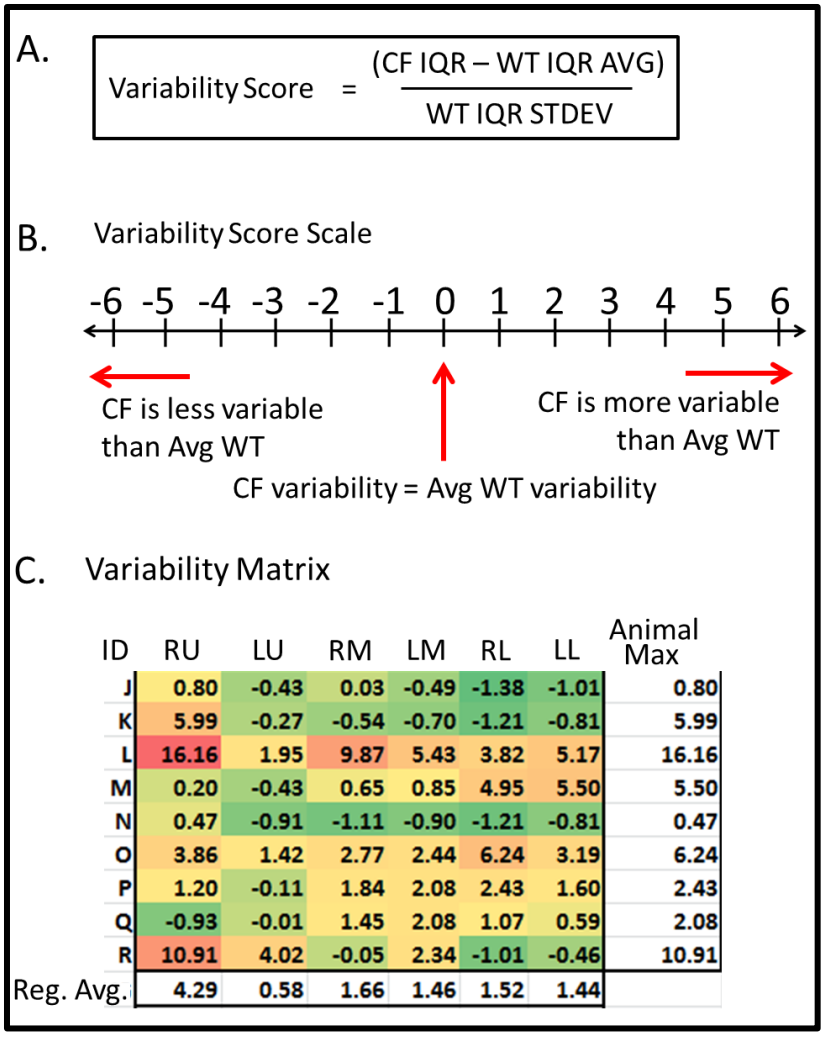

ID	RU	LU	RM	LM	RL	LL	Animal Max
J	0.80	-0.43	0.03	-0.49	-1.38	-1.01	0.80
K	5.99	-0.27	-0.54	-0.70	-1.21	-0.81	5.99
L	16.16	1.95	9.87	5.43	3.82	5.17	16.16
M	0.20	-0.43	0.65	0.85	4.95	5.50	5.50
N	0.47	-0.91	-1.11	-0.90	-1.21	-0.81	0.47
O	3.86	1.42	2.77	2.44	6.24	3.19	6.24
P	1.20	-0.11	1.84	2.08	2.43	1.60	2.43
Q	-0.93	-0.01	1.45	2.08	1.07	0.59	2.08
R	10.91	4.02	-0.05	2.34	-1.01	-0.46	10.91
Reg. Avg.	4.29	0.58	1.66	1.46	1.52	1.44	

Figure 36. Variability Score. (A) The equation used to calculate Variability Score is a modification of a Z-score calculation. It finds the difference in IQR between an individual CF animal from the average non-CF animal and then normalizes this difference by the non-CF standard deviation. (B) A Variability Score of 0 indicates that the CF animal tissue variability equals the average non-CF tissue variability. A score less than 0 indicates CF tissue variability that is less than the non-CF average, and a score greater than 0 indicates that CF tissue variability exceeds the average non-CF variability. (C) Color coded Variability Scores for three week old CF animals. The most variable region is colored red, the least variable green, and intermediate variability is colored with intermediate colors.

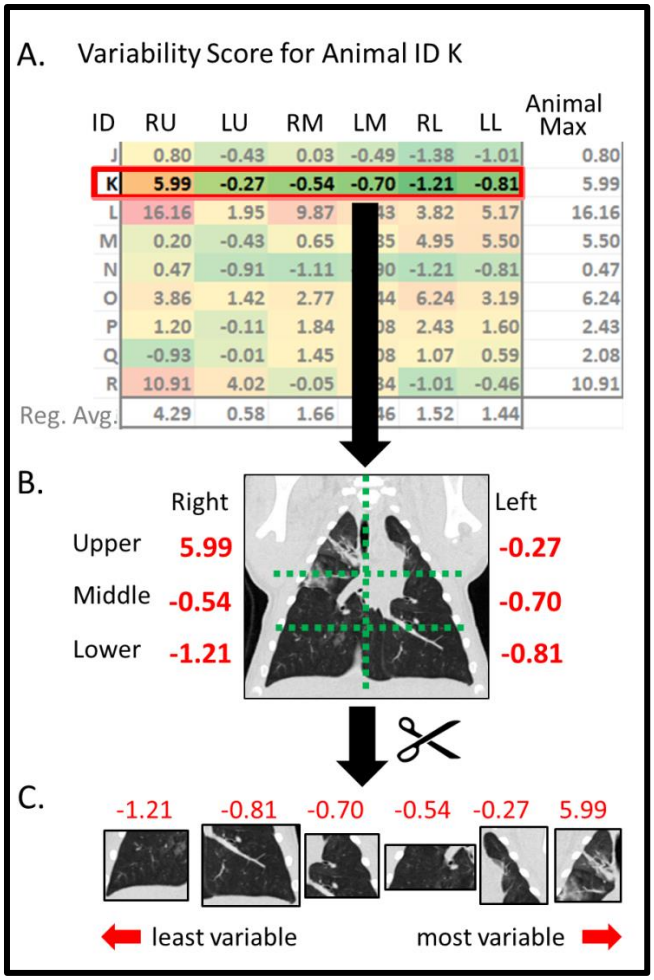

Figure 37. Using the Variability Score, an example. (A) The Variability Score matrix with animal K highlighted. (B) A coronal plane slice from Animal K's inspiratory chest CT scan with the Variability Score listed adjacent to their respective lung zones. (C) This CT image was "cut" into the six lung zones, and ordered from smallest to greatest Variability Score. The visual appearance of the scans corroborates the score; the tissue with the lowest Variability Score is homogenous and dark, while the tissue with the highest Variability Score is patchy in appearance.

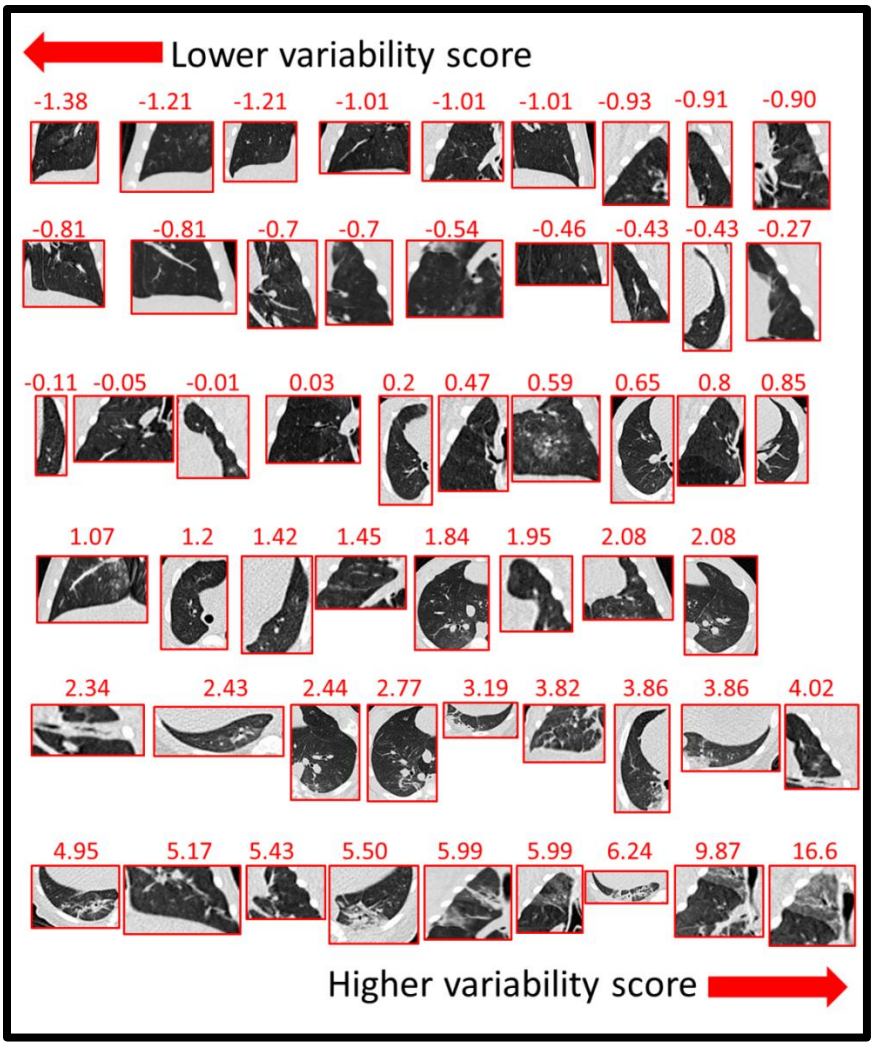

Figure 38. CT images of three week old CF pigs with their Variability Score. This figure is an extension of the previous figure, except rather than showing a scan and Variability Scores for one CF animal, here we are showing scans and Variability Scores for all three week old CF animals. Each zone from each three week old CF animal is shown as a separate image. There are six zones per animal and nine animals total resulting in 54 zones in total. Images are arranged in order from lowest to highest Variability Score. In general, upon visual inspection, the appearance of the tissue in the scan image corresponds to the Variability Score, where more heterogenous tissues have higher Variability Scores and the homogenous tissues lower scores.

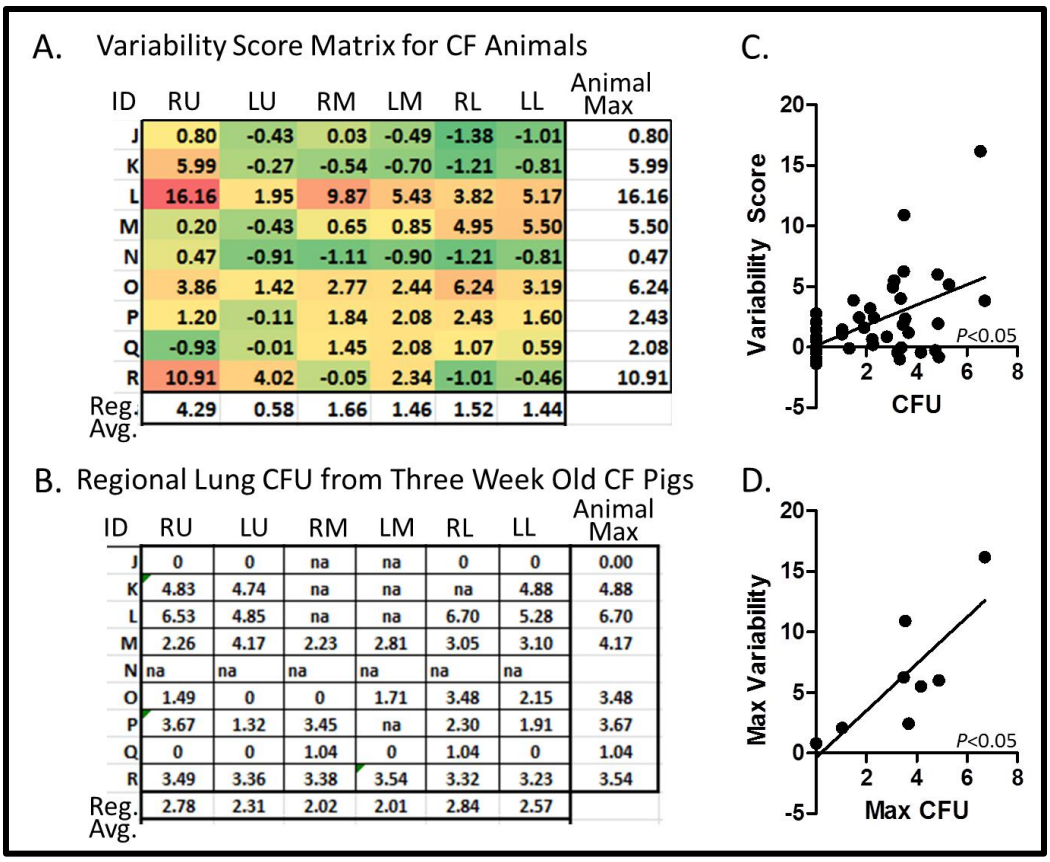

Figure 39. Variability Score and infection correlation. (A) Variability matrix for three week old CF pigs. (B) Regional CFU data for three week old CF pigs. Count in log+1. "na" designates "not any", meaning no specimens were collected for bacterial analysis. (C) There was a statistically significant, linear, positive correlation between regional Variability Score and regional CFU. (D) There was a statistically significant, positive, linear correlation between the within animal maximum Variability Score and the within animal maximum CFU. Pearson's Correlation Coefficient was used to determine the significance of correlation.

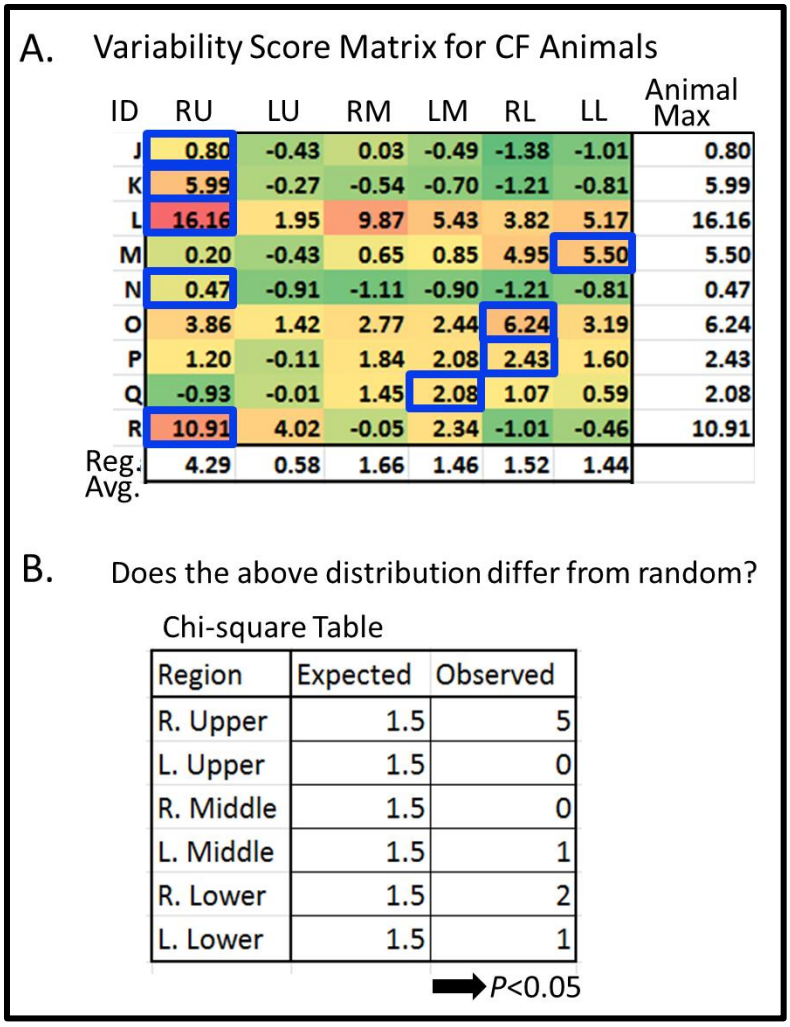

Figure 40. Regional analysis of Variability Score. (A) Boxes enclose the highest Variability Score within animals. (B) Using a Chi-square test we determined that the regional distribution of within animal maximum Variability Score for the three week old CF pig population differed significantly from a random distribution. Chi-square table entries represent number of animals. With 9 animals in the study and six lung zones, we would expect 1.5 animal's most variable zone to be the right upper, and 1.5 the left upper, etc.

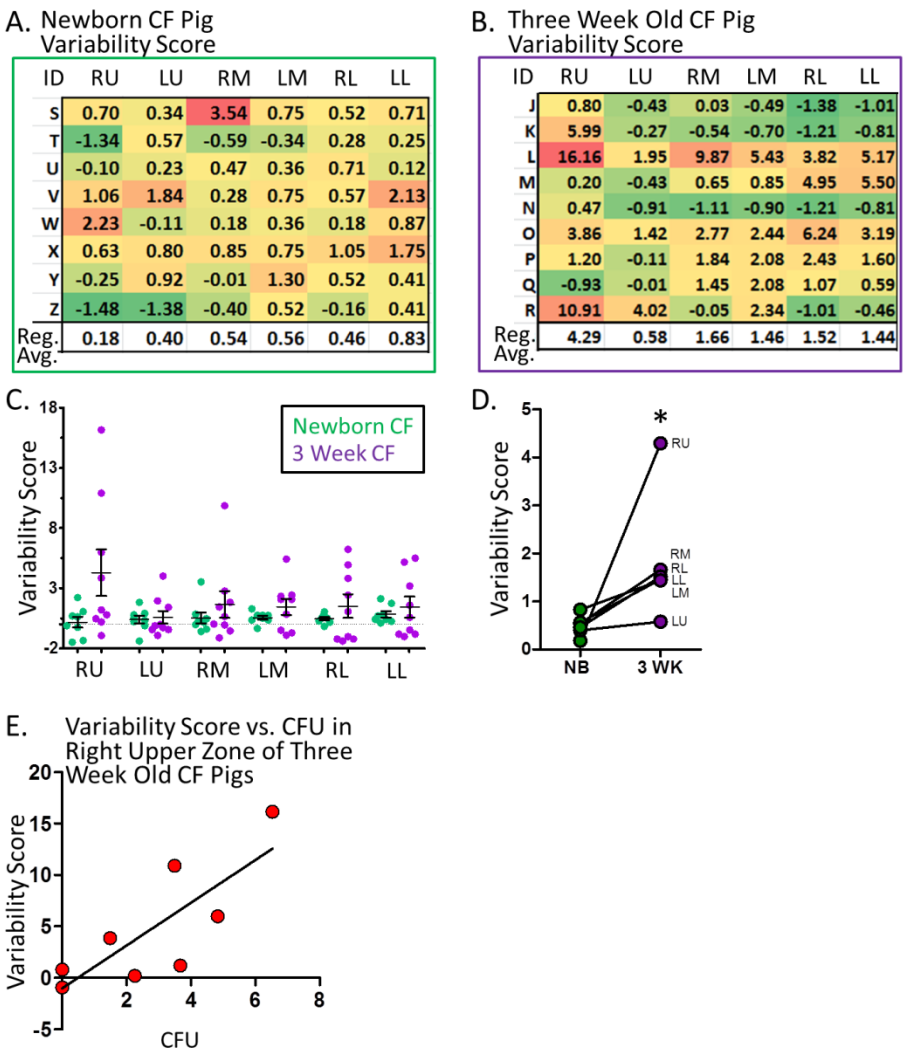

Figure 41. Newborn and three week old CF pig Variability Scores. (A) The newborn CF pig Variability Score table. As the three week old CF pig Variability Score is relative to three week old non-CF animals, the newborn CF pig Variability Scores are relative to newborn non-CF pigs. Color coded by degree of variability. (B) Variability Scores in three week old CF pigs. (C) Variability Scores of newborn and three week old CF pigs. This is a graphical form of the matrices from Part A and B. There were no statistically significant differences between animal groups within any of the six lung zones. However, notice that within each zone three week old CF animals are greater than newborn CF animals on average. Bars represent average ± SEM. (D) Paired newborn (NB) and three week old (3 WK) CF pig average Variability Scores. Each dot represents a regional average from the matrices in A and B, or the average bars in Part C. (E) Variability Score significantly correlates with CFU in the right upper zone of three week old CF pigs. *P<0.05

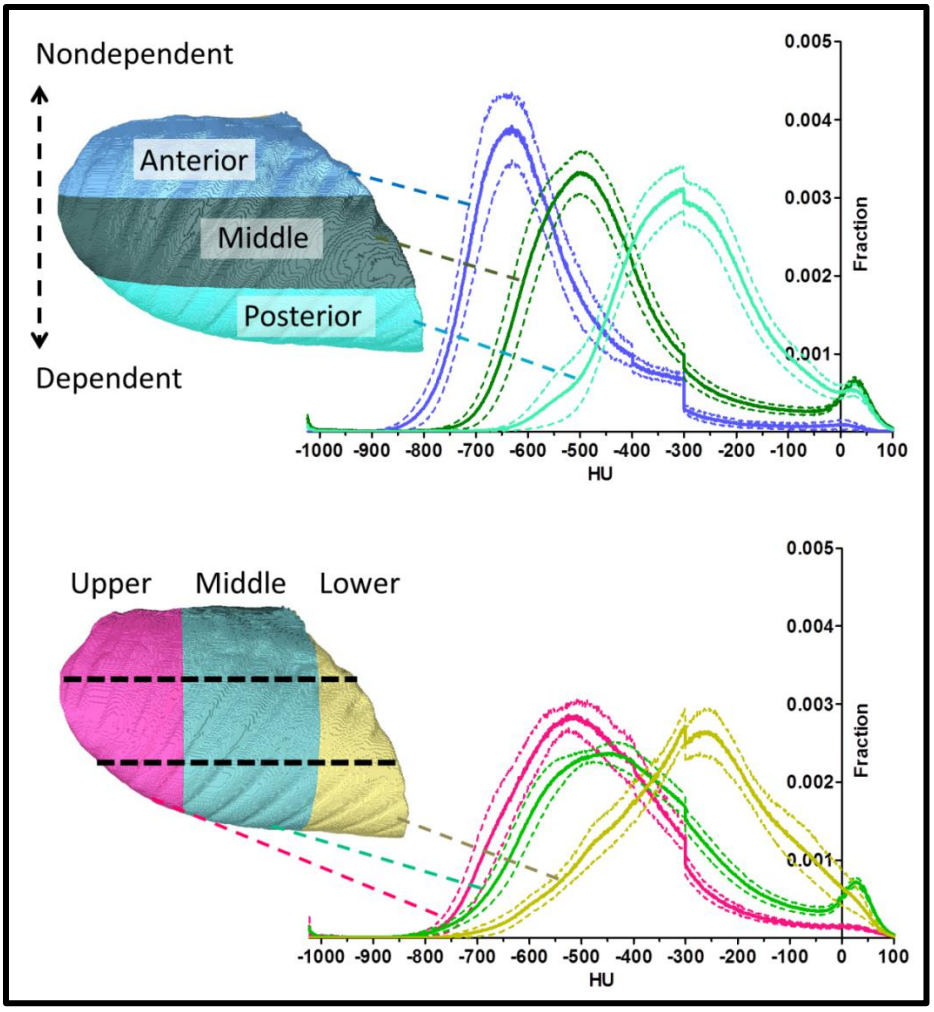

Figure 42. Dependent and independent lung zones in the pig. (Top) In the supine scanned pig, the anterior lung is nondependent and the posterior dependent. HU histograms at 0 cmH_2O of the anterior, middle, and posterior thirds, show the anterior to be the least dense, the posterior the most dense and the middle, intermediate. (Bottom) The lung divided into upper, middle, and lower thirds with accompanying HU histograms at 0 cmH_2O. Dotted lines approximate anterior, middle, and posterior thirds on the lung. The HU histograms indicate the upper lung to be the least dense, the lower the most dense, and the middle of intermediate density.

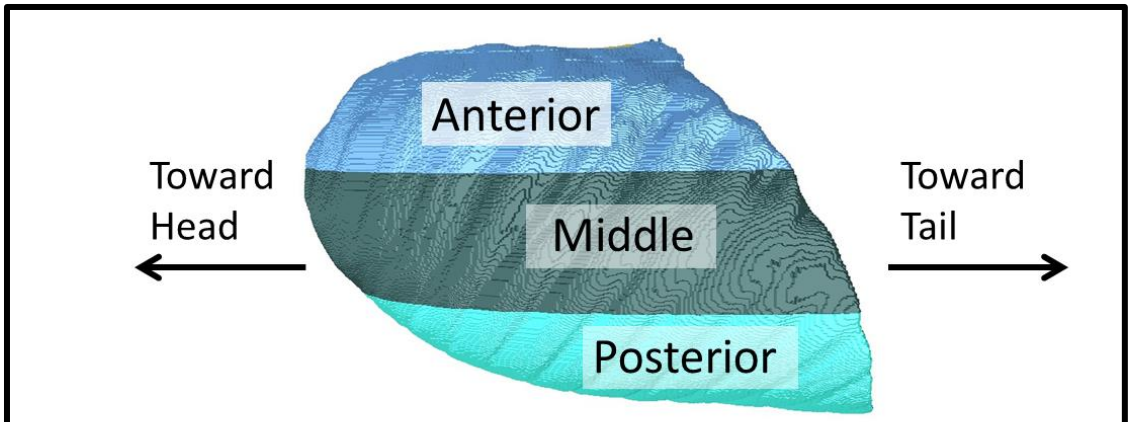

ID	RP	LP	RM	LM	RA	LA	Animal Max	Animal STDEV
J	-0.77	-1.02	0.98	-0.37	-0.25	0.94	0.98	0.85
K	-0.93	-0.72	3.24	-0.75	-0.36	-0.29	3.24	1.59
L	3.76	4.76	16.54	2.93	10.94	3.17	16.54	5.54
M	2.18	4.46	-0.46	-0.56	0.20	0.40	4.46	1.95
N	-1.00	-0.92	-0.19	-0.52	-0.85	-1.60	-0.19	0.48
O	4.89	3.34	2.69	0.20	-0.51	0.48	4.89	2.11
P	1.11	1.39	1.52	0.63	-0.02	0.17	1.52	0.64
Q	0.44	0.90	2.55	2.12	-0.25	0.40	2.55	1.08
R	-0.54	0.54	2.42	2.07	2.64	6.94	6.94	2.57
Reg. Avg.	1.02	1.42	3.25	0.64	1.28	1.18		
Reg. Stdev.	2.17	2.27	5.15	1.39	3.76	2.50		

Figure 43. Three week old CF pig Variability Scores at 25 cmH_2O for anterior, middle, and posterior lung thirds. (Top) Lateral view of lung divided into thirds. (Bottom) Variability Scores for respective zones within respective animals color coded by relative intensity. Boxes enclose the region of greatest Variability Score within an animal. RP = right poster, LP = left posterior, RM = right middle, LM = left middle, RA = right anterior, LA = left anterior.

CHAPTER 5: ACUTE ADMINISTRATION OF IVACAFTOR

5.1 INTRODUCTION

Ivacaftor is a new drug for treatment of people with CF and the *G551D* mutation (and some related mutations) [24, 111-113]. G551D-CFTR reaches the cell surface, as functional CFTR does, however, once there conducts chloride and bicarbonate with very low efficiency. Ivacaftor is an oral, bioavailable, small molecule that induces a conformation change in G551D-CFTR. This conformational change, in turn, increases the channel's open probability [24], and in doing so largely restores function (Figure 44). This process is referred to as "potentiation." Ivacaftor is the first drug for CF that effectively targets CFTR directly, rather than treat symptoms of CFTR's disruption. People with *G551D-CFTR* who take ivacaftor exhibit a rapid and sustained improvement in pulmonary health [26-27, 114-115].

People with CF commonly exhibit a number of lung and airway abnormalities. It is often unclear which of these are primary to CFTR disruption, and which are caused by longstanding lung infection and inflammation (a.k.a. secondary to *CFTR* disruption), which can cause abnormalities independent of CFTR disruption. Separating the two is important. Abnormalities primary to CFTR disruption represent the "roots" of CF lung disease. Identification of these primary defects may enable treatments that target "root" problems.

People with CF commonly exhibit abnormal airway smooth muscle behavior including evidence of airway hyper-reactivity, evidence of increased basal tone, and bronchodilator reversed obstruction to airflow [10-11, 13]. These collectively have been referred to as "CF-asthma [13]." Whether abnormal smooth muscle behavior in people with CF is a primary or secondary consequence of CFTR disruption is unknown. This was the central question of our study.

There are at least two ways to separate primary from secondary defects experimentally. One is to perform studies in neonates with CF. At this age the effects of lung infection and inflammation would likely be limited, thus observed abnormalities

would likely be primary to CFTR disruption. But, studies of people with CF at this age are extremely limited.

An alternate approach is to *acutely restore* CFTR in adults with CF using a CFTR potentiator. This is the approach we used in the current study. We did a before-after drug test in adults with *G551D-CFTR* using ivacaftor. We chose a two day time interval. We reasoned that two days was long enough to "activate" CFTR yet not long enough to appreciably change longstanding (decades) lung infection and inflammation. The implication is that observed changes would likely reflect augmentation of CFTR activity rather than alterations in infection and inflammation, that is, changes would be primary to CFTR.

We formed two hypotheses. First, that ivacaftor would be efficacious over a two day interval. We tested this hypothesis primarily with spirometry and by measuring sweat chloride concentration. Second, based upon evidence of increased basal airway smooth muscle tone in people with CF and newborn CF pigs [18], we hypothesized acute administration of ivacaftor to decrease smooth muscle tone. We tested this by measuring airway distensibility from chest CT scans, with spirometry before and after bronchodilator, and with pulse wave analysis, a method for assessing vascular smooth muscle tone. Twelve people participated in this study. The study presented in this chapter has been previously published, and was funded, in part, by an unrestricted grant from the Vertex Pharmaceuticals Investigator-Initiated Studies Program [60].

5.2 METHODS

Study Design

Twelve adults with CF with at least one *G551D-CFTR* allele were included in this study. None had taken ivacaftor prior to this study. They completed the following tests before and after two days of ivacaftor administration: sweat chloride concentration, inspiratory (TLC) and expiratory (RV) chest CT, spirometry before and after salbutamol

administration, and pulse wave analysis. The people in this study did not otherwise alter their regular treatment regimen. This study was prospective in nature and took place in Dublin, Ireland at St. Vincent's University Hospital. All procedures were reviewed and approved by the Research Ethics Committee of St. Vincent's University Hospital. Study adherence was 100%. Additional methodological description has been previously published [60].

Chest CT and Analysis

Chest CT scans were acquired first at coached TLC (inspiratory scan), and then at coached RV (expiratory scan). Participants were scanned in the supine position. In – plane voxel dimensions were matched on a subject by subject basis between baseline and the two day scans by implementing consistent reconstruction diameters. Participants took three deep breaths prior to scanning to standardize lung history, and for recruitment. Breathing maneuvers were practiced prior to scan acquisition. The CT scanner was a GE HD750. Scan specifications are as follows: 120 kV, 180 mA, 0.625 mm slice thickness with an interval of 0.5 mm, and a pitch of 0.984:1.

Airway and lung measurements were obtained using VIDA Diagnostic's Apollo Software. Measurements, including airway wall thickness, and airway lumen area, were obtained for 42 airways within each scan. These airways included the trachea through RB10 and LB10, plus an additional two airway generations beyond RB1, RB4, RB10, LB1, and LB10 (e.g. LB10a, LB10ai), resulting in one airway "path" for each of the five lung lobes, similar to [116]. Similar to [76], airway distensibility was defined as: (100x[insp. lumen area – exp. lumen area]/exp. lumen area).

Pulse Wave Analysis

We assessed arterial stiffness via pulse wave analysis using a SphymgorCor machine (Core Medical). Participants were in a supine position during measurement

acquisition. AIx measurements were corrected for a heartrate of 75 beats per minute. Pulse wave velocity was calculated as transit distance divided by transit time.

5.3 RESULTS

Demographics

Twelve people participated in this study. All had at least one *G551D-CFTR* allele. For eight of the twelve, the other allele was *F508del-CFTR*. The remaining four second *CFTR* alleles respectively had *G551D*, *P67L*, *R117H*, and *3659delC* mutations. Baseline sweat chloride was elevated in this population, and was on average 94 mmol/l. Average baseline FEV_1 was 64 % of predicted, and ranged from 34 to 101 % of predicted. Participants averaged 31 years of age.

Sweat Chloride and Spirometry

We first had to determine if ivacaftor does anything over only two days, as it is estimated to reach blood serum steady state in 3-5 days [32], and there were no published findings over a two day interval. To test CFTR function we assayed sweat chloride concentration. Sweat chloride is naturally elevated in people with CF. We hypothesized that two days of G551D-CFTR potentiation with ivacaftor would reduce sweat chloride concentration. We observed a significant reduction in sweat chloride (Figure 45A). We assessed lung function with spirometry. We found a significant improvement in FEV_1, FVC, and FEF_{25-75}, (Figure 45B, 45C, 45D).

Air Trapping on CT

Air trapping is the excessive retention of air upon exhalation, is caused by obstruction to airflow, and is one of the earliest radiographic manifestations of CF lung disease in people and pigs [5, 7, 89]. We hypothesized two days of ivacaftor therapy to

reduce air trapping. We assessed air trapping using expiratory (residual volume) chest CT scans, where, like previous studies, we defined air trapping as the percent of lung volume with an HU below -856 (Figure 46) [117]. Air, by definition, has an HU of -1000, and water an HU of 0. Thus, a threshold of -856 HU is designed to enumerate relatively aerated lung regions.

In our study we observed a trend for reduction in whole lung air trapping (*P*=0.052), (Figure 47A). We also assessed air trapping for the upper (toward the head), middle, and lower (toward the feet) thirds of the lung, respectively (Figure 47B). We observed a similar absolute reduction in the level of trapped air for each lung third, however, for only the lower third was this change statistically significant. Hypoperfusion could also reduce the density of lung tissue on CT. However, we observed a statistically significant, linear, positive correlation between air trapping (-856%) and RV/TLC, suggesting that the decrease in air trapping we observed with ivacaftor therapy was likely due to changes in air volume rather than perfusion.

Average inspiratory lung volume increased, and expiratory lung volume decreased with ivacaftor therapy, albeit neither to a statistically significant degree (Figure 47D, 47E). Seven of the twelve participants improved in air trapping and FEV_1 % predicted. Furthermore, there was a significant correlation between change in FEV_1 % predicted and change in air trapping, such that the people who improved the most in FEV_1% also improved the most in air trapping (Figure 47F).

Assessing Smooth Muscle Tone Before and After Acute Ivacaftor Therapy

We found that two days of ivacaftor therapy improved CFTR function and improved lung function as assessed by spirometry and CT-based measures of air trapping, but does it relax airway smooth muscle? We assayed smooth muscle in three ways. First, we measured airway distensibility from chest CT scans. Second, from spirometry before and after bronchodilator, and third, we assessed vascular tone using pulse wave analysis.

Bronchodilator. Salbutamol is a bronchodilator that is commonly used by asthmatics in an aerosolized form [118-119]. Primarily through bronchodilation, it can increase FEV_1 in people with airway narrowing due to increased smooth muscle tone. In the current study, we performed spirometry before and after administration of salbutamol at baseline and after two days of ivacaftor therapy. We hypothesized the improvement in FEV_1 following salbutamol would be decreased after two days of ivacaftor therapy on account of an airway smooth muscle relaxing effect by ivacaftor – ivacaftor will have "pre-relaxed" the airways.

At baseline (before ivacaftor), salbutamol increased FEV_1 by an average of 3.9 ± 0.7% predicted. After two days of ivacaftor therapy the salbutamol response was significantly reduced: 2.1 ± 0.5 % predicted ($P<0.05$, Figure 48). However, from this study we are unable to say if the salbutamol response was reduced on account of "pre-relaxed" airways, or because ivacaftor increased FEV_1 independent of salbutamol, and the reduction in the salbutamol effect was decreased with ivacaftor because of an FEV_1 ceiling effect. None-the-less, a reduction in the salbutamol effect with ivacaftor was consistent with a relaxation of airway smooth muscle by ivacaftor.

Airway distensibility. Smooth muscle tone is a regulator of airway distensibility, the ability of an airway to distend, or reduce in size, in response to pressure changes [76, 120-121]. We hypothesized acute administration of ivacaftor to increase airway distensibility, a result that would be consistent with a decrease in airway smooth muscle tone. To test this hypothesis we acquired chest CT scans at TLC (inspiratory) and RV (expiratory), and calculated airway distensibility of 42 select airway segments (Figure 49). We stratified these airways into three groups based upon their baseline, inspiratory, lumen diameter where "small" airways were <4.5 mm in diameter, "medium" between 4.5 and 6.5 mm in diameter, and "large" airways >6.5 mm in diameter. We found a significant increase in airway distensibility for small airways, but not for medium or large airways (Figure 50A). Expiratory small airway lumen cross-sectional area decreased, on average, with ivacaftor, and average inspiratory lumen cross-sectional area increased, albeit neither change reached statistical significance. There was little change in

expiratory and inspiratory lumen size with ivacaftor for medium and large airways (Figure 50B).

There are at least two ways that airway distensibility could change independent of changes in smooth muscle tone. First, reductions in air trapping could increase airway distensibility. A reduction in air trapping could enhance the effects of periodic deep inspirations, which have been shown to relax airway smooth muscle [91]. However, there was no correlation between change in air trapping and change in airway distensibility. In addition, changes in airway wall thickness could influence airway distensibility. We measured airway wall thickness before and after acute administration of ivacaftor and found no statistically significant changes (Figure 50C).

Vascular smooth muscle tone. Based upon our findings in the lung, we hypothesized that ivacaftor would have an effect on smooth muscle tone systemically. We tested this hypothesis by assaying vascular smooth muscle tone (vascular stiffness) with pulse wave analysis; the assessment of blood pressure waveforms as they propagate through the vasculature.

We first measured augmentation index (AIx). AIx is a measure of the reflected wave's augmentation to systolic blood pressure. A decrease in vascular smooth muscle tone would cause a decrease in AIx. AIx significantly decreased with ivacaftor therapy (Figure 51A). We next measured pulse wave velocity, the propagation velocity of a blood pressure pulse. We observed a significant reduction in pulse wave velocity, a result consistent with a relaxation of vascular smooth muscle (Figure 51B).

We observed an increase in airway distensibility, suggestive of a relaxation of airway smooth muscle tone. We also observed a decrease in pulse wave velocity, suggestive of reduction in vascular smooth muscle tone. If both findings were caused by a relaxation in smooth muscle tone, then we may expect their respective changes with ivacaftor to correlate with each other. We observed a significant correlation between change in small airway distensibility and change in pulse wave velocity on a per person basis (Figure 51C).

5.4 DISCUSSION

The primary objective of this study was to assess smooth muscle function in people with *G551D-CFTR* before and after acute administration of ivacaftor. We tested this in three ways. These included spirometry before and after bronchodilator, airway distensibility as assessed with chest CT scans, and with pulse wave analysis. The results of all three were consistent with a relaxation of smooth muscle tone.

CFTR and Smooth Muscle

Abnormal smooth muscle behavior has been described in people with CF [10, 13], in CF mice [122], and CF pigs [8, 18]. The data from this study suggest that the obstruction commonly observed in people with CF may, at least in part, be caused by abnormal smooth muscle behavior including increased airway smooth muscle tone.

We observed an increase in small airway distensibility, but not in medium or large airway distensibility. Why might this be? Anatomically, in absolute terms, smaller airways have less smooth muscle than larger airways, however, they have more after normalization by airway size [123-124]. Hence, perhaps the small airways were more affected because they had relatively more smooth muscle, although, the effects of chronic infection and inflammation on this pattern of smooth muscle distribution is unknown. In addition, larger airways are known to have more airway cartilage than smaller airways. Perhaps, increased presence of cartilage masked changes in larger airway smooth muscle relaxation. An increase in small but not large airway distensibility following ivacaftor treatment is consistent with a study in asthmatics in which smaller airways responded more to bronchodilators [125].

An increase in small airway distensibility is consistent with a relaxation of airway smooth muscle, however, airway distensibility could also potentially be influenced by changes in other factors such as mucus. We included our measure of vascular stiffness in large part to address potential confounders like these - there is no mucus in the

vasculature. Correlated reductions in small airway distensibility and pulse wave velocity suggest an effect of ivacaftor on smooth muscle tone.

Interestingly, the increase of FEV_1 in response to ivacaftor exceeded that of FEV_1 to salbutamol at baseline. Why might this be? It could be because ivacaftor affects many aspects of lung physiology (e.g. smooth muscle, mucus, etc.) and the increase in FEV_1 represents a summation of all of these effects. In contrast, salbutamol's effect is primarily on smooth muscle, and hence, its effect on FEV_1 represents only a fraction of ivacaftor's. In addition, ivacaftor may have been more effective because through the vasculature it reaches airways that aerosolized salbutamol cannot.

Additional Potential Mechanisms

Our results suggest that improvement in lung function following ivacaftor therapy to be mediated, at least in part, by relaxation of airway smooth muscle. However, it is possible that additional factors contributed to this improvement. One such factor could be inflammation. In fact, a separate study of the same cohort found significant reductions in γ inducible proteins on blood monocytes [126]. However, the GOAL study, which examined a large cohort of people before and after ivacaftor therapy, found no significant changes in sputum inflammatory markers over 6 months of ivacaftor therapy [30]. Moreover, the response of smooth muscle to an acute reduction in inflammation following decades of inflammatory exposure is unknown.

Acute alteration of mucus behavior possibly contributed to improvement in lung function. The GOAL study found improvement in mucociliary clearance over 1 month of ivacaftor therapy in people with *G551D-CFTR* [30]. While enhanced mucociliary clearance may have contributed to the improvement in lung function in the current study, we did not assay mucus, and thus we can only comment on the acute effects of ivacaftor on mucus in a limited manner. However, correlated changes in pulse wave velocity, and airway distensibility, suggest that ivacaftor relaxes smooth muscle.

5.5 CONCLUSIONS

This study had a number of strengths and limitations. Strengths: First, the abbreviated study duration limited changes in factors secondary to CFTR restoration, thus enabling examination of primary factors. Second, assessment of vascular smooth muscle tone using pulse wave analysis provided a measure of smooth muscle tone outside of the lung, and thus independent of pulmonary factors such as mucus, which ivacaftor may have affected. Third, prospective, standardized, high-quality chest CT scans enabled high quality measurement of lung volumes and airway sizes. Fourth, our findings are supported by human and animal studies. For example, a number of studies show smooth muscle to modulate airway distensibility [127-129]. Most airway distensibility studies in asthmatics report reductions in distensibility [130-136]. Moreover, bronchial thermoplasty, which is designed to reduce smooth tone and is used primarily in asthmatics, reduces methacholine induced reductions in airway distensibility [76]. Fifth, in our before-after drug study, subjects served as their own control, thus limiting confounders.

Limitations. First, we did not investigate other proposed mechanisms of CF lung disease including alterations in airway surface liquid pH, airway mucus, or mucociliary clearance. Second, we observed significant changes in smooth muscle tone over a two day interval. Additional studies are required to determine if these changes persist over longer periods of time. Third, our assays were designed to test smooth muscle. Other cell types, such as neurons, exhibit CFTR dependent behavior[137-138]. Additional studies are required to determine the effects of ivacaftor on neurons and other cell types. Last, our study had a relatively small sample size of twelve individuals. Despite this, we were still able to detect significant changes. Moreover, we were satisfied with the number of participants given the rarity of the *G551D* mutation, and the study nature.

The results of this study have a number of implications. First, the improvement in lung function we observed after only two days of ivacaftor was nearly the same as that observed over six months in other ivacaftor studies [26, 28, 139]. This observation suggests that a major component of ivacaftor's mechanism is fast-acting. Second, this study shows that even a study with a limited number of participants and a short study duration

can be informative, particularly when the drug is very effective, like ivacaftor. Third, these data suggest that abnormalities in airway smooth muscle in people with CF are at least in part a direct consequence of CFTR disruption, and that abnormal airway smooth muscle behavior may represent one element of CF lung disease pathogenesis.

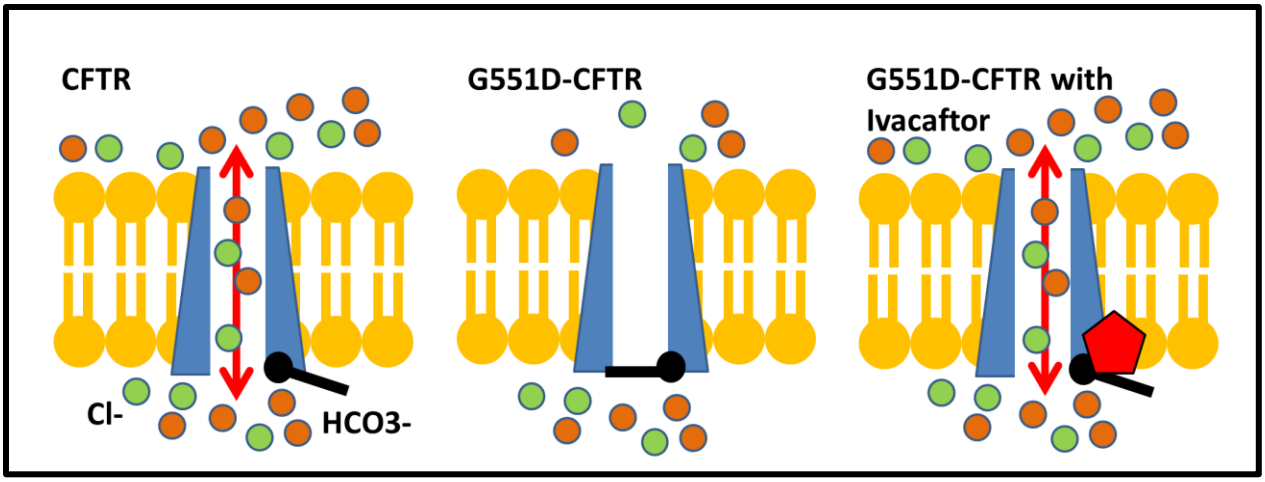

Figure 44. CFTR and ivacaftor. (Left) Functional CFTR at the cell surface channels chloride and bicarbonate. (Middle) G551D-CFTR has a gating mutation that greatly reduces the function of CFTR. (Right) Ivacaftor, red pentagon, induces a conformational change in CFTR structure which increases the open probability of the channel. This process is referred to as "potentiation."

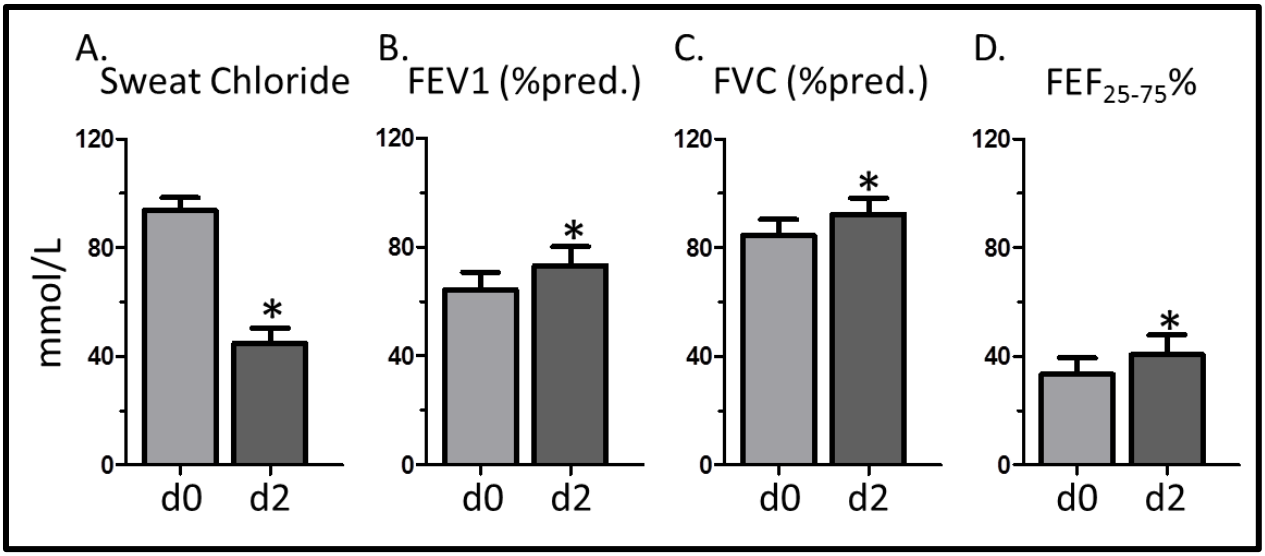

Figure 45. Sweat chloride and spirometry results at baseline (do) and after two days (d2) of ivacaftor therapy. (A) Sweat chloride concentration. (B) FEV_1 % of predicted. (C) Forced vital capacity (FVC) % of predicted. (D) Percent of predicted forced expiratory flow between 25 and 75%. Bars are mean ± SEM. *P<0.05. Figure adapted from [60].

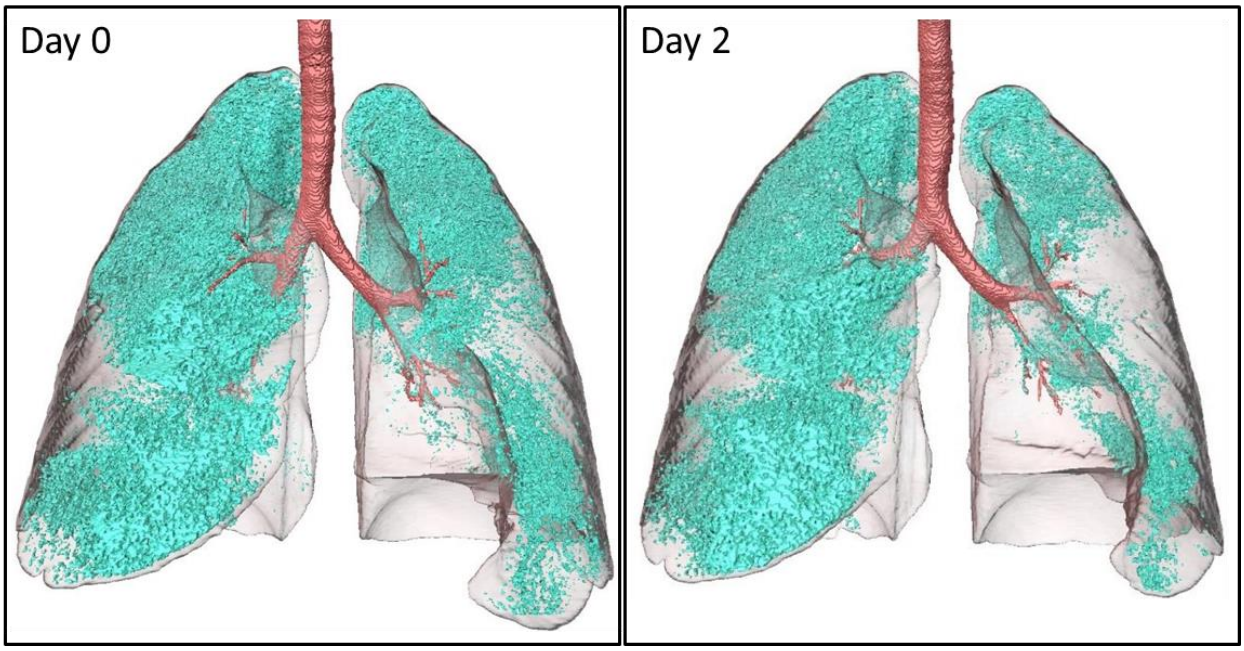

Figure 46. Air trapping before and after ivacaftor. CT scan based renderings of the lungs (semi-transparent), the airways (red), and regions of trapped air (blue) of an individual at baseline (Day 0) and after two days of ivacaftor therapy (Day 2). Trapped air was defined as CT scans voxels with HU below -856. Figure adapted from [60].

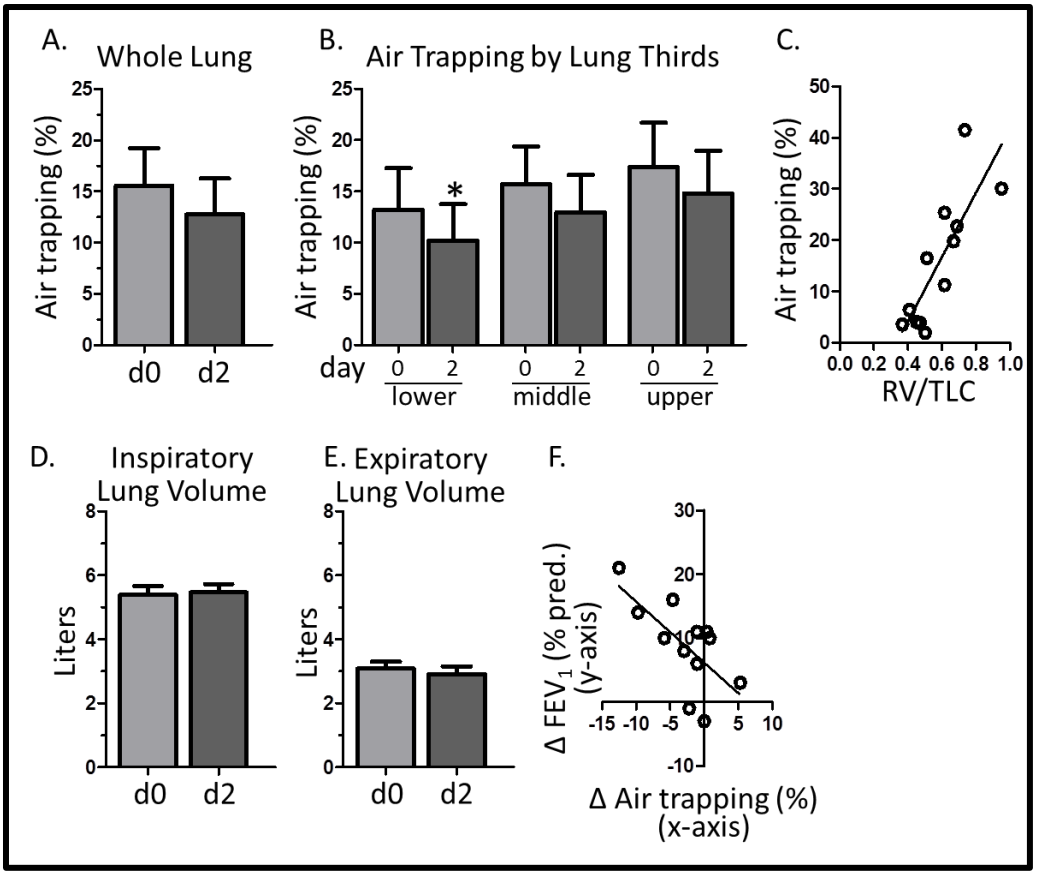

Figure 47. Air trapping and lung volumes from CT at baseline (d0) and after two days of ivacaftor therapy (d2). (A) Whole lung air trapping defined as the percentage of lung volume with an HU below -856 at residual volume. (B) Air trapping by lung thirds. (C) Baseline, percent whole-lung air trapping had a statistically significant linear correlation with baseline RV/TLC. (D) Inspiratory (TLC) lung volume. (E) Expiratory (RV) lung volume. (F) There was a statistically significant linear correlation between change in FEV_1 and change in air trapping with two days of ivacaftor therapy. Bars are mean ± SEM. *P<0.05. Figure adapted from [60].

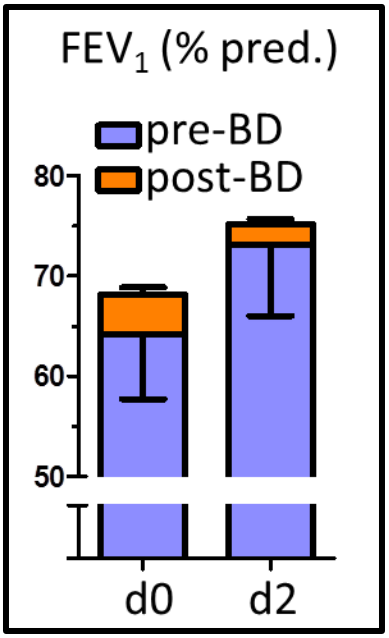

Figure 48. Bronchodilator response. FEV_1 % pred. at baseline (d0) and after two days (d2) of ivacaftor therapy before (blue) and after (orange) salbutamol. Figure adapted from [60].

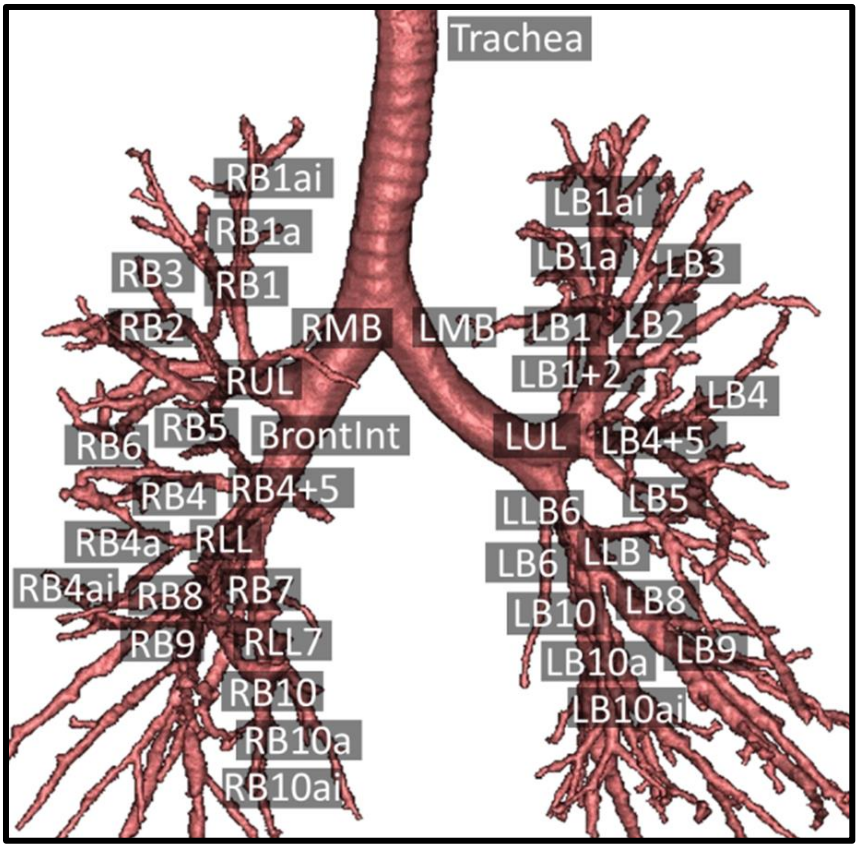

Figure 49. Airway tree nomenclature. We measured 42 airway segments for this study, each is labeled in the tree above, similar to [116].

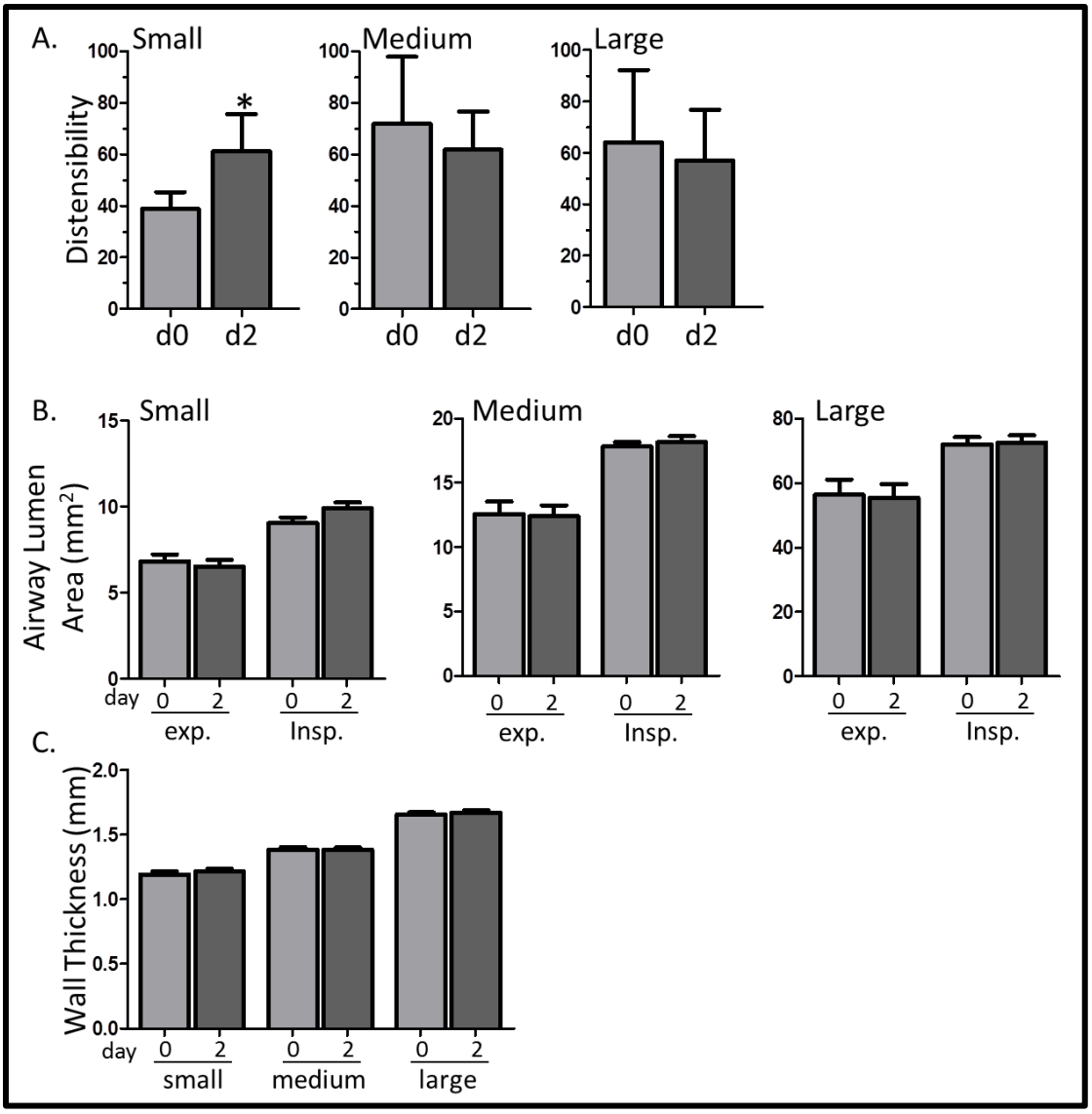

Figure 50. Airway measurements. (A) Airway distensibility in airways categorized as small, medium, and large based upon baseline inspiratory diameter. (B) Airway lumen cross-sectional area on expiration and inspiration for airways designated as small, medium, and large. (C) Airway wall thickness for small, medium, and large airways. Bars are mean ± SEM. *P<0.05. Figure adapted from [60].

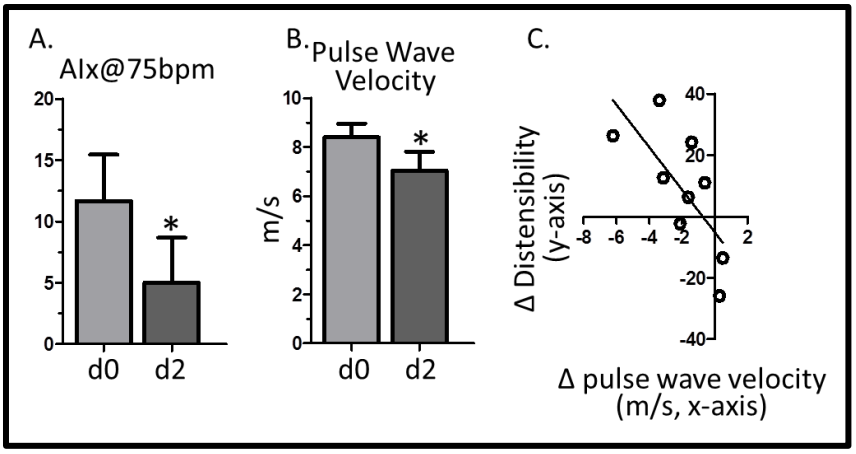

Figure 51. Pulse wave analysis. (A) We observed a reduction in augmentation index adjusted for 75 heartbeats per minute. (B) We observed a reduction in pulse wave velocity. (C) There was a statistically significant, linear correlation between change in small airway distensibility and change in pulse wave velocity on a per person average basis. Bars are mean ± SEM. *P<0.05. Figure adapted from [60].

CHAPTER 6: LUNG STRUCTURE AND FUNCTION IN ADULTS WITH *G551D-CFTR* AFTER ONE YEAR OF IVACAFTOR THERAPY

6.1 INTRODUCTION

Seven of the twelve adults with CF and the *G551D* mutation who participated in our two day ivacaftor study returned approximately one year following initiation of ivacaftor therapy for follow up (Figure 52). Their follow up included a measure of body mass, spirometry, and chest CT. Like the two day study, chest CT scans were obtained at coached TLC and RV. In contrast to the two day study, participants did not do a pulse wave analysis, a sweat chloride test, and spirometry before and after bronchodilator.

Because ivacaftor is a relatively new therapeutic option, its long term effects (~one year) on lung structure and function are largely unknown. The goal of this study was to characterize these effects. Similar to the two day study, this study included airway measurements, lung volumes, lung HU analysis, and spirometry.

Comparison of three time point (baseline, two days of ivacaftor, and one year of ivacaftor) may inform upon underlying mechanisms of improvement in lung function. For example, it could be that all of the changes occur within two days, and there are no changes between two days and one year of ivacaftor. This would suggest that ivacaftor's physiological mechanism is predominantly fast acting. In contrast, if there are changes between all three time points, it would be possible that ivacaftor would have "fast" and "slow" acting mechanisms. We hypothesized that long term administration of ivacaftor would result in sustained improvement in lung function and would limit, and possibly reverse, aspects of CF lung disease apparent on CT.

We encountered problems in the CT scan portion of this project stemming from inconsistent scan reconstruction diameters between study time points. These problems prevented us from completing this project as originally intended. We will discuss this in the upcoming text. Given this, we present the results and discussion in two parts: non-CT assays (body mass and spirometry), and CT assays. The CT scanning and spirometry

methodology were largely the same as the two day study. Hence, we did not include a "Methods" section in this chapter.

6.2 RESULTS AND DISCUSSION – BODY MASS AND SPIROMETRY

Body Mass

People with CF have a nutritional deficit and often fail to gain weight. At baseline the seven people in our study were, on average, 60 ± 6 kg, and after one year of ivacaftor therapy were 62 ± 7 kg (an increase of ~5 lbs., Figure 53). These data are consistent with a study by Rowe *et al.* that reports a mean increase of 2.5 kg (n = 133) over a six month period [30], a study by Ramsey *et al.* that reports a gain of approximately 3 kg (n = 77) over a 48 week interval [26], and additional studies that report weight gains [28, 139-142].

How might CFTR potentiation cause weight gain? One possibility is normalization of intestinal pH. CFTR, largely through its bicarbonate channeling activity, is a modulator of pH. When CFTR is disrupted, pH abnormalities ensue. These pH imbalances are one factor that impair pancreatic and intestinal function in people with CF, which in turn, contribute to malnutrition [143]. One month of ivacaftor therapy has been shown to elevate intestinal pH in people with *G551D-CFTR* [30]. This was a before-ivacaftor, after-ivacaftor study in which participants ingested a "smart pill" that tracks pH as it passes through the digestive tract. It is possible that a normalization of intestinal pH improved nutrient absorption in our cohort, which contributed to their weight gain.

Spirometry

One year of ivacaftor therapy resulted in improved spirometry measures. FEV_1 was 58 ± 7 % predicted at baseline and increased to 73 ± 8 % predicted following one year of ivacaftor therapy (P<0.05, Figure 54A). FVC was 78 ± 7 % predicted at baseline

and 91 ± 7 % predicted after one year of ivacaftor (P<0.05, Figure 54B). FEF_{25-75} improved from 28 ± 7 to 41 ± 11 % predicted (P<0.05, Figure 54C). Interestingly, approximately half of the improvement made over one year in FEV_1, FVC, and FEF_{25-75} occurred within two days of ivacaftor treatment initiation.

The improvement in spirometry made by the seven people in our study was consistent with reported gains over a similar time period (48 weeks) made in other ivacaftor studies [26-27]. It also exceeded the effects of conventional CF therapeutics (non-CFTR modulators). For example, treatment with dornase alfa (a mucolytic) resulted in a 5.8 % of predicted improvement in FEV_1 over 24 weeks of treatment [144], hypertonic saline (a mucolytic) was shown to improve FEV_1 by 3.2 % of predicted through 48 weeks [145], and inhaled tobramycin (an antibiotic) was shown to improve FEV_1 by 12 % of predicted [146]. Ivacaftor may affect lung physiology in a number of ways (e.g. mucus rheology, host defense etc.), and thus its effects on FEV_1 may exceed those of treatments that target just one aspect of pathology, e.g. mucus.

A number of factors may have contributed to improvement in lung function. First, our two day ivacaftor study suggests that ivacaftor relaxes airway smooth muscle, perhaps relieving airway hyper-reactivity and narrowing. It is possible that further relaxation may have occurred over the course of a year. Second, alterations in mucus rheology and behavior likely contributed. In support, Rowe *et al.* reported improvement in mucociliary clearance following one month of ivacaftor therapy [30]. Third, reductions in pulmonary inflammation may have improved lung function. Indeed, in the current study, we observed significant reductions in inflammatory cytokines on bronchoalveolar lavage. Fourth, reduction in pulmonary infection may have improved lung function. Whatever the mechanism(s), the fact that approximately half of the improvement in spirometry occurred within two days of ivacaftor initiation suggests that a major component of ivacaftor's mechanism is fast acting.

6.3 RESULTS AND DISCUSSION – CT SCANS

Airway Wall Thickness

Study participants were CT scanned at coached TLC and RV after one year of ivacaftor therapy, and thus between the three study time points had received a total of six chest CT scans (Figure 55). Similar to the two day study (Chapter 5), we sought to collect airway measurements using Apollo Software.

The first airway measure we report is airway wall thickness. What is known about the effects of ivacaftor on airway wall thickness? Several published studies have either qualitatively or semi-quantitatively (scoring systems) evaluated airway wall thickness on CT before and after ivacaftor therapy. Hoare *et al.*, qualitatively observed airway wall thinning on CT (n=1) over 2 years of ivacaftor therapy [115]. Sheikh *et al.* quantified airway wall thickness on CT using the Brody Scoring system. They report a statistically significant reduction in airway wall thickness over one year of ivacaftor therapy (n = 10) [142]. To our knowledge, there are no published reports of airway wall thickening in response to ivacaftor therapy. Based upon the findings of these studies, we hypothesized airway wall thinning over one year of ivacaftor therapy.

Similar to the two day ivacaftor study, we measured airway wall thickness in 42 specific airway segments (see Figure 49 for a list and schematic of these airways). Over two days of ivacaftor therapy there were no statistically significant changes in airway wall thickness in these 42 airways. However, one year of ivacaftor therapy resulted in airway wall thickening (Figure 56A). This was a surprising finding, because it disagreed with published findings, and is difficult to explain physiologically especially given the reduction in inflammation and improvement in lung health we observed in these individuals.

Based upon our discovery, we formed a new hypothesis: in this population, ivacaftor therapy reduced the *rate* of airway wall thickening (Figure 56B). For this study, we collected CT scans at baseline, after two days of ivacaftor therapy, and after one year of ivacaftor therapy. We were going to test our new hypothesis by obtaining additional

chest CT scans from before initiation of ivacaftor (e.g. from one year prior to our baseline scans), and additional scans from after ivacaftor therapy (e.g. two years after initiation of ivacaftor). Then to test our hypothesis, we would then collect airway wall thickness measurements and determine the rate of change in wall thickness over time.

Before we were able to obtain these additional chest CT scans, we realized there was a problem with our new hypothesis. The increase in wall thickness between baseline and one year of ivacaftor therapy were so pronounced (an absolute increase of nearly 0.1 mm), that it did not seem that a rate greater than 0.1 mm/year, as we hypothesized the pre-ivacaftor rate to be, was physiologically plausible.

Based upon this, we began searching for non-physiologic explanations. We discovered that the XY dimension (mm units) of the CT scan voxels were matched within each scan subject between the baseline, and two day scans, but not the one year scans (Figure 56C). The XY voxel size was increased for each individual in the study, and the increase in voxel size strongly correlated with the increase in airway wall thickness (Figure 56D). Thus, it appeared that a measured increase in wall thickness was, at least in part, "caused" by a non-physiologic factor: inconsistent voxel size.

Voxel Size in CT Scans

We were unable to say if changes observed over one year of ivacaftor therapy were due to physiological changes, or due to measurement errors stemming from inconsistent CT scan parameters. Our interpretation was confounded. This realization also raised a number of questions. Is inconsistent voxel size our only problem, or were additional scanning parameters not matched as well? Can we "correct" our scans without having to rescan our study participants? What effect does voxel size have on image quality? How does a change in XY voxel size, but not slice thickness, affect Apollo's airway and parenchymal measurements? Where do we go from here? We will next address these questions in turn.

Is inconsistent voxel size our only problem, or were additional scanning parameters not matched as well? Generation of CT scans is a multistep process (Figure 57). It can be simplified into two broad steps, each having their respective parameters. Inconsistencies in the parameters for either of these broad steps could potentially alter image qualities. The two broad steps are scan acquisition and scan reconstruction. We found that all parameters at the level of scan acquisition were consistent between the baseline, two day, and one year scans. These included parameters such as scan voltage, current, and others. In addition, all scans were acquired using a single CT scanner at a single CT scanning facility.

After scan acquisition, the information for the CT scan is stored in a non-viewable raw data format. These raw data need to be reconstructed in order to produce a viewable CT scan. There are a number of parameters at the level of reconstruction that can influence CT scan qualities. One such factor is reconstruction kernel. Reconstruction kernels can be thought of as an image filter. There are "sharp" reconstruction kernels that maintain high frequency information, and there are "blurry" reconstruction kernels that generally reduce spatial resolution (but also image noise). Importantly, we used the same reconstruction kernel for all of our scans.

A reconstruction parameter that was not matched was reconstruction diameter. This inconsistency caused our alteration in voxel dimension. In CT scanning there is a "Field of Measurement (FOM)," and there is an image "Field of View (FOV)." These are different from each other. The FOM is the entire area that was CT scanned. The FOV is the area that is reconstructed into a viewable CT image. The FOV is usually a fraction of the FOM, and cannot exceed FOM. Both the FOM and the FOV are circular in cross-section and centered about the same axis. The diameter of the FOV is known as the reconstruction diameter and can be set by the CT scan technician at scan reconstruction. Reconstruction diameter directly affects the physical dimensions of XY voxel size (e.g. in mm). Each scan (at least on the scanner we used for this study) is 512 x 512 voxels by default in the XY plane (the transverse plane in a typical chest CT scan). Voxel size is determined by dividing the reconstruction diameter by the number of voxels, in this case 512 (Figure 58). Thus, an increase in reconstruction diameter, which

is what we observed in our one year scans, results in an increase in XY voxel size. According to Hsieh *et al.*, one can reduce voxel size by maintaining a constant reconstruction diameter while increasing the matrix size, however, this is rarely done in practice due to "reconstruction complexity and storage" issues[147]. (The contents of this paragraph were based upon the texts of Kalender and Hsieh.[147-148])

Can we "correct" our scans without having to rescan our study participants? If the error had occurred at the level of scan acquisition, then we would likely have to rescan the study participants in order to correct the scans. Of course, if we rescanned the subjects today, the scans would no longer be one year, post ivacaftor scans, but ~four year post ivacaftor scans. However, the error occurred at the level of scan reconstruction. In this case, the scan technicians should be able to complete a new scan reconstruction with the correct reconstruction diameter, provided they kept the raw image data. (These scans were acquired in Dublin, Ireland. Our collaborators in Ireland have kept the raw data, and have been working to correct these scans.)

What effect does voxel size have on image quality? Alterations in reconstruction diameter result in alterations in voxel size. Voxel size, in turn, may affect image resolution. Generally, there is a tradeoff between FOV and resolution. Large FOVs image a wider area but at less resolution. Smaller FOVs image a smaller physical space but at increased resolution. Figure 59 and Figure 60 illustrate this in photography. In our study, the reconstruction diameter happened to be larger in the one year scans than the baseline scans for all 7 participants. This led to increased voxel size, likely reducing image resolution, which in turn, may have introduced measurement artifact. Note that reconstruction diameter is only one of many factors that influence image resolution. Importantly, all of these other factors were consistent between our scans.

How does a change in XY voxel size, but not slice thickness, affect Apollo's airway and parenchymal measurements? It is likely complex, and is possibly dependent upon the orientation of the airway respective to the X, Y, and Z-axis (Figure 61). Would an airway wall thickness measurement along the z-axis be affected by alterations in XY voxel size? How much would the measurement be affected if acquired along an axis

oblique to the z-axis? Would airway wall thickness measurements be affected differently than airway lumen diameter measurements, and lung parenchymal measurements?

Given the complexity in predicting the effect of voxel size on Apollo's airway and parenchymal measurements, we elected to explore it empirically. We did a "*quick and dirty"*, n=1, experiment where we performed airway and lung measurements in a chest CT scan, and then altered the XY voxel size dimensions in the scan and repeated the measurements. While in our ivacaftor scans, the voxel size changed due to differences in reconstruction diameter, in this n=1 study we altered the voxel size by downsampling in a post-processing step. The mechanism is different, but both result in an increase of XY voxel size. The goal of this mini-study was to help determine which of our one year ivacaftor measurements are likely accurate and which are not.

More specifically, we took one inspiratory chest CT scan (from our ivacaftor scan set), performed airway measurements and HU analysis. The XY voxel size was 0.566 x 0.566 mm. We then downsampled by a factor of two, in a post-processing step, resulting in a voxel size of 1.13 x 1.13 mm, and repeated our measurements. We did not downsample the z-axis, so the original and downsampled scan each have the same number of slices (566); this is akin to our one year ivacaftor scans, as altered reconstruction diameter does not affect the voxel z-dimension.

We recognized that downsampling as a post-processing step is different than altering the reconstruction diameter, and that downsampling by a factor of two probably reduces resolution considerably more than a ~5% reduction in reconstruction diameter. This downsampling exercise is simply intended to provide some direction regarding which data we can use for this thesis. One could conduct a rigorous study testing the effects of reconstruction diameter on Apollo's airway and lung measurements, however, such a study is beyond the scope of the work presented here.

Figure 62 shows a slice from the original CT scan and the downsampled scan with resulting airway tree and lung segmentations. Visually, it is difficult to see differences in scan resolution. Although, if looked upon very closely, the downsampled scan is more

"blurry." The downsampled airway tree segmentation has less branches, and the lung segmentation appears more quantized.

We measured lumen cross-sectional area, lumen diameter, and airway wall thickness for the 42 airways we measured in the two day ivacaftor study. Lumen diameter, lumen area, and airway thickness were all significantly greater in the downsampled scan (Figure 63).

Might the effect of voxel size on airway measurements depend upon the size of the airway measurement? According to Kalender, "…a negative influence of [reconstruction diameter] is largely excluded when the pixel size is smaller than the diameter of the smallest resolvable detail by a factor of two or more (Nyquist condition) [148]." Based upon this we thought an alteration of voxel size would have a greater effect on large measurements (e.g. trachea diameter) than small measures (e.g. diameter of airway RB10). Thus, we stratified our airway measurements based upon airway size. We divided the 42 airways into three groups, (n = 14 per group) based upon airway diameter in the original scan. The 14 airways with the smallest diameter were labeled as "small." The 14 largest airways were labeled, "large," and the intermediate 14 were labeled "medium."

Lumen diameter was significantly greater in the downsampled scan for small airways but no different for medium or large airways. Lumen area was significantly greater in the downsampled scans for small, and large airways, but no different in medium airways. Wall thickness was greatly elevated in the downsampled scan for small, medium, and large airways (Figure 64 & 65).

To further examine the relationship between the size of measurement and voxel size, we also made XY plots where the x-axis was airway measurement in the original scan, and the y-axis was percent change between the downsampled, and original scan. We made an XY plot for airway lumen diameter in the original scan vs. % change in airway lumen diameter between scans, and similar graphs for lumen cross-sectional area, and wall thickness. None of the graphs had a statistically significant correlation (graphs not shown).

Does voxel size affect HU histogram statistics? To test this we collected whole lung histograms from the original and downsampled scan. Upon visual inspection, we found the HU histograms from the original and downsampled scan to be nearly identical (Figure 66). Histogram statistics were nearly identical between the scans as well.

What do we learn from this mini-study? We have learned that in measuring airways, Apollo is sensitive to alterations in voxel size. Thus, when using Apollo, it is important to match scan parameters, particularly in before-after matched scans like in the present study. Might changes in voxel size affect our pig CT scans? We believe that alterations in voxel size minimally affect HU and lung volume measures. Thus, we believe those measures to be accurate for our CF and non-CF pig scans. Alterations in voxel size could potentially affect our airway measurements. However, our key findings in the three week old CF pig airways included reduced airway circularity, and proximal airway size reduction. We believe these findings are correct, because they agree with 1) results from newborn histological analysis showing reduced airways size and circularity 2) agree with CT scan based studies in newborn non-CF and CF pigs, 3) agree with our micro-CT analysis of newborn non-CF and CF tracheal lobes, and 4) agree with fetal pig histological data.

Where do we go from here? First, as mentioned previously, we are working with our collaborators in Dublin, Ireland to correctly reconstruct the CT scans from the raw image data. If we obtain these scans, we plan to continue with our study as originally intended. Second, we could complete a rigorous study evaluating the effects of reconstruction diameter on Apollo airway and parenchymal measurements. This study could have the following general study design: compare Apollo airway and parenchymal measurements for a set of scans reconstructed at varying diameters. Third, given the scenario, how should we proceed with this project for this written thesis? In our quick and dirty, n=1 study, we found that voxel size significantly affects airway measurements, even of large airways, but minimally affects lung parenchymal measurements. Based upon this observation, we will not interpret our airway measurement findings from our one year ivacaftor study. Instead, we will discuss the results we expected to get. However, we will interpret the lung parenchymal results (chiefly, lung volume, and HU

histogram statistics) from our one year ivacaftor study, albeit, keeping in mind the obvious caveat.

Expected Airway Measurements After One Year of Ivacaftor Therapy

What effect would we expect ivacaftor to have on bronchiectasis? We expect it to have the same effect reported by other studies. Interestingly, study results have been mixed. Sheikh *et al.* reported an improvement in bronchiectasis, first on an n=1 case study [141]. They later used the Brody Scoring system to evaluate 10 people with CF before and after at least one year of ivacaftor therapy, and found a significant improvement in bronchiectasis [142]. Hoare *et al.*, in an n=1 case study, reports "stabilization" of bronchiectasis over one year of ivacaftor therapy [115]. Chassagnon *et al.* used CT scan scoring to quantify bronchiectasis on CT in adults with CF (n=22) before and after ivacaftor therapy. They found that bronchiectasis became significantly worse over an average of 33 months of ivacaftor therapy [149]. Taken together, there are reports of improvement in bronchiectasis, stabilization of bronchiectasis, and worsening of bronchiectasis following approximately one year of ivacaftor therapy.

Let us more closely consider the publications of Chassagnon and Sheikh, which have differing results regarding the effects of ivacaftor on bronchiectasis. What might account for their differences? Methodologically, these studies differ from each other. First, the Chassagnon CT scan scorers were blinded to the study design, while the Sheikh scorers were not. Second, the Chassagnon CT scans included numerous slices, while the Sheikh studies were limited to 4 slices. Hence, methodological differences may have contributed to their differing results. In addition, the Chassagnon study, which was published after the Sheikh studies, discusses why their results differ from those of Sheikh. Chassagnon *et al.* mention the possibility that airway wall thinning and clearance of accumulated airway mucus may have been erroneously scored as improvement in bronchiectasis by Sheikh et *al.* [149].

Sheikh *et al.* report improvement in bronchiectasis. Is reversal of bronchiectasis possible? Although bronchiectasis is generally regarded as irreversible [150-151], there are a few reports of reversible bronchiectasis in the literature. For example, Gaillard *et al.* report a reversal of bronchiectasis in children (average age 5.8 years) [151]. They longitudinally examined 22 children with a radiological diagnosis of bronchiectasis. A number of these children had asthma, and a number had recurring infection (none had CF). They report improvement in bronchiectasis in 14 of 22 children (median scan interval of 21 months), including 6 that had complete resolution of bronchiectasis. This study suggests that bronchiectasis can be reversible under certain conditions (e.g. young age, and mild severity). This study may suggest the reversal of bronchiectasis reported by Sheikh *et al.* to be plausible.

What would we expect in our study? We believe the Chassagnon study to have a stronger methodology than the Sheikh study, and hence, we believe it more likely the results of our study to agree with those of Chassagnon than Sheikh. A worsening of bronchiectasis over one year of ivacaftor therapy would likely manifest as an increase in airway dilatation. We would expect our airway measurements to reflect this.

What are the published effects of ivacaftor on airway wall thickness? Here, there is general agreement between different published findings. Hoare *et al.* reports airway wall thinning on CT after two years of ivacaftor therapy in an n=1 case study [115]. Sheikh *et al.* reports significant wall thinning on CT [142]. Similarly, Chassagnon *et al.* also reports significant wall thinning with ivacaftor [149]. Based upon the results of these studies, we would expect airway walls to thin in our ivacaftor population over one year of ivacaftor therapy.

Of course, airway lumen diameter and airway wall thickness are not independent measures. It is possible that reduction in airway wall thickness would result in an increase in airway lumen diameter independent of intrinsic airway dilatation (Figure 67). It is possible that the worsening of bronchiectasis reported by Chassagnon was a consequence of this. If we observed an increase in airway lumen diameter in the one year ivacaftor scans, we would have to determine how much of it was simply due to reduction in airway wall thickness.

What causes airway wall thickening and what are the functional consequences of airway wall thickening? Airway wall thickening is generally regarded as remodeling caused by infection and inflammation. A study by Horsley *et al.* provides supportive evidence of this. They examined inflammatory markers and airway anatomy on CT (with a scoring system) at the time of exacerbation and after IV antibiotics in adults (median age 23 years) with CF [152]. Following antibiotic therapy, they report a significant reduction in inflammatory markers and airway wall thickness [152]. (They did not report a bronchiectasis score, but in the text regarded it as "irreversible."[152]) Functionally, wall thickening and remodeling may interfere with smooth muscle behavior [153], and may contribute to airway narrowing and airway hyper-responsiveness [154].

Lung Volumes and HU Histograms

Inspiratory lung volume did not significantly change after two days or one year of ivacaftor therapy (Figure 68). Inspiratory HU histograms changed very little with ivacaftor therapy. Inspiratory, whole lung, mean HU, mode HU, and IQR HU did not change significantly with ivacaftor.

Expiratory lung volume reduced over one year of ivacaftor therapy. The whole lung, expiratory histograms also shifted rightward. The histogram statistics reflect this rightward shift as there was a statistically significant increase in mean HU, and mode HU. There was not a statistically significant change in whole lung IQR HU.

Similar to other studies we used an -856 HU threshold to quantify the volume of trapped air in the lung [60, 117]. We observed a significant reduction in whole lung air trapping (Figure 70, Figure 71). Approximately half of the reduction in air trapping that occurred over one year of ivacaftor therapy occurred within two days of ivacaftor therapy.

What might have caused the improvement in air trapping? Alterations in airway mucus may have contributed. We did not assay the effects of ivacaftor on airway mucus for the current study, but other research groups have. Both Sheikh and Chassagnon *et al.*

reported statistically significant improvement in airway mucus accumulation following one year of ivacaftor therapy [142, 149]. Additionally, Rowe *et al.* report improved mucociliary clearance using gamma scintigraphy imaging [30]. The Sheikh, Chassagnon, and Rowe studies did not report air trapping, and thus, these studies do not provide a link between air trapping and mucus in CF. However, Robinson *et al.* report improvement in air trapping following mucolytic therapy, thus providing some connection between airway mucus and air trapping [92]. Reduction in airway reactivity may have contributed to the improvement in air trapping. We observed relaxation of airway smooth muscle following two days of ivacaftor therapy with concomitant reduction in air trapping [60]. Perhaps, over one year of ivacaftor therapy, there was further relaxation of smooth muscle, which contributed to a further improvement in air trapping.

6.4 CONCLUSION

Strengths of this study include: 1) high-quality, prospectively obtained, standardized, chest CT scans at both TLC and RV enable a rigorous and detailed analysis. 2) This would be the first long term (~1 year) ivacaftor, CT scan study with results based upon actual measurement (e.g. volume in cm^3, wall thickness in mm etc.) rather than scoring systems. Limitations of this study include: 1) Inconsistent voxel size between scans confounded our interpretation of airway measurements. 2) We had only seven study participants. However, we were satisfied with the number of participants given the rarity of the mutation and the nature of the study. Moreover, we observed significant changes over only two days of ivacaftor therapy with a limited number of participants. 3) It would be interesting to "reverse" the study design. More specifically, take these people off of ivacaftor, and see if the changes observed while on ivacaftor revert. This could be done over two days and one year. Over two days, we would hypothesize an increase in smooth muscle tone, evidenced by an increase in AIx, pulse wave velocity, and a decrease in airway distensibility. This result would provide strong supportive evidence

of an effect of CFTR on smooth muscle function. While such a study would be informative, it would be unethical to conduct in people, although, it could be done with a *G551D-CFTR* pig with ivacaftor treatment.

Through this study we have learned an important lesson: it is important to match CT scanning parameters, especially in before-after studies, and especially when using computerized airway measurement approaches. It is also important to keep the raw image data. After identifying the voxel size confounder, we decided to investigate the effects of voxel size upon Apollo's airway and lung measurements. We learned that Apollo's airway measurement apparatus is likely more sensitive to changes in voxel dimension than its lung volume and HU histogram measurement apparatus. Interestingly, if we "correct" for voxel size, then there is airway wall thinning after one year of ivacaftor therapy. This result would be consistent with that of other publications. If indeed our lung and HU histogram measurements are correct, our data suggest that a major component of ivacaftor's mechanism is fast acting, as approximately one-third of the change in RV between baseline and one year occurred within two days. Our two-day study suggests that changes in airway smooth muscle are one contributing factor. As previously mentioned, we plan to repeat scan reconstruction, except with correct reconstruction diameters. This will be the first long term (~one year) ivacaftor study to report actual measurements (e.g. in mm) rather than the results of visual scoring.

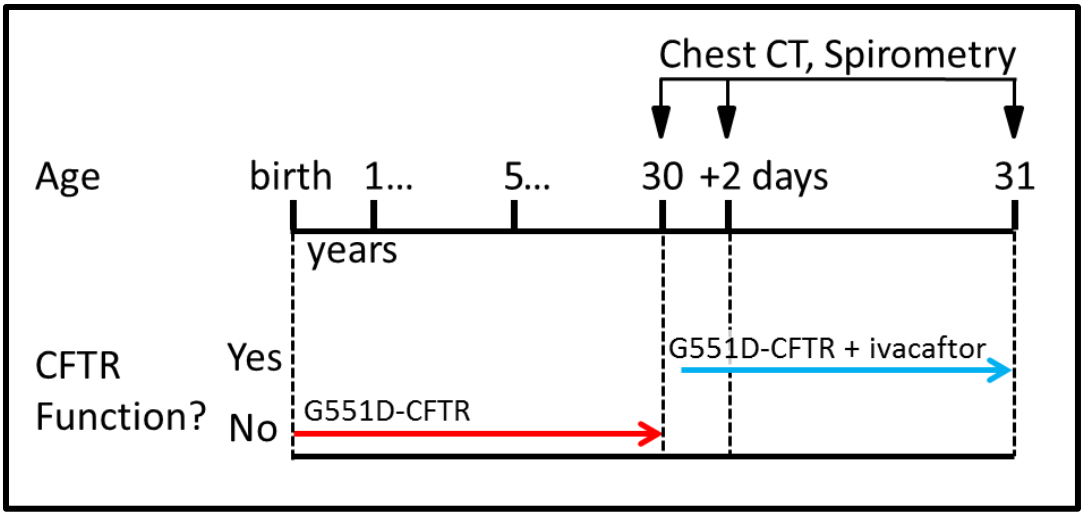

Figure 52. Ivacaftor project study design. Adults with CF and the G551D mutation were assessed with chest CT and spirometry at baseline, after two days of ivacaftor therapy, and after approximately one year of ivacaftor therapy.

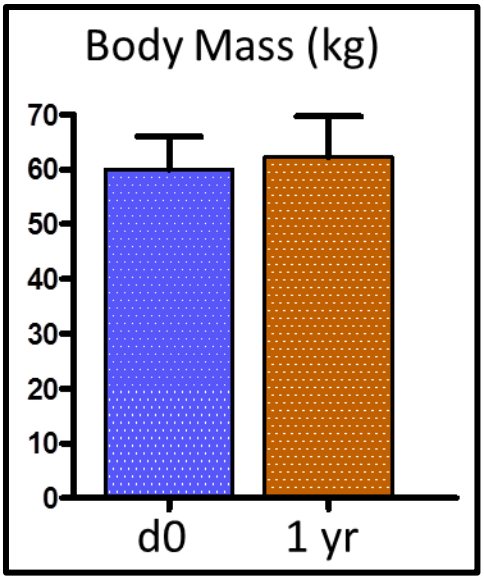

Figure 53. Body Mass. At baseline participants (n = 7) average 60.0 ± 6.0 kg, and after ~one year of ivacaftor therapy were, on average, 62.3 ± 7.4 kg. Changes not statistically significant.

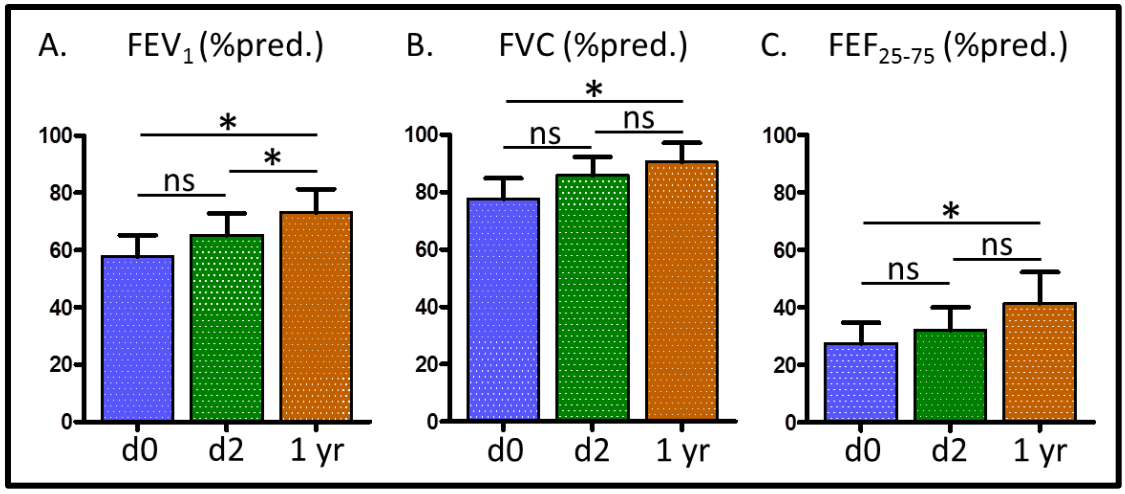

Figure 54. Spirometry at baseline (d0), after two days of ivacaftor therapy (d2), and after one year of ivacaftor therapy (1 yr). (A) FEV_1 % of predicted. (B) FVC % of predicted. (C) FEF_{25-75} % of predicted. *P<0.05. Statistical testing with Friedman Test with Dunn's Multiple Comparison Post-Test. N=7 at each time point.

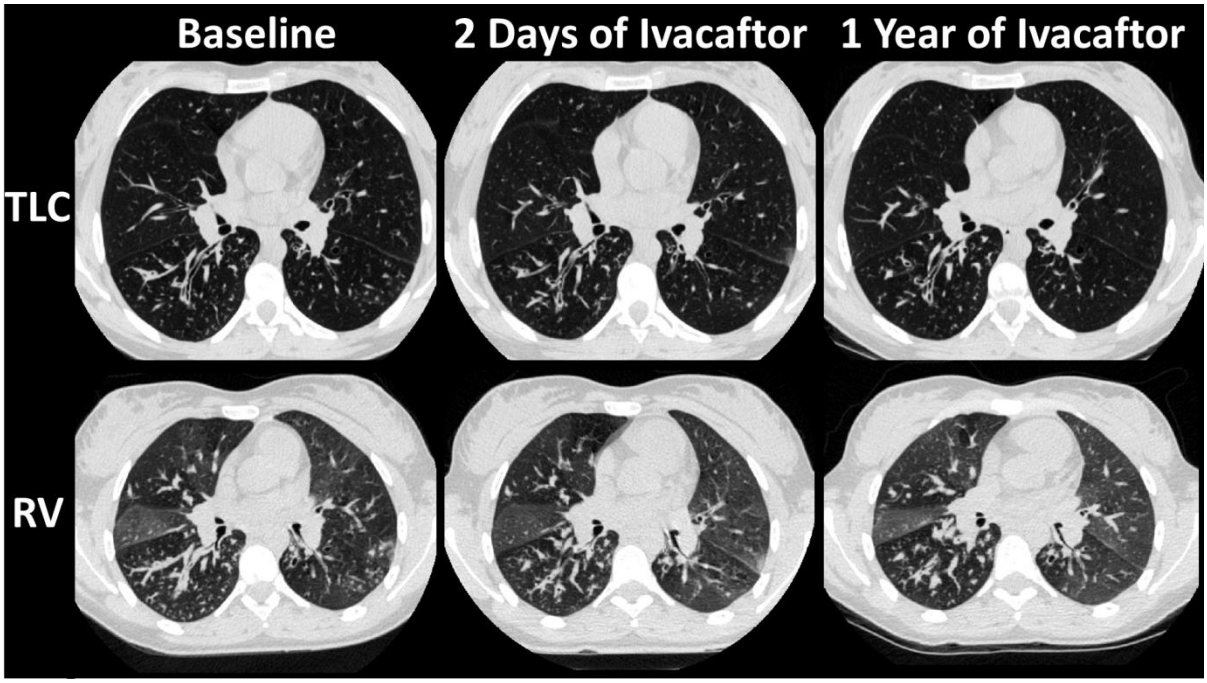

Figure 55. Chest CT. Chest CT scan slices acquired at TLC and RV at baseline (pre-ivacaftor), after two days of ivacaftor therapy, and after one year of ivacaftor therapy. Shown slices are anatomically matched as well as possible.

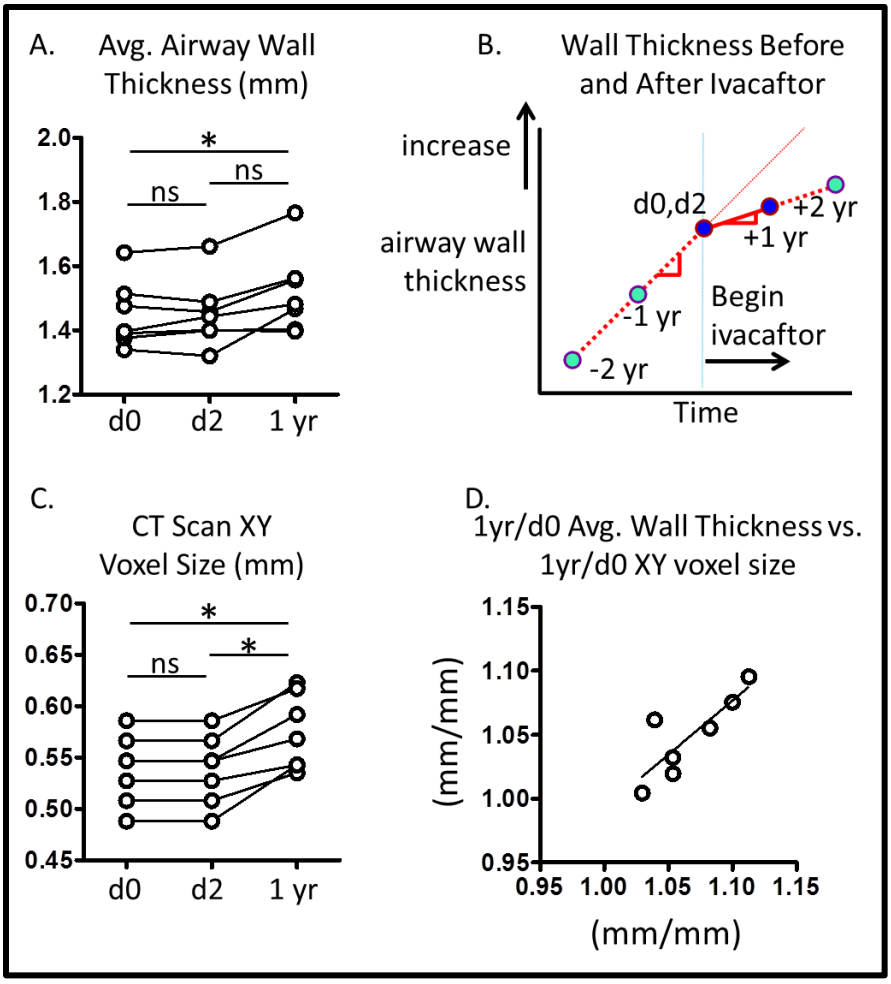

Figure 56. Airway wall thickness and voxel size. (A) Average airway wall thickness at baseline (d0), after two days (d2), and one year (1 yr) of ivacaftor therapy. (B) Perhaps ivacaftor reduced the rate of airway wall thickening. Day 0 and Day 2 are known time-points. Minus 2 years, minus 1 year and plus 1 year are speculative. (C) CT scan XY voxel dimension. (D) 1yr/d0 average airway wall thickness vs. 1yr/d0 XY voxel size. *P<0.05 with Friedman test with Dunn's Multiple Comparison Post-Test.

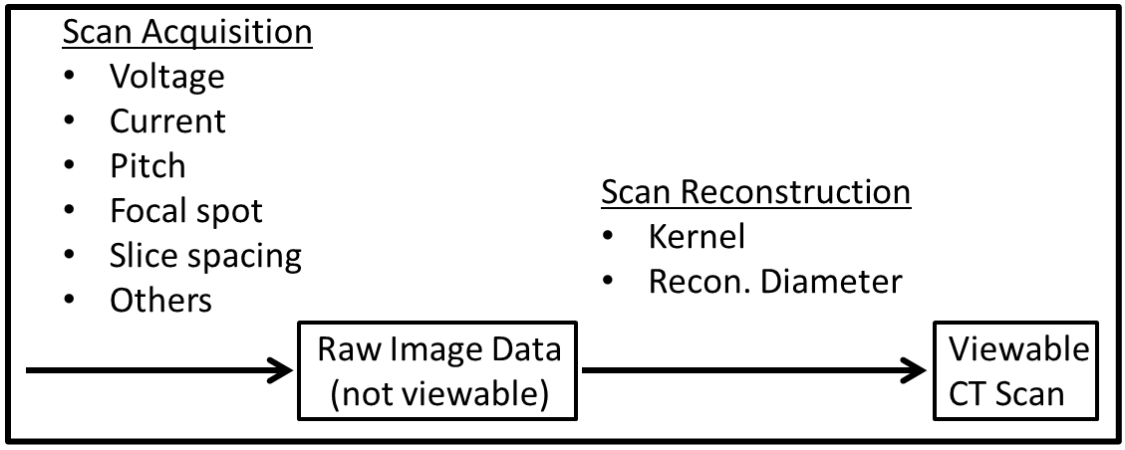

Figure 57. CT scan generation pipeline. Generating CT scans is a multi-step process. The first is scan acquisition. There are a number of "scanner settings" that can be altered (e.g. scanner voltage, current, etc.) that affect image characteristics. The information obtained from scan acquisition is stored in a non-viewable "raw" data file. This file is then "reconstructed" into a viewable CT scan. A number of "reconstruction settings" may affect CT scan image characteristics. For example, there are various reconstruction kernels that each uniquely affect image characteristics such as sharpness and noise. An additional reconstruction setting is the reconstruction diameter. This sets the diameter of the viewable scan and may impact the voxel dimensions.

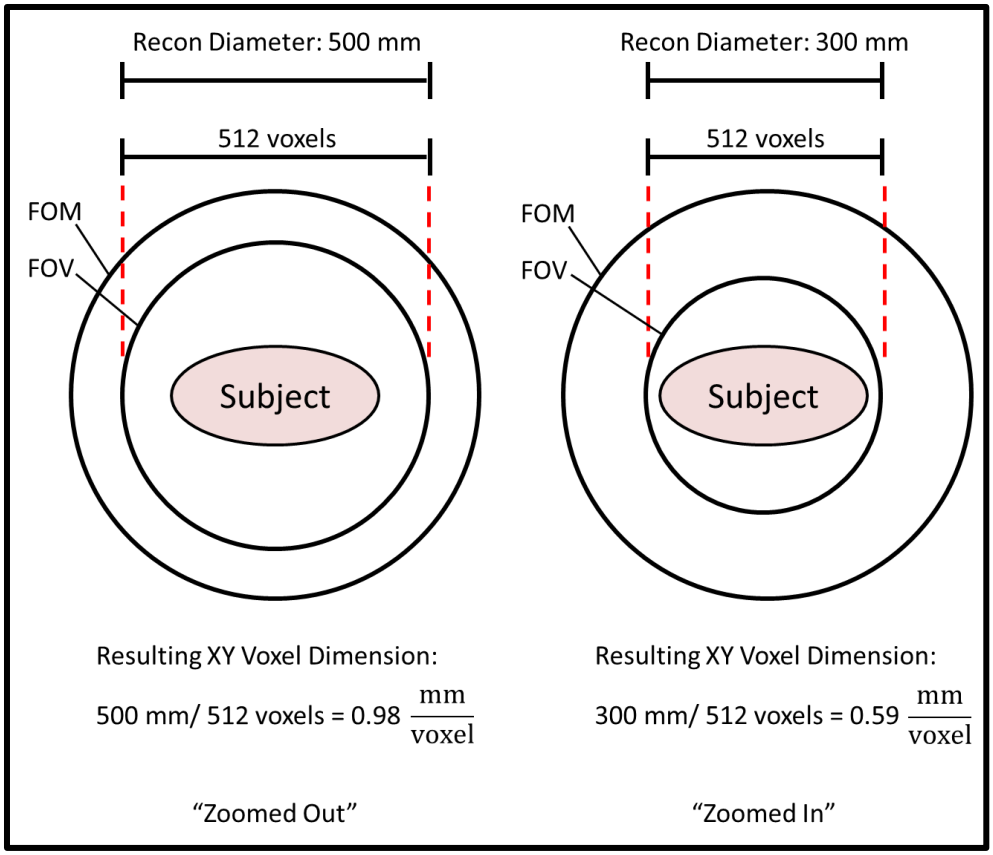

Figure 58. Reconstruction diameter and XY voxel dimension. Consider two examples. On the left the reconstruction diameter was set to 500 mm. The reconstruction diameter sets the field of view (FOV), a sub-region of the Field of Measurement (FOM). The image matrix is 512 x 512 voxels. Thus, each resulting voxel is 0.98 mm in XY side length, relatively "zoomed out." On the right, the reconstruction diameter was set to 300 mm, resulting in a tighter fit around the scan subject. The image matrix is still 512 x 512 voxels, and thus the resulting voxel, in the XY plane, has sides of 0.59 mm. This scan is relatively "zoomed in," and as a result would have relatively better spatial resolution.

Figure 59. "Reconstruction Diameter" in photography. This is a photographic analog to the reconstruction diameter in CT. Each picture has the same number of pixels (4000 x 2248), similar to CT scans of differing FOV (512 x 512). However, the top photo imaged a larger physical space. It is relatively "zoomed out." Thus, each pixel in the top photo represents more physical space (0.49 mm/pixel), than in the lower image (0.11 mm/pixel). The change in XY pixel size affects resolution characteristics.

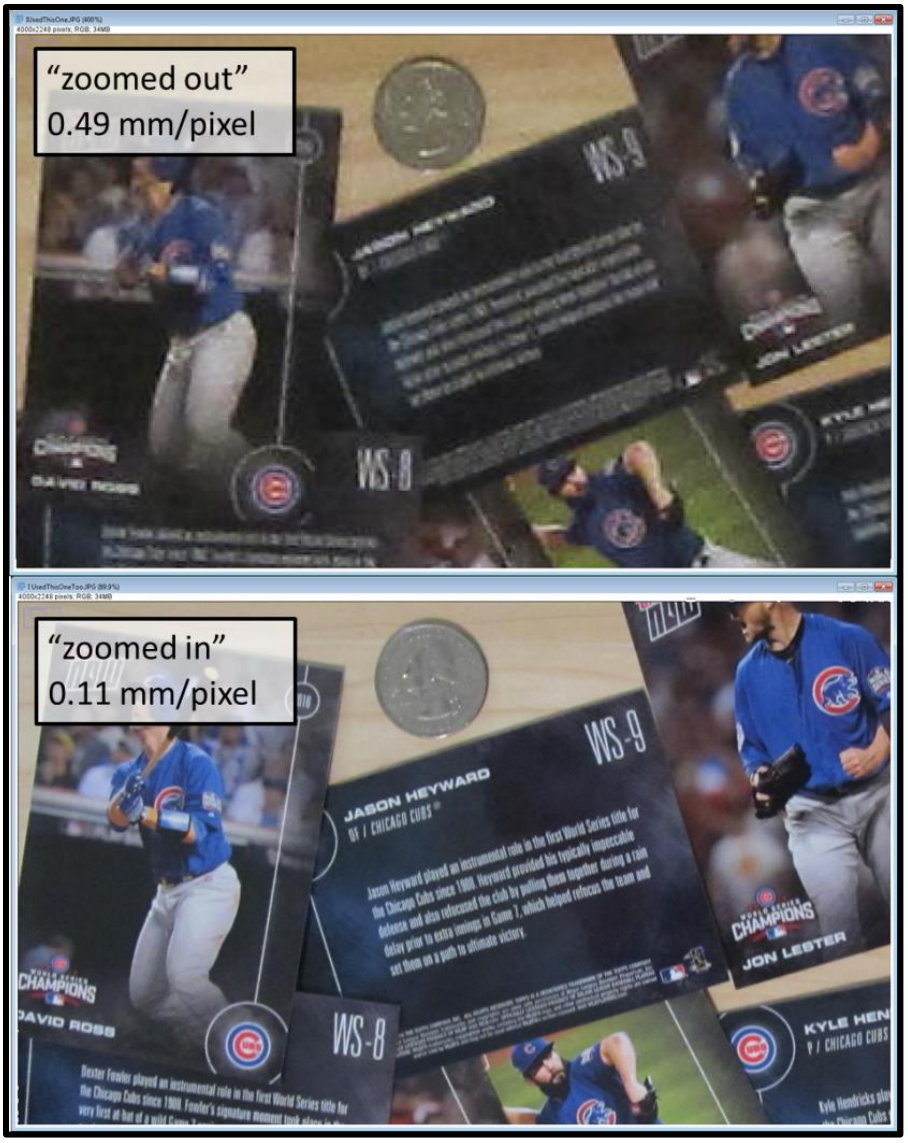

Figure 60. Pixel size and resolution. A subsection of each photo from the prior figure were enlarged and respectively magnified until size matched (the quarter is the same size in each photo). The "zoomed out" image has noticeably worse spatial resolution. This example also illustrates that magnifying a "zoomed out" image does not restore its spatial resolution.

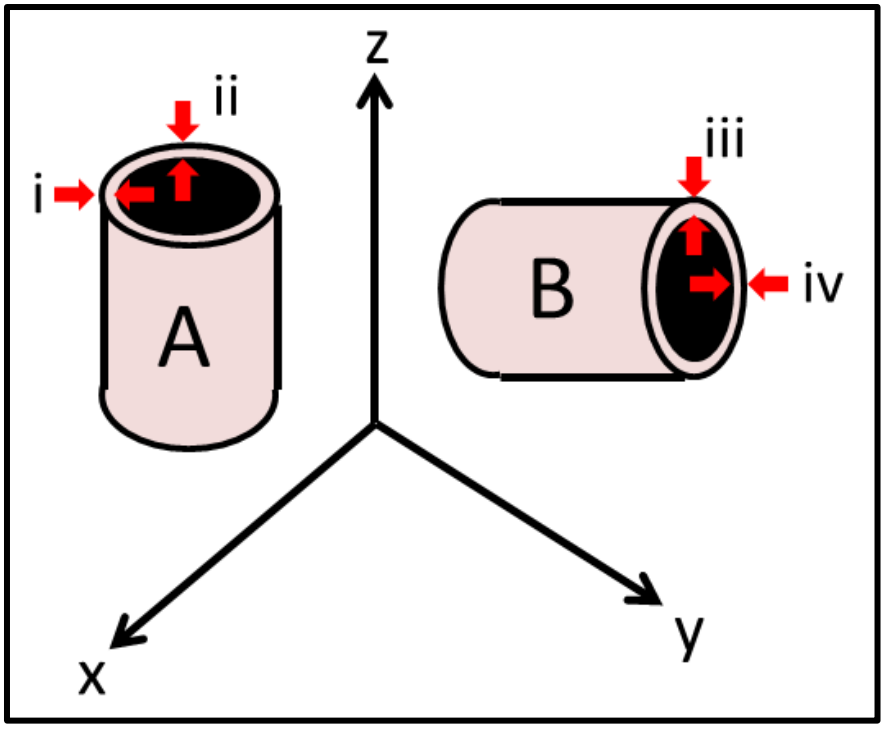

Figure 61. XY voxel size and axis of measurement. In our scan set, in-plane voxel size was increased but slice thickness (z-axis length of voxel) was not. The impact of voxel size on measurement may depend upon the axis of measurement. Consider several examples. Airway A is longitudinally oriented along the z-axis, and its cross-section, as shown, is in the XY plane. Both of its airway wall measurements are in the XY plane, and so may be affected by alterations in XY voxel size. In contrast, airway wall thickness measure "iii" is along the z-axis. Would this measurement be altered even if there was no change in slice thickness? Airway B has wall thickness measurements that are along the z-axis, but also oblique to the z-axis, and perpendicular to the z-axis: iv. The effects of changes of in-plane, but not cross-plane voxel size on Apollo's airway measurements is likely complex.

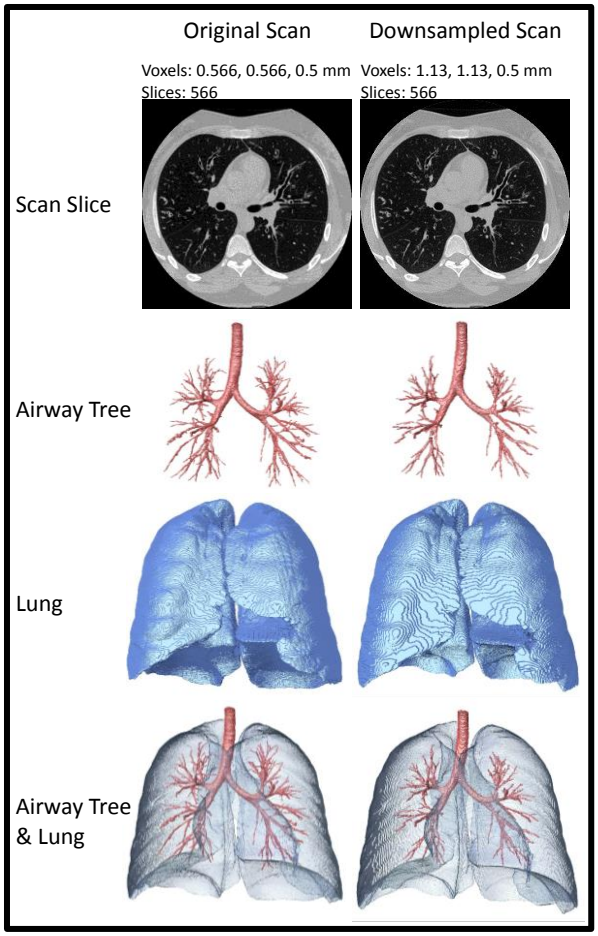

Figure 62. Original and downsampled scan. XY voxel size and number of slices in the original and downsampled (by 2x) scan are listed alongside a slice from each scan and Apollo's automatically generated airway segmentation, and lung segmentation. The airway tree from the downsampled scan has relatively less branches. The lung segmentation from the downsampled scan is relatively more quantized.

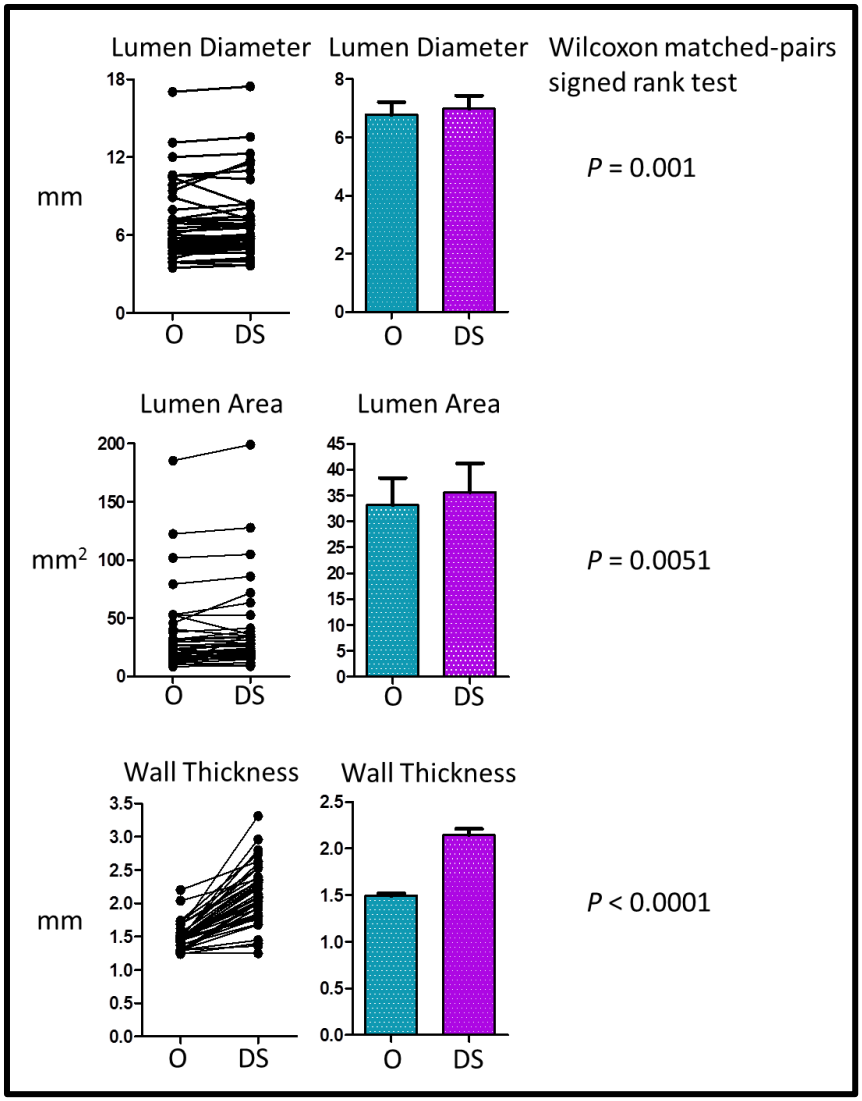

Figure 63. Airway measurements in the original and downsampled scan. We measured lumen diameter, lumen area, and wall thickness in 42 airways in the original and downsampled scan. All three were significantly greater from the downsampled scan than from the original scan. The graphs on the left show these data as connected line and dot graphs, with the corresponding bar graphs on the right. Bars are mean ± SEM.

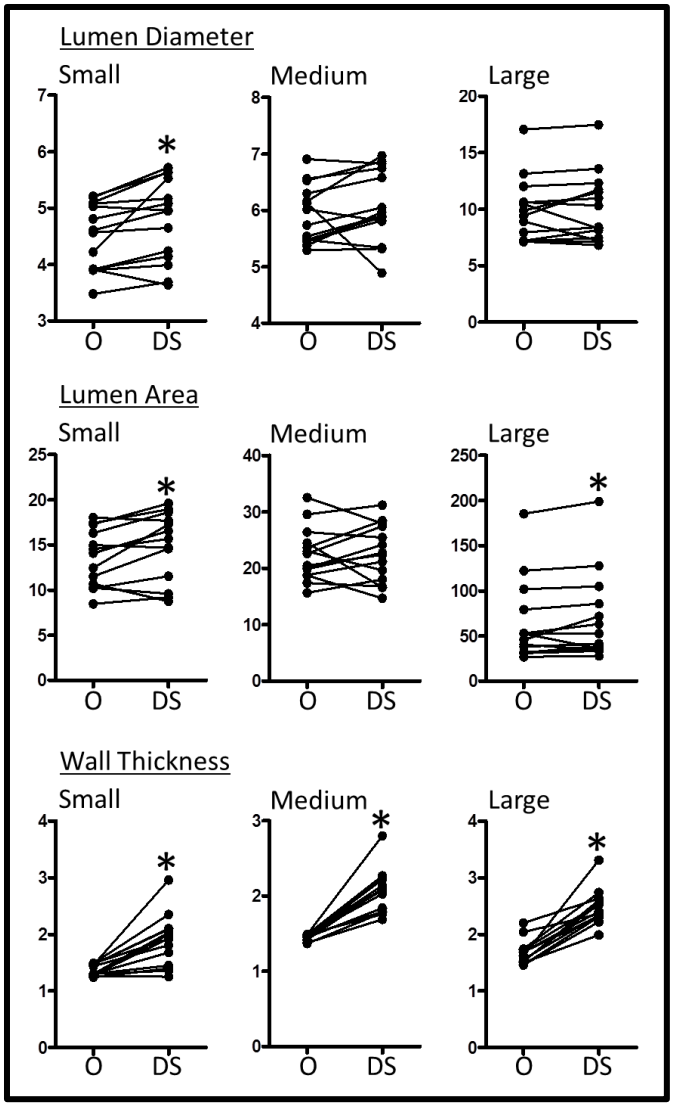

Figure 64. Airway measurements in the original and downsampled scan stratified by airway size. We divided our 42 airways into three groups of 14 based upon their lumen diameter in the original scan. Groups included "small," "medium," and "large." "O" denotes original scan, and "DS" denotes downsampled scan. *P<0.05 with Wilcoxon matched-pairs, signed rank test.

	Original	Down-Sampled	Percent Change	P-Value
Diameter Small	4.50±0.16	4.79±0.20	+6.5	S
Diameter Medium	5.93±0.14	6.07±0.17	+2.4	NS
Diameter Large	9.90±0.75	10.10±0.82	+2.0	NS
Lumen Area Small	13.6±0.85	14.8±1.0	+9.3	S
Lumen Area Medium	22.4±1.26	22.6±1.35	+1.1	NS
Lumen Area Large	63.8±12.0	68.0±12.9	+2.0	S
Wall Thickness Small	1.36±0.03	1.88±0.12	+38	S
Wall Thickness Medium	1.45±0.01	2.06±0.07	+42	S
Wall Thickness Large	1.66±0.06	2.49±0.08	+50	S

Figure 65. Airway measurements for airway size groups from the original and downsampled scan. Data represent mean ± SEM. "S" denotes significant with Wilcoxon matched-pairs, signed rank test, and "NS" denotes not significant.

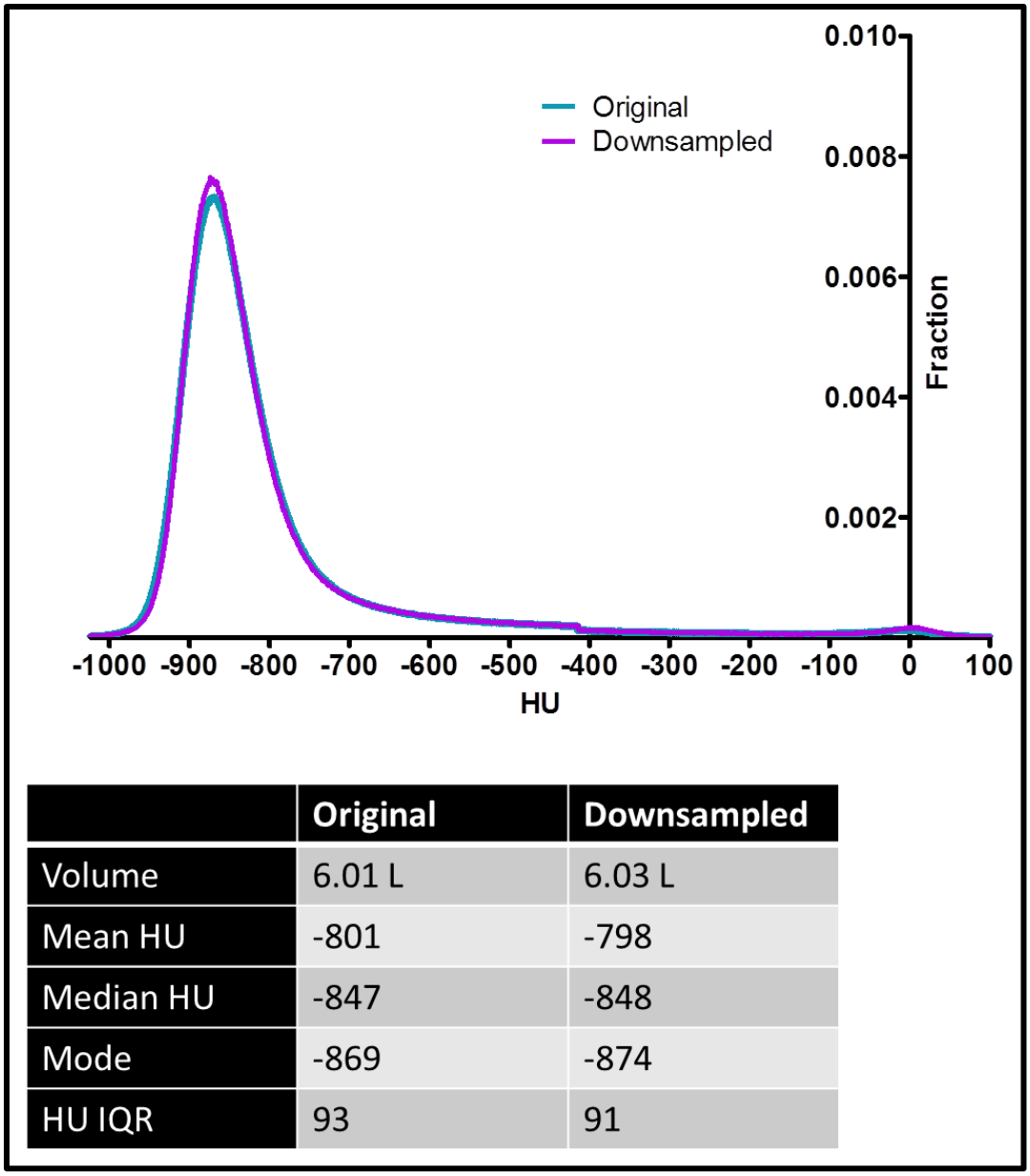

	Original	Downsampled
Volume	6.01 L	6.03 L
Mean HU	-801	-798
Median HU	-847	-848
Mode	-869	-874
HU IQR	93	91

Figure 66. HU histograms and statistics from the original and downsampled scan. This scan was acquired at coached TLC. There are two HU histogram curves in the graph, however, it is difficult to distinguish both due to overlap.

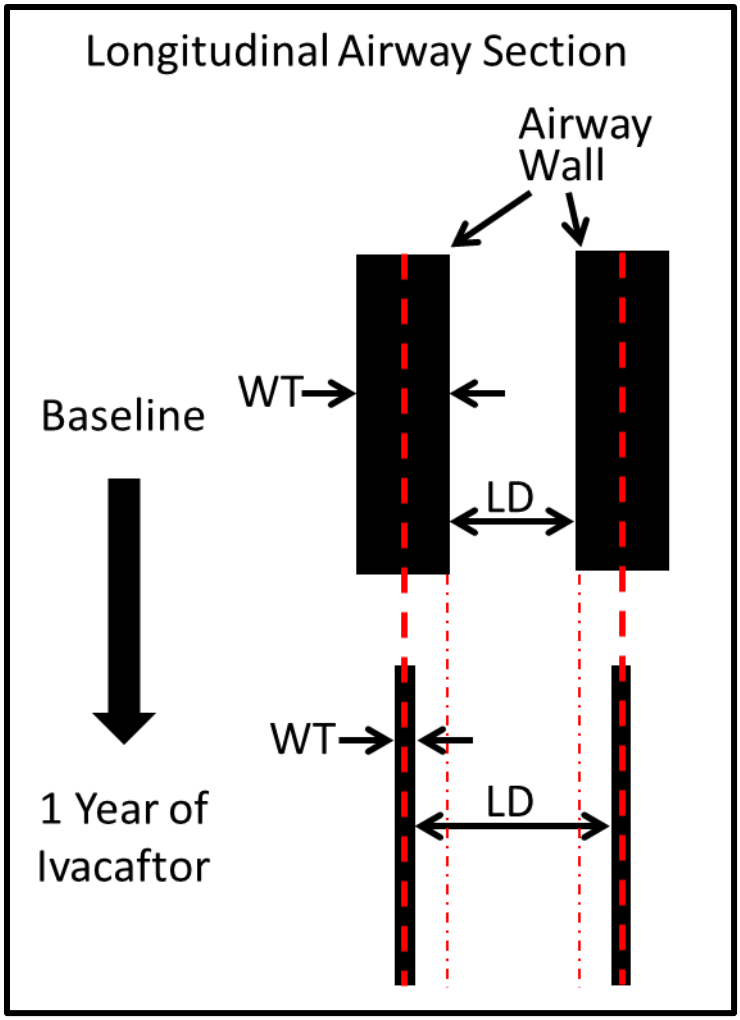

Figure 67. Possible changes in airway wall thickness and lumen diameter following one year of ivacaftor therapy. Diagram shows a longitudinally cut airway with the wall thickness (WT), and lumen diameter (LD) highlighted. Dashed lines highlight the center of the airway walls and baseline inner airway walls, respectively. Airway wall thinning following ivacaftor therapy could result in an increase in airway lumen diameter, even if the lumen diameter measured from airway wall centerline to centerline does not change. Airway wall thinning exaggerated for illustration purposes.

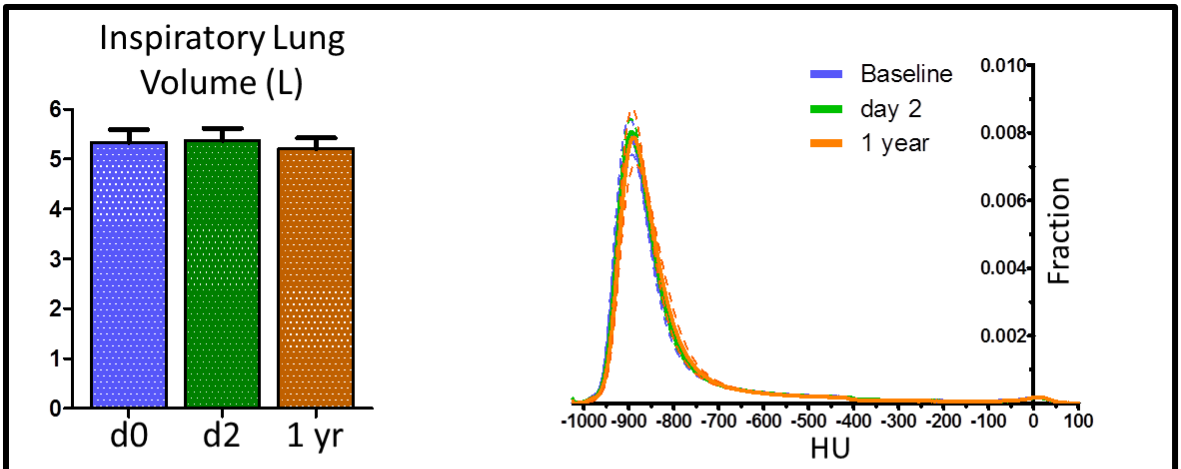

Inspiratory	Baseline	Day 2	1 year	P-Value
Mean HU	-813±8	-814±6	-810±8	NS
Mode HU	-892±6	-892±3	-884±7	NS
IQR HU	90±7	91±5	95±11	NS

Figure 68. Inspiratory HU histograms at baseline, after two days, and after one year of ivacaftor therapy. (Top left) Lung volume. (Top right) HU histograms at each of the three time points. Lines and dotted lines are avg. ± SEM, respectively. (Bottom) HU histogram statistics. N=7. P-value from a Wilcoxon matched-pairs, signed rank test.

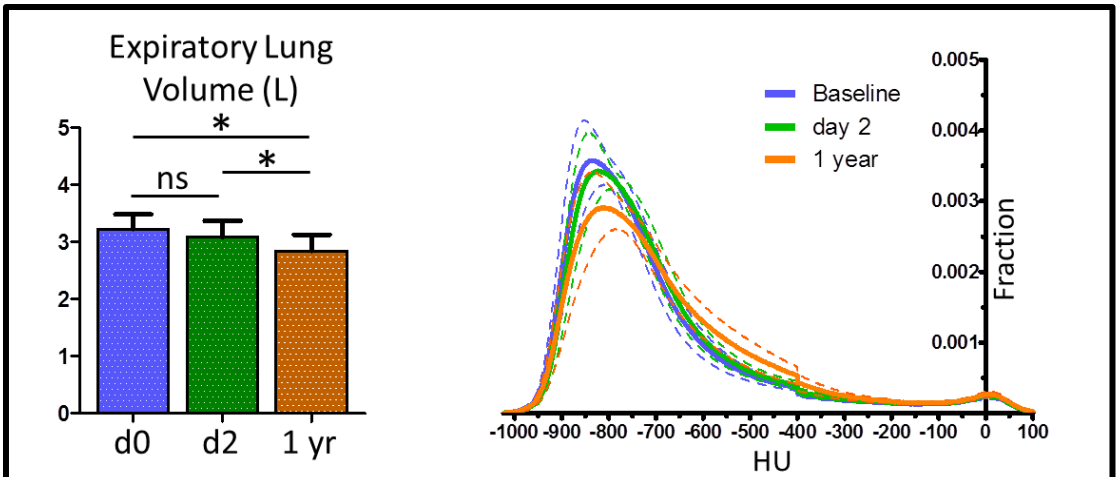

Expiratory	Baseline	Day 2	1 year	P-Value
Mean HU	-704±20	-690±20	-667±28	S
Mode HU	-814±20	-803±21	-793±25	S
IQR HU	170±13	178±13	199±14	NS

Figure 69. Expiratory HU histograms at baseline, after two days, and after one year of ivacaftor therapy. (Top left) Lung volume. (Top right) HU histograms at each of the three time points. Lines and dotted lines are avg. ± SEM, respectively. (Bottom) HU histogram statistics. N=7. P-value from a Wilcoxon matched-pairs, signed rank test.

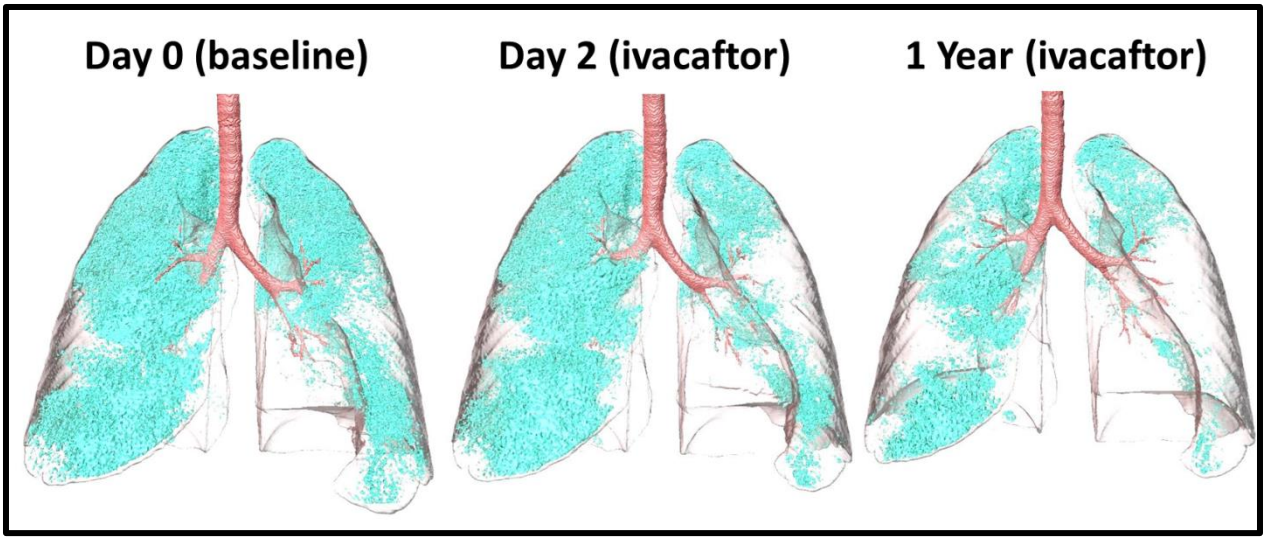

Figure 70. -856 HU threshold segmentation. Three dimensional rendering of the lungs (semi-transparent) and airways at baseline, after two days and one year of ivacaftor therapy. HU values less than -856 are highlighted in blue.

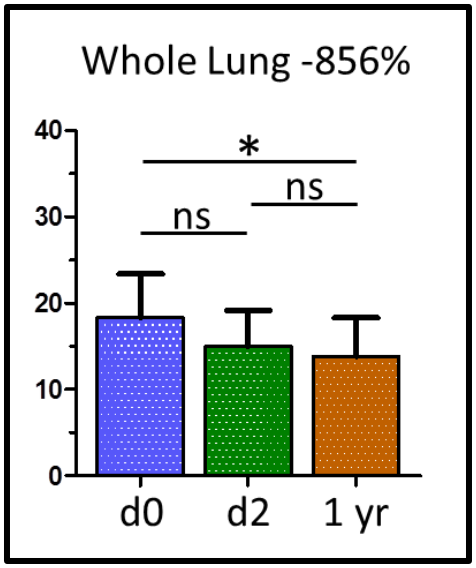

Figure 71. Air trapping at baseline, two days, and one year of ivacaftor therapy. We used a -856 HU threshold to estimate the percent volume of trapped air in the whole lung. N=7 at each time point.

REFERENCES

1. Cystic Fibrosis Foundation. https://www.cff.org/ (accessed September 8th, 2015).

2. Shah, V. S.; Meyerholz, D. K.; Tang, X. X.; Reznikov, L.; Abou Alaiwa, M.; Ernst, S. E.; Karp, P. H.; Wohlford-Lenane, C. L.; Heilmann, K. P.; Leidinger, M. R.; Allen, P. D.; Zabner, J.; McCray, P. B., Jr.; Ostedgaard, L. S.; Stoltz, D. A.; Randak, C. O.; Welsh, M. J., Airway acidification initiates host defense abnormalities in cystic fibrosis mice. *Science* **2016,** *351* (6272), 503-7.

3. Pezzulo, A. A.; Tang, X. X.; Hoegger, M. J.; Alaiwa, M. H.; Ramachandran, S.; Moninger, T. O.; Karp, P. H.; Wohlford-Lenane, C. L.; Haagsman, H. P.; van Eijk, M.; Banfi, B.; Horswill, A. R.; Stoltz, D. A.; McCray, P. B., Jr.; Welsh, M. J.; Zabner, J., Reduced airway surface pH impairs bacterial killing in the porcine cystic fibrosis lung. *Nature* **2012,** *487* (7405), 109-13.

4. Sly, P. D.; Gangell, C. L.; Chen, L.; Ware, R. S.; Ranganathan, S.; Mott, L. S.; Murray, C. P.; Stick, S. M.; Investigators, A. C., Risk factors for bronchiectasis in children with cystic fibrosis. *N Engl J Med* **2013,** *368* (21), 1963-70.

5. Sly, P. D.; Brennan, S.; Gangell, C.; de Klerk, N.; Murray, C.; Mott, L.; Stick, S. M.; Robinson, P. J.; Robertson, C. F.; Ranganathan, S. C.; Australian Respiratory Early Surveillance Team for Cystic, F., Lung disease at diagnosis in infants with cystic fibrosis detected by newborn screening. *American journal of respiratory and critical care medicine* **2009,** *180* (2), 146-52.

6. Stoltz, D. A.; Meyerholz, D. K.; Pezzulo, A. A.; Ramachandran, S.; Rogan, M. P.; Davis, G. J.; Hanfland, R. A.; Wohlford-Lenane, C.; Dohrn, C. L.; Bartlett, J. A.; Nelson, G. A. t.; Chang, E. H.; Taft, P. J.; Ludwig, P. S.; Estin, M.; Hornick, E. E.; Launspach, J. L.; Samuel, M.; Rokhlina, T.; Karp, P. H.; Ostedgaard, L. S.; Uc, A.; Starner, T. D.; Horswill, A. R.; Brogden, K. A.; Prather, R. S.; Richter, S. S.; Shilyansky, J.; McCray, P. B., Jr.; Zabner, J.; Welsh, M. J., Cystic fibrosis pigs develop lung disease and exhibit defective bacterial eradication at birth. *Science translational medicine* **2010,** *2* (29), 29ra31.

7. Adam, R. J.; Michalski, A. S.; Bauer, C.; Abou Alaiwa, M. H.; Gross, T. J.; Awadalla, M. S.; Bouzek, D. C.; Gansemer, N. D.; Taft, P. J.; Hoegger, M. J.; Diwakar, A.; Ochs, M.; Reinhardt, J. M.; Hoffman, E. A.; Beichel, R. R.; Meyerholz, D. K.; Stoltz, D. A., Air trapping and airflow obstruction in newborn cystic fibrosis piglets. *American journal of respiratory and critical care medicine* **2013,** *188* (12), 1434-41.

8. Meyerholz, D. K.; Stoltz, D. A.; Namati, E.; Ramachandran, S.; Pezzulo, A. A.; Smith, A. R.; Rector, M. V.; Suter, M. J.; Kao, S.; McLennan, G.; Tearney, G. J.; Zabner, J.; McCray, P. B., Jr.; Welsh, M. J., Loss of cystic fibrosis transmembrane conductance regulator function produces abnormalities in tracheal development in neonatal pigs and young children. *American journal of respiratory and critical care medicine* **2010,** *182* (10), 1251-61.

9. Chapman, D. G.; Pascoe, C. D.; Lee-Gosselin, A.; Couture, C.; Seow, C. Y.; Pare, P. D.; Salome, C. M.; King, G. G.; Bosse, Y., Smooth muscle in the maintenance of increased airway resistance elicited by methacholine in humans. *American journal of respiratory and critical care medicine* **2014,** *190* (8), 879-85.

10. Michoud, M. C.; Robert, R.; Hassan, M.; Moynihan, B.; Haston, C.; Govindaraju, V.; Ferraro, P.; Hanrahan, J. W.; Martin, J. G., Role of the cystic fibrosis transmembrane conductance channel in human airway smooth muscle. *American journal of respiratory cell and molecular biology* **2009,** *40* (2), 217-22.

11. Regamey, N.; Ochs, M.; Hilliard, T. N.; Muhlfeld, C.; Cornish, N.; Fleming, L.; Saglani, S.; Alton, E. W.; Bush, A.; Jeffery, P. K.; Davies, J. C., Increased airway smooth muscle mass in children with asthma, cystic fibrosis, and non-cystic fibrosis bronchiectasis. *American journal of respiratory and critical care medicine* **2008,** *177* (8), 837-43.

12. Hays, S. R.; Ferrando, R. E.; Carter, R.; Wong, H. H.; Woodruff, P. G., Structural changes to airway smooth muscle in cystic fibrosis. *Thorax* **2005,** *60* (3), 226-8.

13. Balfour-Lynn, I. M.; Elborn, J. S., "CF asthma": what is it and what do we do about it? *Thorax* **2002,** *57* (8), 742-8.

14. Sanchez, I.; Powell, R. E.; Pasterkamp, H., Wheezing and airflow obstruction during methacholine challenge in children with cystic fibrosis and in normal children. *The American review of respiratory disease* **1993,** *147* (3), 705-9.

15. Hiatt, P.; Eigen, H.; Yu, P.; Tepper, R. S., Bronchodilator responsiveness in infants and young children with cystic fibrosis. *The American review of respiratory disease* **1988,** *137* (1), 119-22.

16. Kent, B. D.; Lane, S. J.; van Beek, E. J.; Dodd, J. D.; Costello, R. W.; Tiddens, H. A., Asthma and cystic fibrosis: a tangled web. *Pediatric pulmonology* **2014,** *49* (3), 205-13.

17. Vandebrouck, C.; Melin, P.; Norez, C.; Robert, R.; Guibert, C.; Mettey, Y.; Becq, F., Evidence that CFTR is expressed in rat tracheal smooth muscle cells and contributes to bronchodilation. *Respiratory research* **2006,** *7*, 113.

18. Cook, D. P.; Rector, M. V.; Bouzek, D. C.; Michalski, A. S.; Gansemer, N. D.; Reznikov, L. R.; Li, X.; Stroik, M. R.; Ostedgaard, L. S.; Abou Alaiwa, M. H.; Thompson, M. A.; Prakash, Y. S.; Krishnan, R.; Meyerholz, D. K.; Seow, C. Y.; Stoltz, D. A., Cystic Fibrosis Transmembrane Conductance Regulator in Sarcoplasmic Reticulum of Airway Smooth Muscle. Implications for Airway Contractility. *American journal of respiratory and critical care medicine* **2016,** *193* (4), 417-26.

19. Cooney, A. L.; Abou Alaiwa, M. H.; Shah, V. S.; Bouzek, D. C.; Stroik, M. R.; Powers, L. S.; Gansemer, N. D.; Meyerholz, D. K.; Welsh, M. J.; Stoltz, D. A.; Sinn, P. L.; McCray, P. B., Jr., Lentiviral-mediated phenotypic correction of cystic fibrosis pigs. *JCI Insight* **2016,** *1* (14).

20. Steines, B.; Dickey, D. D.; Bergen, J.; Excoffon, K. J.; Weinstein, J. R.; Li, X.; Yan, Z.; Alaiwa, M. H.; Shah, V. S.; Bouzek, D. C.; Powers, L. S.; Gansemer, N. D.; Ostedgaard, L. S.; Engelhardt, J. F.; Stoltz, D. A.; Welsh, M. J.; Sinn, P. L.; Schaffer, D. V.; Zabner, J., CFTR gene transfer with AAV improves early cystic fibrosis pig phenotypes. *JCI Insight* **2016,** *1* (14), e88728.

21. Wainwright, C. E.; Elborn, J. S.; Ramsey, B. W.; Marigowda, G.; Huang, X.; Cipolli, M.; Colombo, C.; Davies, J. C.; De Boeck, K.; Flume, P. A.; Konstan, M. W.; McColley, S. A.; McCoy, K.; McKone, E. F.; Munck, A.; Ratjen, F.; Rowe, S. M.; Waltz, D.; Boyle, M. P.; Group, T. S.; Group, T. S., Lumacaftor-Ivacaftor in Patients with Cystic Fibrosis Homozygous for Phe508del CFTR. *N Engl J Med* **2015,** *373* (3), 220-31.

22. Stoltz, D. A.; Meyerholz, D. K.; Welsh, M. J., Origins of cystic fibrosis lung disease. *N Engl J Med* **2015,** *372* (4), 351-62.

23. Armstrong, D. S.; Grimwood, K.; Carlin, J. B.; Carzino, R.; Gutierrez, J. P.; Hull, J.; Olinsky, A.; Phelan, E. M.; Robertson, C. F.; Phelan, P. D., Lower airway inflammation in infants and young children with cystic fibrosis. *American journal of respiratory and critical care medicine* **1997,** *156* (4 Pt 1), 1197-204.

24. Van Goor, F.; Hadida, S.; Grootenhuis, P. D.; Burton, B.; Cao, D.; Neuberger, T.; Turnbull, A.; Singh, A.; Joubran, J.; Hazlewood, A.; Zhou, J.; McCartney, J.; Arumugam, V.; Decker, C.; Yang, J.; Young, C.; Olson, E. R.; Wine, J. J.; Frizzell, R. A.; Ashlock, M.; Negulescu, P., Rescue of CF airway epithelial cell function in vitro by a CFTR potentiator, VX-770. *Proceedings of the National Academy of Sciences of the United States of America* **2009,** *106* (44), 18825-30.

25. Eckford, P. D.; Li, C.; Ramjeesingh, M.; Bear, C. E., Cystic fibrosis transmembrane conductance regulator (CFTR) potentiator VX-770 (ivacaftor) opens the defective channel gate of mutant CFTR in a phosphorylation-dependent but ATP-independent manner. *J Biol Chem* **2012,** *287* (44), 36639-49.

26. Ramsey, B. W.; Davies, J.; McElvaney, N. G.; Tullis, E.; Bell, S. C.; Drevinek, P.; Griese, M.; McKone, E. F.; Wainwright, C. E.; Konstan, M. W.; Moss, R.; Ratjen, F.; Sermet-Gaudelus, I.; Rowe, S. M.; Dong, Q.; Rodriguez, S.; Yen, K.; Ordonez, C.; Elborn, J. S.; Group, V. X. S., A CFTR potentiator in patients with cystic fibrosis and the G551D mutation. *N Engl J Med* **2011,** *365* (18), 1663-72.

27. Accurso, F. J.; Rowe, S. M.; Clancy, J. P.; Boyle, M. P.; Dunitz, J. M.; Durie, P. R.; Sagel, S. D.; Hornick, D. B.; Konstan, M. W.; Donaldson, S. H.; Moss, R. B.; Pilewski, J. M.; Rubenstein, R. C.; Uluer, A. Z.; Aitken, M. L.; Freedman, S. D.; Rose, L. M.; Mayer-Hamblett, N.; Dong, Q.; Zha, J.; Stone, A. J.; Olson, E. R.; Ordonez, C. L.; Campbell, P. W.; Ashlock, M. A.; Ramsey, B. W., Effect of VX-770 in persons with cystic fibrosis and the G551D-CFTR mutation. *N Engl J Med* **2010,** *363* (21), 1991-2003.

28. Davies, J. C.; Wainwright, C. E.; Canny, G. J.; Chilvers, M. A.; Howenstine, M. S.; Munck, A.; Mainz, J. G.; Rodriguez, S.; Li, H.; Yen, K.; Ordonez, C. L.; Ahrens, R.; Group, V. X. S., Efficacy and safety of ivacaftor in patients aged 6 to 11 years with cystic fibrosis with a G551D mutation. *American journal of respiratory and critical care medicine* **2013,** *187* (11), 1219-25.

29. McKone, E. F.; Borowitz, D.; Drevinek, P.; Griese, M.; Konstan, M. W.; Wainwright, C.; Ratjen, F.; Sermet-Gaudelus, I.; Plant, B.; Munck, A.; Jiang, Y.; Gilmartin, G.; Davies, J. C.; Group, V. X. S., Long-term safety and efficacy of ivacaftor in patients with cystic fibrosis who have the Gly551Asp-CFTR mutation: a phase 3, open-label extension study (PERSIST). *The Lancet. Respiratory medicine* **2014,** *2* (11), 902-10.

30. Rowe, S. M.; Heltshe, S. L.; Gonska, T.; Donaldson, S. H.; Borowitz, D.; Gelfond, D.; Sagel, S. D.; Khan, U.; Mayer-Hamblett, N.; Van Dalfsen, J. M.; Joseloff, E.; Ramsey, B. W.; Network, G. I. o. t. C. F. F. T. D., Clinical mechanism of the cystic fibrosis transmembrane conductance regulator potentiator ivacaftor in G551D-mediated cystic fibrosis. *American journal of respiratory and critical care medicine* **2014,** *190* (2), 175-84.

31. Sawicki, G. S.; McKone, E. F.; Pasta, D. J.; Millar, S. J.; Wagener, J. S.; Johnson, C. A.; Konstan, M. W., Sustained Benefit from Ivacaftor Demonstrated by Combining Clinical Trial and Cystic Fibrosis Patient Registry Data. *American journal of respiratory and critical care medicine* **2015,** *192* (7), 836-42.

32. Kalydeco - Highlights of Prescribing Information. Administration, F. a. D., Ed. 2012; p 13.

33. Park, R. W.; Grand, R. J., Gastrointestinal manifestations of cystic fibrosis: a review. *Gastroenterology* **1981,** *81* (6), 1143-61.

34. Holsclaw, D. S.; Eckstein, H. B.; Nixon, H. H., Meconium Ileus. A 20-Year Review of 109 Cases. *Am J Dis Child* **1965,** *109*, 101-13.

35. Donnison, A. B.; Shwachman, H.; Gross, R. E., A review of 164 children with meconium ileus seen at the Children's Hospital Medical Center, Boston. *Pediatrics* **1966,** *37* (5), 833-50.

36. Macdonald, J. A.; Trusler, G. A., Meconium ileus: an eleven-year review at the Hospital for Sick Children, Toronto. *Canadian Medical Association journal* **1960,** *83*, 881-5.

37. Andersen, D. H., Cystic fibrosis of the pancreas and its relation to celiac disease - A clinical and pathologic study. *American Journal of Diseases of Children* **1938,** *56* (2), 344-399.

38. Rowe, S. M.; Miller, S.; Sorscher, E. J., Mechanisms of disease: Cystic fibrosis. *N Engl J Med* **2005,** *352* (19), 1992-2001.

39. Anguiano, A.; Oates, R. D.; Amos, J. A.; Dean, M.; Gerrard, B.; Stewart, C.; Maher, T. A.; White, M. B.; Milunsky, A., Congenital bilateral absence of the vas deferens. A primarily genital form of cystic fibrosis. *JAMA* **1992,** *267* (13), 1794-7.

40. Augarten, A.; Yahav, Y.; Kerem, B. S.; Halle, D.; Laufer, J.; Szeinberg, A.; Dor, J.; Mashiach, S.; Gazit, E.; Madgar, I., Congenital bilateral absence of vas deferens in the absence of cystic fibrosis. *Lancet* **1994,** *344* (8935), 1473-4.

41. Welsh, M. J.; Smith, A. E., Cystic fibrosis. *Sci Am* **1995,** *273* (6), 52-9.

42. Meyer, K. C.; Sharma, A., Regional variability of lung inflammation in cystic fibrosis. *American journal of respiratory and critical care medicine* **1997,** *156* (5), 1536-40.

43. Maffessanti, M.; Candusso, M.; Brizzi, F.; Piovesana, F., Cystic fibrosis in children: HRCT findings and distribution of disease. *Journal of thoracic imaging* **1996,** *11* (1), 27-38.

44. Kerem, E.; Viviani, L.; Zolin, A.; MacNeill, S.; Hatziagorou, E.; Ellemunter, H.; Drevinek, P.; Gulmans, V.; Krivec, U.; Olesen, H.; Group, E. P. R. S., Factors associated with FEV1 decline in cystic fibrosis: analysis of the ECFS patient registry. *The European respiratory journal : official journal of the European Society for Clinical Respiratory Physiology* **2014,** *43* (1), 125-33.

45. Wyckoff, T. J.; Thomas, B.; Hassett, D. J.; Wozniak, D. J., Static growth of mucoid Pseudomonas aeruginosa selects for non-mucoid variants that have acquired flagellum-dependent motility. *Microbiology* **2002,** *148* (Pt 11), 3423-30.

46. Whiteley, M.; Bangera, M. G.; Bumgarner, R. E.; Parsek, M. R.; Teitzel, G. M.; Lory, S.; Greenberg, E. P., Gene expression in Pseudomonas aeruginosa biofilms. *Nature* **2001,** *413* (6858), 860-4.

47. Tiddens, H. A., Detecting early structural lung damage in cystic fibrosis. *Pediatric pulmonology* **2002,** *34* (3), 228-31.

48. Fink, *Clinical Practice in Respiratory Care*. Lippincott Williams & Wilkins: New York, 1999.

49. van Haren, E. H.; Lammers, J. W.; Festen, J.; van Herwaarden, C. L., Bronchodilator response in adult patients with cystic fibrosis: effects on large and small airways. *The European respiratory journal : official journal of the European Society for Clinical Respiratory Physiology* **1991,** *4* (3), 301-7.

50. Eggleston, P. A.; Rosenstein, B. J.; Stackhouse, C. M.; Alexander, M. F., Airway hyperreactivity in cystic fibrosis. Clinical correlates and possible effects on the course of the disease. *Chest* **1988,** *94* (2), 360-5.

51. Weinberger, M., Airways reactivity in patients with CF. *Clin Rev Allergy Immunol* **2002,** *23* (1), 77-85.

52. Rogers, C. S.; Stoltz, D. A.; Meyerholz, D. K.; Ostedgaard, L. S.; Rokhlina, T.; Taft, P. J.; Rogan, M. P.; Pezzulo, A. A.; Karp, P. H.; Itani, O. A.; Kabel, A. C.; Wohlford-Lenane, C. L.; Davis, G. J.; Hanfland, R. A.; Smith, T. L.; Samuel, M.; Wax, D.; Murphy, C. N.; Rieke, A.; Whitworth, K.; Uc, A.; Starner, T. D.; Brogden, K. A.; Shilyansky, J.; McCray, P. B., Jr.; Zabner, J.; Prather, R. S.; Welsh, M. J., Disruption of the CFTR gene produces a model of cystic fibrosis in newborn pigs. *Science* **2008,** *321* (5897), 1837-41.

53. Rogers, C. S.; Abraham, W. M.; Brogden, K. A.; Engelhardt, J. F.; Fisher, J. T.; McCray, P. B., Jr.; McLennan, G.; Meyerholz, D. K.; Namati, E.; Ostedgaard, L. S.; Prather, R. S.; Sabater, J. R.; Stoltz, D. A.; Zabner, J.; Welsh, M. J., The porcine lung as a potential model for cystic fibrosis. *American journal of physiology. Lung cellular and molecular physiology* **2008,** *295* (2), L240-63.

54. Meyerholz, D. K.; Stoltz, D. A.; Pezzulo, A. A.; Welsh, M. J., Pathology of gastrointestinal organs in a porcine model of cystic fibrosis. *The American journal of pathology* **2010,** *176* (3), 1377-89.

55. Hoegger, M. J.; Fischer, A. J.; McMenimen, J. D.; Ostedgaard, L. S.; Tucker, A. J.; Awadalla, M. A.; Moninger, T. O.; Michalski, A. S.; Hoffman, E. A.; Zabner, J.; Stoltz, D. A.; Welsh, M. J., Cystic fibrosis. Impaired mucus detachment disrupts mucociliary transport in a piglet model of cystic fibrosis. *Science* **2014,** *345* (6198), 818-22.

56. Hoegger, M. J.; Awadalla, M.; Namati, E.; Itani, O. A.; Fischer, A. J.; Tucker, A. J.; Adam, R. J.; McLennan, G.; Hoffman, E. A.; Stoltz, D. A.; Welsh, M. J., Assessing mucociliary transport of single particles in vivo shows variable speed and preference for the ventral trachea in newborn pigs. *Proceedings of the National Academy of Sciences of the United States of America* **2014**.

57. Tang, X. X.; Ostedgaard, L. S.; Hoegger, M. J.; Moninger, T. O.; Karp, P. H.; McMenimen, J. D.; Choudhury, B.; Varki, A.; Stoltz, D. A.; Welsh, M. J., Acidic pH increases airway surface liquid viscosity in cystic fibrosis. *The Journal of clinical investigation* **2016,** *126* (3), 879-91.

58. Ostedgaard, L. S.; Meyerholz, D. K.; Chen, J. H.; Pezzulo, A. A.; Karp, P. H.; Rokhlina, T.; Ernst, S. E.; Hanfland, R. A.; Reznikov, L. R.; Ludwig, P. S.; Rogan, M. P.; Davis, G. J.; Dohrn, C. L.; Wohlford-Lenane, C.; Taft, P. J.; Rector, M. V.; Hornick, E.; Nassar, B. S.; Samuel, M.; Zhang, Y.; Richter, S. S.; Uc, A.; Shilyansky, J.; Prather, R. S.; McCray, P. B., Jr.; Zabner, J.; Welsh, M. J.; Stoltz, D. A., The DeltaF508 mutation causes CFTR misprocessing and cystic fibrosis-like disease in pigs. *Science translational medicine* **2011,** *3* (74), 74ra24.

59. West, *Respiratory Physiology*. Lippincott Williams & Wilkins: New York, 2012.

60. Adam, R. J.; Hisert, K. B.; Dodd, J. D.; Grogan, B.; Launspach, J. L.; Barnes, J. K.; Gallagher, C. G.; Sieren, J. P.; Gross, T. J.; Fischer, A. J.; Cavanaugh, J. E.; Hoffman, E. A.; Singh, P. K.; Welsh, M. J.; McKone, E. F.; Stoltz, D. A., Acute administration of ivacaftor to people with cystic fibrosis and a G551D-CFTR mutation reveals smooth muscle abnormalities. *JCI Insight* **2016,** *1* (4), e86183.

61. Prince, *Medical Imaging Signals and Systems*. Prentice Hall: 2005.

62. Schreiber, J. J.; Anderson, P. A.; Rosas, H. G.; Buchholz, A. L.; Au, A. G., Hounsfield units for assessing bone mineral density and strength: a tool for osteoporosis management. *J Bone Joint Surg Am* **2011,** *93* (11), 1057-63.

63. Soldevilla, M. S.; McKenna, M. E.; Wiggins, S. M.; Shadwick, R. E.; Cranford, T. W.; Hildebrand, J. A., Cuvier's beaked whale (Ziphius cavirostris) head tissues: physical properties and CT imaging. *J Exp Biol* **2005,** *208* (12), 2319-2332.

64. Jia, Y. C.; Beltran, C.; Indelicato, D. J.; Flampouri, S.; Li, Z. F.; Merchant, T. E., Proton therapy dose distribution comparison between Monte Carlo and a treatment planning system for pediatric patients with ependymoma. *Med Phys* **2012,** *39* (8), 4742-4747.

65. Muller, N. L.; Staples, C. A.; Miller, R. R.; Abboud, R. T., "Density mask". An objective method to quantitate emphysema using computed tomography. *Chest* **1988,** *94* (4), 782-7.

66. Gevenois, P. A.; De Vuyst, P.; de Maertelaer, V.; Zanen, J.; Jacobovitz, D.; Cosio, M. G.; Yernault, J. C., Comparison of computed density and microscopic morphometry in pulmonary emphysema. *American journal of respiratory and critical care medicine* **1996,** *154* (1), 187-92.

67. Markstaller, K.; Eberle, B.; Kauczor, H. U.; Scholz, A.; Bink, A.; Thelen, M.; Heinrichs, W.; Weiler, N., Temporal dynamics of lung aeration determined by dynamic CT in a porcine model of ARDS. *Br J Anaesth* **2001,** *87* (3), 459-68.

68. Puybasset, L.; Cluzel, P.; Gusman, P.; Grenier, P.; Preteux, F.; Rouby, J. J., Regional distribution of gas and tissue in acute respiratory distress syndrome. I. Consequences for lung morphology. CT Scan ARDS Study Group. *Intensive Care Med* **2000,** *26* (7), 857-69.

69. Gharib, R.; Joos, H. A.; Hilty, L. B., Sweat Chloride Concentration; a Comparative Study in Children with Bronchial Asthma and with Cystic Fibrosis. *Am J Dis Child* **1965,** *109*, 66-8.

70. Verschakelen, J. A.; Vanfraeyenhoven, L.; Laureys, G.; Demedts, M.; Baert, A. L., Differences in Ct Density between Dependent and Nondependent Portions of the Lung - Influence of Lung-Volume. *Am J Roentgenol* **1993,** *161* (4), 713-717.

71. Chen, C. H.; Nevo, E.; Fetics, B.; Pak, P. H.; Yin, F. C.; Maughan, W. L.; Kass, D. A., Estimation of central aortic pressure waveform by mathematical transformation of radial tonometry pressure. Validation of generalized transfer function. *Circulation* **1997,** *95* (7), 1827-36.

72. Wilkinson, I. B.; MacCallum, H.; Cockcroft, J. R.; Webb, D. J., Inhibition of basal nitric oxide synthesis increases aortic augmentation index and pulse wave velocity in vivo. *Br J Clin Pharmacol* **2002,** *53* (2), 189-92.

73. Fischer, A. J.; Singh, S. B.; Adam, R. J.; Stoltz, D. A.; Baranano, C. F.; Kao, S.; Weinberger, M. M.; McCray, P. B., Jr.; Starner, T. D., Tracheomalacia is associated with lower FEV1 and Pseudomonas acquisition in children with CF. *Pediatric pulmonology* **2014,** *49* (10), 960-70.

74. McDermott, S.; Barry, S. C.; Judge, E. E.; Collins, S.; de Jong, P. A.; Tiddens, H. A.; McKone, E. F.; Gallagher, C. C.; Dodd, J. D., Tracheomalacia in adults with cystic fibrosis: determination of prevalence and severity with dynamic cine CT. *Radiology* **2009,** *252* (2), 577-86.

75. Nakakuki, S., Bronchial tree, lobular division and blood vessels of the pig lung. *The Journal of veterinary medical science / the Japanese Society of Veterinary Science* **1994,** *56* (4), 685-9.

76. Brown, R. H.; Wizeman, W.; Danek, C.; Mitzner, W., Effect of bronchial thermoplasty on airway distensibility. *The European respiratory journal : official journal of the European Society for Clinical Respiratory Physiology* **2005,** *26* (2), 277-82.

77. Broackes-Carter, F. C.; Mouchel, N.; Gill, D.; Hyde, S.; Bassett, J.; Harris, A., Temporal regulation of CFTR expression during ovine lung development: implications for CF gene therapy. *Human molecular genetics* **2002,** *11* (2), 125-31.

78. Trezise, A. E.; Chambers, J. A.; Wardle, C. J.; Gould, S.; Harris, A., Expression of the cystic fibrosis gene in human foetal tissues. *Human molecular genetics* **1993,** *2* (3), 213-8.

79. McCray, P. B., Jr.; Wohlford-Lenane, C. L.; Snyder, J. M., Localization of cystic fibrosis transmembrane conductance regulator mRNA in human fetal lung tissue by in situ hybridization. *The Journal of clinical investigation* **1992,** *90* (2), 619-25.

80. Green, M.; Mead, J.; Turner, J. M., Variability of maximum expiratory flow-volume curves. *Journal of applied physiology: respiratory, environmental and exercise physiology* **1974,** *37* (1), 67-74.

81. Mortola, J. P., Dysanaptic lung growth: an experimental and allometric approach. *J Appl Physiol Respir Environ Exerc Physiol* **1983,** *54* (5), 1236-41.

82. Rock, J. R.; Futtner, C. R.; Harfe, B. D., The transmembrane protein TMEM16A is required for normal development of the murine trachea. *Developmental biology* **2008,** *321* (1), 141-9.

83. King, G. G.; Carroll, J. D.; Muller, N. L.; Whittall, K. P.; Gao, M.; Nakano, Y.; Pare, P. D., Heterogeneity of narrowing in normal and asthmatic airways measured by HRCT. *The European respiratory journal : official journal of the European Society for Clinical Respiratory Physiology* **2004,** *24* (2), 211-8.

84. King, G. G.; Downie, S. R.; Verbanck, S.; Thorpe, C. W.; Berend, N.; Salome, C. M.; Thompson, B., Effects of methacholine on small airway function measured by forced oscillation technique and multiple breath nitrogen washout in normal subjects. *Respiratory physiology & neurobiology* **2005,** *148* (1-2), 165-77.

85. Arthur, G., Gene therapy in cystic fibrosis: from lab benches to lungs. *The Lancet. Respiratory medicine* **2015,** *3* (7), 521-2.

86. Bonvin, E.; Le Rouzic, P.; Bernaudin, J. F.; Cottart, C. H.; Vandebrouck, C.; Crie, A.; Leal, T.; Clement, A.; Bonora, M., Congenital tracheal malformation in cystic fibrosis transmembrane conductance regulator-deficient mice. *The Journal of physiology* **2008,** *586* (13), 3231-43.

87. Tuggle, K. L.; Birket, S. E.; Cui, X.; Hong, J.; Warren, J.; Reid, L.; Chambers, A.; Ji, D.; Gamber, K.; Chu, K. K.; Tearney, G.; Tang, L. P.; Fortenberry, J. A.; Du, M.; Cadillac, J. M.; Bedwell, D. M.; Rowe, S. M.; Sorscher, E. J.; Fanucchi, M. V., Characterization of defects in ion transport and tissue development in cystic fibrosis transmembrane conductance regulator (CFTR)-knockout rats. *PloS one* **2014,** *9* (3), e91253.

88. Diwakar, A.; Adam, R. J.; Michalski, A. S.; Tamegnon, M. M.; Fischer, A. J.; Launspach, J. L.; Horan, R. A.; Kao, S. C.; Chaloner, K.; Meyerholz, D. K.; Stoltz, D. A., Sonographic evidence of abnormal tracheal cartilage ring structure in cystic fibrosis. *Laryngoscope* **2015**.

89. Hall, G. L.; Logie, K. M.; Parsons, F.; Schulzke, S. M.; Nolan, G.; Murray, C.; Ranganathan, S.; Robinson, P.; Sly, P. D.; Stick, S. M.; Arest, C. F.; Berry, L.; Garratt, L.; Massie, J.; Mott, L.; Poreddy, S.; Simpson, S., Air trapping on chest CT is associated with worse ventilation distribution in infants with cystic fibrosis diagnosed following newborn screening. *PloS one* **2011,** *6* (8), e23932.

90. Tepper, L. A.; Utens, E. M.; Caudri, D.; Bos, A. C.; Gonzalez-Graniel, K.; Duivenvoorden, H. J.; van der Wiel, E. C.; Quittner, A. L.; Tiddens, H. A., Impact of bronchiectasis and trapped air on quality of life and exacerbations in cystic fibrosis. *The European respiratory journal : official journal of the European Society for Clinical Respiratory Physiology* **2013,** *42* (2), 371-9.

91. West, A. R.; Needi, E. T.; Mitchell, H. W.; McFawn, P. K.; Noble, P. B., Airways dilate to simulated inspiratory but not expiratory manoeuvres. *The European respiratory journal : official journal of the European Society for Clinical Respiratory Physiology* **2012,** *40* (2), 455-61.

92. Robinson, T. E.; Goris, M. L.; Zhu, H. J.; Chen, X.; Bhise, P.; Sheikh, F.; Moss, R. B., Dornase alfa reduces air trapping in children with mild cystic fibrosis lung disease: a quantitative analysis. *Chest* **2005,** *128* (4), 2327-35.

93. Wandtke, J. C.; Hyde, R. W.; Fahey, P. J.; Utell, M. J.; Plewes, D. B.; Goske, M. J.; Fischer, H. W., Measurement of lung gas volume and regional density by computed tomography in dogs. *Invest Radiol* **1986,** *21* (2), 108-17.

94. Adams, H.; Bernard, M. S.; McConnochie, K., An appraisal of CT pulmonary density mapping in normal subjects. *Clinical radiology* **1991,** *43* (4), 238-42.

95. Hedlund, L. W.; Vock, P.; Effmann, E. L., Evaluating Lung Density by Computed-Tomography. *Semin Respir Med* **1983,** *5* (1), 76-&.

96. Kreel, L., Computer tomography in the evaluation of pulmonary asbestosis. Preliminary experiences with the EMI general purpose scanner. *Acta Radiol Diagn (Stockh)* **1976,** *17* (4), 405-12.

97. Lynch, D. A.; Brasch, R. C.; Hardy, K. A.; Webb, W. R., Pediatric pulmonary disease: assessment with high-resolution ultrafast CT. *Radiology* **1990,** *176* (1), 243-8.

98. Davis, S. D.; Fordham, L. A.; Brody, A. S.; Noah, T. L.; Retsch-Bogart, G. Z.; Qaqish, B. F.; Yankaskas, B. C.; Johnson, R. C.; Leigh, M. W., Computed tomography reflects lower airway inflammation and tracks changes in early cystic fibrosis. *American journal of respiratory and critical care medicine* **2007,** *175* (9), 943-50.

99. Dakin, C. J.; Numa, A. H.; Wang, H.; Morton, J. R.; Vertzyas, C. C.; Henry, R. L., Inflammation, infection, and pulmonary function in infants and young children with cystic fibrosis. *American journal of respiratory and critical care medicine* **2002,** *165* (7), 904-10.

100. Hilliard, T. N.; Sukhani, S.; Francis, J.; Madden, N.; Rosenthal, M.; Balfour-Lynn, I.; Bush, A.; Davies, J. C., Bronchoscopy following diagnosis with cystic fibrosis. *Arch Dis Child* **2007,** *92* (10), 898-9.

101. Welsh, M. J., Targeting the basic defect in cystic fibrosis. *N Engl J Med* **2010,** *363* (21), 2056-7.

102. Abbott, G. F.; Rosado-de-Christenson, M. L.; Rossi, S. E.; Suster, S., Imaging of small airways disease. *Journal of thoracic imaging* **2009,** *24* (4), 285-98.

103. Awadalla, M.; Miyawaki, S.; Abou Alaiwa, M. H.; Adam, R. J.; Bouzek, D. C.; Michalski, A. S.; Fuld, M. K.; Reynolds, K. J.; Hoffman, E. A.; Lin, C. L.; Stoltz, D. A., Early Airway Structural Changes in Cystic Fibrosis Pigs as a Determinant of Particle Distribution and Deposition. *Annals of biomedical engineering* **2013**.

104. Vic, P.; Tassin, E.; Turck, D.; Gottrand, F.; Launay, V.; Farriaux, J. P., [Frequency of gastroesophageal reflux in infants and in young children with cystic fibrosis]. *Arch Pediatr* **1995,** *2* (8), 742-6.

105. Vinocur, C. D.; Marmon, L.; Schidlow, D. V.; Weintraub, W. H., Gastroesophageal reflux in the infant with cystic fibrosis. *Am J Surg* **1985,** *149* (1), 182-6.

106. Scott, R. B.; O'Loughlin, E. V.; Gall, D. G., Gastroesophageal reflux in patients with cystic fibrosis. *The Journal of pediatrics* **1985,** *106* (2), 223-7.

107. Khan, T. Z.; Wagener, J. S.; Bost, T.; Martinez, J.; Accurso, F. J.; Riches, D. W., Early pulmonary inflammation in infants with cystic fibrosis. *American journal of respiratory and critical care medicine* **1995,** *151* (4), 1075-82.

108. Balough, K.; McCubbin, M.; Weinberger, M.; Smits, W.; Ahrens, R.; Fick, R., The relationship between infection and inflammation in the early stages of lung disease from cystic fibrosis. *Pediatric pulmonology* **1995,** *20* (2), 63-70.

109. Aldallal, N.; McNaughton, E. E.; Manzel, L. J.; Richards, A. M.; Zabner, J.; Ferkol, T. W.; Look, D. C., Inflammatory response in airway epithelial cells isolated from patients with cystic fibrosis. *American journal of respiratory and critical care medicine* **2002,** *166* (9), 1248-56.

110. Perez, A.; Issler, A. C.; Cotton, C. U.; Kelley, T. J.; Verkman, A. S.; Davis, P. B., CFTR inhibition mimics the cystic fibrosis inflammatory profile. *American journal of physiology. Lung cellular and molecular physiology* **2007,** *292* (2), L383-95.

111. Char, J. E.; Wolfe, M. H.; Cho, H. J.; Park, I. H.; Jeong, J. H.; Frisbee, E.; Dunn, C.; Davies, Z.; Milla, C.; Moss, R. B.; Thomas, E. A.; Wine, J. J., A little CFTR goes a long way: CFTR-dependent sweat secretion from G551D and R117H-5T cystic fibrosis subjects taking ivacaftor. *PloS one* **2014,** *9* (2), e88564.

112. Yu, H.; Burton, B.; Huang, C. J.; Worley, J.; Cao, D.; Johnson, J. P., Jr.; Urrutia, A.; Joubran, J.; Seepersaud, S.; Sussky, K.; Hoffman, B. J.; Van Goor, F., Ivacaftor potentiation of multiple CFTR channels with gating mutations. *Journal of cystic fibrosis : official journal of the European Cystic Fibrosis Society* **2012,** *11* (3), 237-45.

113. De Boeck, K.; Munck, A.; Walker, S.; Faro, A.; Hiatt, P.; Gilmartin, G.; Higgins, M., Efficacy and safety of ivacaftor in patients with cystic fibrosis and a non-G551D gating mutation. *Journal of cystic fibrosis : official journal of the European Cystic Fibrosis Society* **2014,** *13* (6), 674-80.

114. Davies, J.; Sheridan, H.; Bell, N.; Cunningham, S.; Davis, S. D.; Elborn, J. S.; Milla, C. E.; Starner, T. D.; Weiner, D. J.; Lee, P. S.; Ratjen, F., Assessment of clinical response to ivacaftor with lung clearance index in cystic fibrosis patients with a G551D-CFTR mutation and preserved spirometry: a randomised controlled trial. *The Lancet. Respiratory medicine* **2013,** *1* (8), 630-8.

115. Hoare, S.; McEvoy, S.; McCarthy, C. J.; Kilcoyne, A.; Brady, D.; Gibney, B.; Gallagher, C. G.; McKone, E. F.; Dodd, J. D., Ivacaftor imaging response in cystic fibrosis. *American journal of respiratory and critical care medicine* **2014,** *189* (4), 484.

116. Smith, B. M.; Hoffman, E. A.; Rabinowitz, D.; Bleecker, E.; Christenson, S.; Couper, D.; Donohue, K. M.; Han, M. K.; Hansel, N. N.; Kanner, R. E.; Kleerup, E.; Rennard, S.; Barr, R. G., Comparison of spatially matched airways reveals thinner airway walls in COPD. The Multi-Ethnic Study of Atherosclerosis (MESA) COPD Study and the Subpopulations and Intermediate Outcomes in COPD Study (SPIROMICS). *Thorax* **2014,** *69* (11), 987-96.

117. Busacker, A.; Newell, J. D., Jr.; Keefe, T.; Hoffman, E. A.; Granroth, J. C.; Castro, M.; Fain, S.; Wenzel, S., A multivariate analysis of risk factors for the air-trapping asthmatic phenotype as measured by quantitative CT analysis. *Chest* **2009,** *135* (1), 48-56.

118. Ullman, A.; Svedmyr, N., Salmeterol, a new long acting inhaled beta 2 adrenoceptor agonist: comparison with salbutamol in adult asthmatic patients. *Thorax* **1988,** *43* (9), 674-8.

119. Castle, W.; Fuller, R.; Hall, J.; Palmer, J., Serevent nationwide surveillance study: comparison of salmeterol with salbutamol in asthmatic patients who require regular bronchodilator treatment. *BMJ* **1993,** *306* (6884), 1034-7.

120. Olsen, C. R.; Stevens, A. E.; McIlroy, M. B., Rigidity of tracheae and bronchi during muscular constriction. *Journal of applied physiology: respiratory, environmental and exercise physiology* **1967,** *23* (1), 27-34.

121. Jensen, A.; Atileh, H.; Suki, B.; Ingenito, E. P.; Lutchen, K. R., Selected contribution: airway caliber in healthy and asthmatic subjects: effects of bronchial challenge and deep inspirations. *Journal of applied physiology* **2001,** *91* (1), 506-15; discussion 504-5.

122. Wallace, H. L.; Southern, K. W.; Connell, M. G.; Wray, S.; Burdyga, T., Abnormal tracheal smooth muscle function in the CF mouse. *Physiological reports* **2013,** *1* (6), e00138.

123. Matsuba, K.; Thurlbeck, W. M., A morphometric study of bronchial and bronchiolar walls in children. *The American review of respiratory disease* **1972,** *105* (6), 908-13.

124. James, A.; Carroll, N., Airway smooth muscle in health and disease; methods of measurement and relation to function. *The European respiratory journal : official journal of the European Society for Clinical Respiratory Physiology* **2000,** *15* (4), 782-9.

125. Kelly, V. J.; Brown, N. J.; King, G. G.; Thompson, B. R., The bronchodilator response of in vivo specific airway compliance in adults with asthma. *Annals of biomedical engineering* **2011,** *39* (3), 1125-35.

126. Hisert, K. B.; Schoenfelt, K. Q.; Cooke, G.; Grogan, B.; Launspach, J. L.; Gallagher, C. G.; Donnelly, S. C.; McKone, E. F.; Welsh, M. J.; Singh, P. K.; Becker, L., Ivacaftor-induced proteomic changes suggest monocyte defects may contribute to the pathogenesis of cystic fibrosis. *American journal of respiratory cell and molecular biology* **2015**.

127. Hahn, H. L.; Watson, A.; Wilson, A. G.; Pride, N. B., Influence of bronchomotor tone on airway dimensions and resistance in excised dog lungs. *J Appl Physiol Respir Environ Exerc Physiol* **1980,** *49* (2), 270-8.

128. Gunst, S. J.; Stropp, J. Q.; Service, J., Mechanical modulation of pressure-volume characteristics of contracted canine airways in vitro. *Journal of applied physiology* **1990,** *68* (5), 2223-9.

129. Brown, R. H.; Mitzner, W.; Bulut, Y.; Wagner, E. M., Effect of lung inflation in vivo on airways with smooth muscle tone or edema. *Journal of applied physiology* **1997,** *82* (2), 491-9.

130. Brown, N. J.; Salome, C. M.; Berend, N.; Thorpe, C. W.; King, G. G., Airway distensibility in adults with asthma and healthy adults, measured by forced oscillation technique. *American journal of respiratory and critical care medicine* **2007,** *176* (2), 129-37.

131. Kermode, J. A.; Brown, N. J.; Hardaker, K. M.; Farah, C. S.; Berend, N.; King, G. G.; Salome, C. M., The effect of airway remodelling on airway hyper-responsiveness in asthma. *Respiratory medicine* **2011,** *105* (12), 1798-804.

132. Pyrgos, G.; Scichilone, N.; Togias, A.; Brown, R. H., Bronchodilation response to deep inspirations in asthma is dependent on airway distensibility and air trapping. *Journal of applied physiology* **2011,** *110* (2), 472-9.

133. Kelly, V. J.; Brown, N. J.; Sands, S. A.; Borg, B. M.; King, G. G.; Thompson, B. R., Effect of airway smooth muscle tone on airway distensibility measured by the forced oscillation technique in adults with asthma. *Journal of applied physiology* **2012,** *112* (9), 1494-503.

134. Brown, R. H.; Scichilone, N.; Mudge, B.; Diemer, F. B.; Permutt, S.; Togias, A., High-resolution computed tomographic evaluation of airway distensibility and the effects of lung inflation on airway caliber in healthy subjects and individuals with asthma. *American journal of respiratory and critical care medicine* **2001,** *163* (4), 994-1001.

135. Johns, D. P.; Wilson, J.; Harding, R.; Walters, E. H., Airway distensibility in healthy and asthmatic subjects: effect of lung volume history. *Journal of applied physiology* **2000,** *88* (4), 1413-20.

136. Brown, R. H.; Mitzner, W.; Wagner, E.; Permutt, S.; Togias, A., Airway distension with lung inflation measured by HRCT. *Academic radiology* **2003,** *10* (10), 1097-103.

137. Reznikov, L. R.; Dong, Q.; Chen, J. H.; Moninger, T. O.; Park, J. M.; Zhang, Y.; Du, J.; Hildebrand, M. S.; Smith, R. J.; Randak, C. O.; Stoltz, D. A.; Welsh, M. J., CFTR-deficient pigs display peripheral nervous system defects at birth. *Proceedings of the National Academy of Sciences of the United States of America* **2013,** *110* (8), 3083-8.

138. Reznikov, L. R., Cystic Fibrosis and the Nervous System. *Chest* **2016**.

139. Harrison, M. J.; Murphy, D. M.; Plant, B. J., Ivacaftor in a G551D homozygote with cystic fibrosis. *N Engl J Med* **2013,** *369* (13), 1280-2.

140. Sheikh, S. I.; Long, F. R.; McCoy, K. S.; Johnson, T.; Ryan-Wenger, N. A.; Hayes, D., Jr., Ivacaftor Improves Appearance of Sinus Disease on Computerized Tomography in Cystic Fibrosis Patients with G551D mutation. *Clinical otolaryngology : official journal of ENT-UK ; official journal of Netherlands Society for Oto-Rhino-Laryngology & Cervico-Facial Surgery* **2014**.

141. Hayes, D., Jr.; Long, F. R.; McCoy, K. S.; Sheikh, S. I., Improvement in bronchiectasis on CT imaging in a pediatric patient with cystic fibrosis on ivacaftor therapy. *Respiration; international review of thoracic diseases* **2014,** *88* (4), 345.

142. Sheikh, S. I.; Long, F. R.; McCoy, K. S.; Johnson, T.; Ryan-Wenger, N. A.; Hayes, D., Jr., Computed tomography correlates with improvement with ivacaftor in cystic fibrosis patients with G551D mutation. *Journal of cystic fibrosis : official journal of the European Cystic Fibrosis Society* **2015,** *14* (1), 84-9.

143. De Lisle, R. C.; Borowitz, D., The cystic fibrosis intestine. *Cold Spring Harbor perspectives in medicine* **2013,** *3* (9), a009753.

144. Fuchs, H. J.; Borowitz, D. S.; Christiansen, D. H.; Morris, E. M.; Nash, M. L.; Ramsey, B. W.; Rosenstein, B. J.; Smith, A. L.; Wohl, M. E., Effect of aerosolized recombinant human DNase on exacerbations of respiratory symptoms and on pulmonary function in patients with cystic fibrosis. The Pulmozyme Study Group. *N Engl J Med* **1994,** *331* (10), 637-42.

145. Elkins, M. R.; Robinson, M.; Rose, B. R.; Harbour, C.; Moriarty, C. P.; Marks, G. B.; Belousova, E. G.; Xuan, W.; Bye, P. T.; National Hypertonic Saline in Cystic Fibrosis Study, G., A controlled trial of long-term inhaled hypertonic saline in patients with cystic fibrosis. *N Engl J Med* **2006,** *354* (3), 229-40.

146. Ramsey, B. W.; Pepe, M. S.; Quan, J. M.; Otto, K. L.; Montgomery, A. B.; Williams-Warren, J.; Vasiljev, K. M.; Borowitz, D.; Bowman, C. M.; Marshall, B. C.; Marshall, S.; Smith, A. L., Intermittent administration of inhaled tobramycin in patients with cystic fibrosis. Cystic Fibrosis Inhaled Tobramycin Study Group. *N Engl J Med* **1999,** *340* (1), 23-30.

147. Hsieh, *Computed Tomography Principles, Design, Artifiacts, and Recent Advances*. Second Edition ed.; Wiley Interscience: Washington, USA, 2009.

148. Kalender, *Computed Tomography: Fundamentals, System Technology, Image Quality, Applications*. 3rd ed.; Publicis: Germany, 2011.

149. Chassagnon, G.; Hubert, D.; Fajac, I.; Burgel, P. R.; Revel, M. P.; investigators, Long-term computed tomographic changes in cystic fibrosis patients treated with ivacaftor. *The European respiratory journal : official journal of the European Society for Clinical Respiratory Physiology* **2016,** *48* (1), 249-52.

150. Whitwell, F., A study of the pathology and pathogenesis of bronchiectasis. *Thorax* **1952,** *7* (3), 213-39.

151. Gaillard, E. A.; Carty, H.; Heaf, D.; Smyth, R. L., Reversible bronchial dilatation in children: comparison of serial high-resolution computer tomography scans of the lungs. *Eur J Radiol* **2003,** *47* (3), 215-20.

152. Horsley, A. R.; Davies, J. C.; Gray, R. D.; Macleod, K. A.; Donovan, J.; Aziz, Z. A.; Bell, N. J.; Rainer, M.; Mt-Isa, S.; Voase, N.; Dewar, M. H.; Saunders, C.; Gibson, J. S.; Parra-Leiton, J.; Larsen, M. D.; Jeswiet, S.; Soussi, S.; Bakar, Y.; Meister, M. G.; Tyler, P.; Doherty, A.; Hansell, D. M.; Ashby, D.; Hyde, S. C.; Gill, D. R.; Greening, A. P.; Porteous, D. J.; Innes, J. A.; Boyd, A. C.; Griesenbach, U.; Cunningham, S.; Alton, E. W., Changes in physiological, functional and structural markers of cystic fibrosis lung disease with treatment of a pulmonary exacerbation. *Thorax* **2013,** *68* (6), 532-9.

153. Pare, P. D.; Roberts, C. R.; Bai, T. R.; Wiggs, B. J., The functional consequences of airway remodeling in asthma. *Monaldi Arch Chest Dis* **1997,** *52* (6), 589-96.

154. McParland, B. E.; Macklem, P. T.; Pare, P. D., Airway wall remodeling: friend or foe? *Journal of applied physiology* **2003,** *95* (1), 426-34.